EPA 600/R-14/261 | September 2014 | www.epa.gov/research

United States
Environmental Protection
Agency

Adsorption and Desorption of Chemical Warfare Agents on Activated Carbon: Impact of Temperature and Relative Humidity

Office of Research and Development
National Homeland Security Research Center

Adsorption and Desorption of Chemical Warfare Agents on Activated Carbon: Impact of Temperature and Relative Humidity

National Homeland Security Research Center
Office of Research and Development
U.S. Environmental Protection Agency
Research Triangle Park, NC 27711

DISCLAIMER

The United States Environmental Protection Agency (EPA), through its Office of Research and Development (ORD) funded and managed the research described here through EPA Contract Number EP-C-10-001 with Battelle. This report has been subjected to the Agency's review and has been approved for publication as an Environmental Protection Agency report. Note that approval does not signify that the contents necessarily reflect the views of the Agency. Mention of trade names, products, or services does not convey official EPA approval, endorsement, or recommendation.

Questions concerning this document or its application should be addressed to:

Lukas Oudejans, Ph.D.
Decontamination and Consequence Management Division
National Homeland Security Research Center
Office of Research and Development
U.S. Environmental Protection Agency (MD-E343-06)
109 T.W. Alexander Dr.
Research Triangle Park, NC 27709
Phone: 919-541-2973
Fax: 919-541-0496
E-mail: Oudejans.Lukas@epa.gov

ACKNOWLEDGMENTS

The following individuals are acknowledged for review of this document:

United States Environmental Protection Agency:

Office of Solid Waste and Emergency Response, Office of Emergency Management

Shannon Serre (on detail from Office of Research and Development, National Homeland Security Research Center)

Office of Solid Waste and Emergency Response, Office of Superfund Remediation & Technology Innovation

Dave Mickunas

Office of Research and Development, National Homeland Security Research Center

Paul Lemieux

Ramona Sherman (QA review)

Contributions of the following organizations to the development of this document are gratefully acknowledged.

Battelle Memorial Institute

TABLE OF CONTENTS

LIST OF FIGURES

LIST OF TABLES

ABBREVIATIONS AND ACRONYMS

ASTM	American Society for Testing and Materials, now ASTM International
ASZM	copper, silver, zinc, molybdenum
BPL	bituminous pulverized low (ash)
^{o}C	degree(s) Celsius
cm	centimeter(s)
CCV	continuing calibration verification
CWA	chemical warfare agent
DMMP	dimethyl methylphosphonate
EPA	U.S. Environmental Protection Agency
FID	flame ionization detector
FPD	flame photometric detector
ft^2	square foot
g	gram(s)
GB	isopropyl methylphosphonofluoridate, nerve agent (sarin)
GC	gas chromatograph
HD	bis(2-chloroethyl)sulfide, blister agent (sulfur mustard)
HEPA	high-efficiency particulate air
HF	hydrofluoric acid
HMRC	Hazardous Materials Research Center
h	hour(s)
HVAC	heating, ventilation, and air conditioning
ID	inner diameter
IDLH	immediately dangerous to life or health
in	inch(es)
L	liter(s)
Lpm	liter(s) per minute
m	meter(s)
m^2	square meter(s)
m^3	cubic meter(s)
MFC	mass flow controller
MFM	mass flow meter

µL	microliter(s)
mg	milligram(s)
min	minute(s)
mL	milliliter(s)
mm	millimeter(s)
NHSRC	National Homeland Security Research Center
NIST	National Institute of Standards and Technology
OD	outer diameter
ppm	part(s) per million
QA	quality assurance
QC	quality control
r^2	coefficient of determination
RH	relative humidity
RPD	relative percentage of difference
s	second(s)
SOP	standard operating procedure
SOW	statement of work
SST	solid sorbent tube
STEL	short term exposure limit
T	temperature
TDG	thiodiglycol
TEDA	triethylenediamine
TGD	thickened soman
TIC	toxic industrial chemical
TSA	technical systems audit
VX	ethyl({2-[bis(propan-2-yl)amino]ethyl}sulfanyl)(methyl)phosphinate, nerve agent

EXECUTIVE SUMMARY

This project supports the mission of the U.S. Environmental Protection Agency's (EPA) Office of Research and Development's (ORD) Homeland Security Research Program (HSRP) to conduct research and develop scientific products that improve the capability of EPA to carry out its homeland security responsibilities. The known threat of a chemical agent release in a building or transportation hub is necessitating the EPA's National Homeland Security Research Center (NHSRC) to develop of a research program to evaluate potential decontamination strategies. The EPA may be tasked to clean up or provide technical support related to these agents after a release in buildings. Knowledge of how effective many of the available fumigation technologies are against chemical agents is currently being developed by NHSRC for various fumigation methods such as (modified) hydrogen peroxide vapor, chlorine dioxide vapor, and hot (humid) air.

Hot air has been assessed for the gaseous decontamination of sarin (GB), VX, sulfur mustard (HD), and thickened soman (TGD) from indoor building materials as a less complicated alternative to (modified) hydrogen peroxide vapor or chlorine dioxide vapor. Enhanced volatilization of chemical warfare agents (CWAs) by increasing the temperature through introduction of hot (humid) air into a building using the existing building heating, ventilation and air conditioning (HVAC) system is a valuable and relatively low cost decontamination option for an indoor facility. Such approach would require a uniform heat distribution of such facility as to avoid cold spots that could act as sinks for volatilized agent vapor. Negative air machines/air scrubbers outfitted with carbon filters and air heating elements could also be considered to remove chemical agents from indoor environments. Either way, collective protection (filtration) systems would be required to either prevent transfer of the CWA vapor to the outside environment or to adsorb the agent during recirculation of (building) air. The heated air that is generated would cause an increase in carbon temperature that is likely to impact the carbon adsorption characteristics, resulting in a potentially poorer carbon adsorption performance with shorter breakthrough times. This impact on the carbon adsorption characteristics would lead to an unintended earlier release of hazardous agent in the effluent of the carbon bed.

The objective of this study was to determine the dynamic adsorption and desorption performance of activated carbon beds through measurement of the initial breakthrough and desorption curves at ambient and elevated temperatures. Results from this evaluation can be

used by responders to assess the capability of carbon filters in HVAC applications to capture the CWA under ambient and elevated temperature conditions. The measurement of desorption of the CWA from the activated carbon would indicate whether off-gassing from activated carbon air filters is a potential concern when these filters are removed from service as part of the waste management.

Four types of activated carbons, Calgon Carbon ASZM-TEDA (6 × 16 mesh and 12 × 30 mesh), IONEX Research IONEX 03-001 (8 × 16 mesh), and Cabot Norit® Vapure™ 612 (6 × 12 mesh) were tested against two chemical warfare agents, namely, sarin (*O*-Isopropyl methylphosphonofluoridate, GB) and sulfur mustard (bis(2-chloroethyl) sulfide, HD). Each of these carbons is used frequently in either HVAC carbon filters or respirator cartridges. Vapor challenges for adsorption and desorption performance were performed for the activated carbon types with various mesh sizes, as summarized in Table ES-1. All carbons were in equilibrium with the environmental conditions prior to the start of the agent challenge.

Table ES-1. Summary of tested conditions. Numbers refer to number of tests at identified condition.

Carbon Type	Mesh Size	Agent	Temperature (°C) / RH			Bed Depth (cm)
			25/dry[a]	55/dry	55/humid	
Calgon Carbon ASZM-TEDA™	6 × 16	GB	1			2.5
			1			3.0
			2			3.5
IONEX Research IONEX 03-001	8 × 16	GB	2	2	1[b]	3.5
Norit® Vapure™ 612	6 × 12	GB	2	2		3.5
Calgon Carbon ASZM-TEDA™	12 × 30	GB	1	1		2.5
IONEX Research IONEX 03-001	8 × 16	HD	1	1	1[c] [50 % RH]	2.5
Calgon Carbon ASZM-TEDA™	12 × 30	HD	1	1	1 [20 % RH]	2.5
Calgon Carbon ASZM-TEDA™	6 × 16	HD	1			2.5

[a] dry: < 10 % relative humidity (RH)

[b] attempted; detection of hydrofluoric acid (HF) in effluent prevented test

[c] incomplete test due to condensation in sample line

The target test challenge concentration was 1,500 milligrams/cubic meter (mg/m^3) of GB and 500 mg/m^3 HD. Both concentrations were derived from a release of 1 liter (L) of liquid agent into a 168 square meter (m^2) (2000 square foot [ft^2]) office-type area (no air exchange assumed) with the HD concentration limited by its saturation concentration.

Three environmental conditions were considered, namely, dry RH less than 10 %) conditions at 25 ºC as a reference condition and 55 ºC temperature (T) while a more humid (50 % RH targeted) condition was included at 55 ºC. The 55 ºC temperature is considered to be close to the upper boundary temperature that can be used during hot air fumigation without damage (e.g., to electrical wiring inside a building).

Summary of Results for GB

Among the four types of activated carbons tested, the ASZM-TEDA (12 × 30 mesh) and IONEX 03-001 carbons demonstrated the best GB adsorption performance, with the IONEX 03-001 carbon bed effluent concentration held at <0.04 mg/m^3 for 85 and 170 minutes (min) at 25 ºC/dry and 55 ºC/dry conditions, respectively. Comparable adsorption curves were obtained for the GB vapor on the ASZM-TEDA (12 × 30 mesh) carbon bed as the effluent concentration was held at < 0.04 mg/m^3 for 140 min at 25 ºC/dry conditions. Note that the ASZM-TEDA (12 × 30 mesh) carbon results are based on a 2.5 centimeters (cm) bed depth while the other coarser carbons were tested with a 3.5 cm bed depth. This shallower bed depth selection was based on observations (i.e., lack of measurable breakthrough) for HD for a 2.5 cm bed depth. Immediate breakthrough occurred with both the ASZM-TEDA (6 × 16 mesh) and Vapure™ 612 carbon beds, as the GB concentration in the effluent steadily increased initially, albeit very gradually.

Contrary to anticipated results, increasing the temperature from 25 ºC/dry to 55 ºC/dry did not appear to affect carbon bed adsorption performance adversely for the coarser (low mesh size) carbons. Significantly better adsorption performance was measured for the IONEX 03-001 carbon bed and better adsorption performance was observed for the Vapure™ 612 carbon in the initial stages of the adsorption phase. There is no definitive explanation for this observation. Prolonged (>16 hours [h]) preconditioning at 55 ºC/dry was believed to be a factor, because the carbon might desorb contaminants or water vapor out of the carbon pores to increase the

adsorption capacity. A weight loss of 4 and 5 %, respectively, was associated with preconditioning the IONEX 03-001 and Vapure™ 612 carbon at 55 ºC/dry conditions. Increasing temperature from 25 °C/dry to 55 °C/dry shifted the onset of GB adsorption to shorter times for the finer ASZM-TEDA (12 × 30 mesh), in line with expectations.

GB desorption from the carbon bed was observed for all four types of carbons after the GB challenge was stopped and clean air was pulled through the carbon bed at the flow and T/RH conditions equivalent to the adsorption test. In general, the GB concentration downstream of the carbon bed, as a result of GB desorbing from the carbon, decreased quickly in the initial stages of desorption and then leveled off. The desorption behavior was dependent on temperature. After an initial drop in GB concentration downstream of the carbon (effluent stream), the GB concentration continued to decrease with time as 25 ºC, dry clean air continued to flow through the carbon bed. Conversely, after an initial decrease in GB concentration, the GB concentration in the effluent gradually increased with time as 55 ºC, dry clean air continued to flow through the carbon bed. Consequently, GB desorption may pose more risk at the higher temperature of 55 ºC, because of the slowly increasing trend of the desorption concentration with time.

Adsorption studies at higher RH were originally planned. However, HF was detected in the effluent of a preliminary test at 55 ºC/50 % RH using a shallow IONEX 03-001 carbon bed. Consequently, tests originally planned at the higher RH conditions were not executed to prevent catastrophic failure of the sensitive analytical equipment that measured the effluent GB vapor. Hydrolysis of GB results in the formation of HF as a decomposition product and is expected to be enhanced/faster at high temperature and RH. Since HF is highly corrosive, tests should be conducted to quantify the formation of HF under different T/RH conditions. The results would indicate whether HF formation is a potential risk to, e.g., the metal ductwork in HVAC applications. Using the aforementioned release scenario and assuming complete hydrolysis of GB with no air exchange, the HF concentration could be as high as 260 parts per million (ppm). This concentration is at the lower end of laboratory studies that investigate the impact of HF on (electronic) equipment. A further assessment of the impact that HF may have on metal ductwork was beyond the scope of this study.

Desorption from the carbon beds was persistent for all types of carbons tested, with desorption concentrations sustained at levels of three to four order of magnitude higher than the short term exposure limit (STEL) (i.e., 0.0001 mg/m^3 for GB) after 10 hours of desorption. Only

a small quantity of the adsorbed GB, however, was desorbed. After desorption for up to ten hours, less than 1 % of the adsorbed GB had been desorbed at both 25 ºC/dry and 55 ºC/dry conditions for all three types of carbons tested.

Summary of Results for HD

In HD vapor challenge tests, the ASZM-TEDA (12 × 30 mesh) carbon out-performed the IONEX 03-001 carbon and the ASZM-TEDA (6 × 16 mesh) carbon. No evidence of breakthrough was observed after nearly six hours of HD vapor exposure under all three sets of test conditions using the ASZM-TEDA (12 × 30 mesh) carbon. The IONEX 03-001 carbon began exhibiting breakthrough behavior at approximately three to four hours. Comparison of the ASZM-TEDA (12 × 30 mesh) results to the ASZM-TEDA (6 × 16 mesh) results under the 25 ºC/dry conditions indicated that the difference in particle size in the carbon bed was the primary reason for this difference in breakthrough behavior.

Similar to the observation made in GB testing, increasing the test temperature from 25 ºC to 55 ºC did not appear to impact the HD vapor adsorption behavior of the IONEX 03-001 carbon significantly. Desorption of HD, however, was more rapid at 55 ºC compared to the 25 ºC test conditions.

Testing HD vapor adsorption and desorption at 55 ºC/humid conditions was complicated by the formation of condensation in the post-MINICAMS® sample flow system. Thiodiglycol (TDG), the primary HD hydrolysis product, was detected in effluent samples at the conclusion of the challenge period and in an extracted sample of the ASZM-TEDA (12 × 30 mesh) test carbon exposed to HD. Neither the IONEX 03-001 nor the ASZM-TEDA (12 × 30 mesh) carbon achieved HD vapor breakthrough during the test under the 55 ºC/humid conditions.

Table ES-2 summarizes the changes in breakthrough times when comparing them to the reference breakthrough time(s) observed at 25 °C/dry test condition.

Table ES-2. Summary of trends in breakthrough times with respect to 25 °C/dry adsorption results.

		GB		HD	
Carbon Type	**Mesh Size**	**55 °C/dry**	**55 °C/humid**	**55 °C/dry**	**55 °C/humid**
Calgon Carbon ASZM-TEDA™	6 × 16	ND	NA[a]	NA	NA
Calgon Carbon ASZM-TEDA™	12 × 30	--	NA[a]	+/-	+/-
IONEX Research IONEX 03-001	8 × 16	++	ND[a]	==	++[b]
Norit® Vapure™ 612	6 × 12	--	NA[a]	NA	NA

++: longer breakthrough time
==: equal breakthrough time; no discernable impact
--: shorter breakthrough times
+/-: no breakthrough observed for any condition
ND: Not Determined
NA: Not Attempted
[a] Not determined due to observed formation of HF in effluent
[b] Enhanced HD hydrolysis extends breakthrough time

Results from this study are limited to one targeted concentration per CWA. Different concentrations will result in different breakthrough times. However, the impact of temperature and RH, the main objective of this study, would be as shown in this report. It is evident from the results that most carbons tested at the 3.5 cm bed depth are unable to keep the effluent at or below recommended safe vapor concentration levels. As such, a deeper bed or multiple shallower beds in series are recommended.

Breakthrough time comparisons made in this report assume that the impact of temperature, bed thickness and RH are independent. Any dependence among these parameters, if present, could not have been estimated in this study because of the lack of replicates for most of the experimental test conditions. The inherent difficulty of using CWAs in large quantities (milliliters (mL) of agent consumed per test) limits a more thorough research effort including sufficient replicates to identify the actual accuracy of each breakthrough test.

Impact of Study

This research provides information on the impact of temperature and RH on the performance of activated carbon beds as to capture chemical warfare agent vapors. The observed changes in breakthrough times for GB and HD at elevated temperatures and RH will provide decision makers with information for the use of these activated carbon to capture the effluent at elevated temperatures. This will facilitate their use as part of a hot air decontamination technology.

1.0 INTRODUCTION

The primary mission of the U.S. Environmental Protection Agency's (EPA's) Office of Research and Development's (ORD's) Homeland Security Research Program (HSRP) is to conduct research and develop scientific products that improve the capability of EPA to carry out its homeland security responsibilities. The known threat of a chemical agent release in a building or transportation hub is necessitating the U.S. EPA's National Homeland Security Research Center (NHSRC) to develop of a research program that evaluates potential decontamination strategies. The EPA may be tasked to clean up these agents after a release in buildings. Knowledge of how effective many of the available fumigation technologies are against chemical warfare agents (CWAs) is currently being obtained by NHSRC for various fumigation methods such as (modified) hydrogen peroxide vapor [Wagner et al., 2007, EPA 2010], chlorine dioxide vapor [EPA 2009, EPA 2011], and hot (humid) air. Hot air has been assessed for the gaseous decontamination of sarin (GB), VX, sulfur mustard (HD), and thickened soman (TGD) as a less complicated alternative to, for example, (modified) hydrogen peroxide vapor or chlorine dioxide vapor. The effluent during hot air fumigation is likely to contain CWA (and/or by-product) vapors well above the airborne exposure limit. These vapors therefore need to be captured before release of the CWA-loaded hot air to the exterior. Such capture is expected to occur from air flows at elevated temperatures and humidity because of the nature of the decontamination system. The elevated temperatures and relative humidity may affect the ability of carbon in the air filtration system to capture the CWA (or CWA decontamination by-products or decomposition products). The measurement of desorption of the CWA from the activated carbon would indicate whether off-gassing from activated carbon air filters is a potential concern when these filters are removed from service.

There are limitations on the highest temperatures that could be used during hot air decontamination. Aside from the technical difficulties associated with reaching high temperatures inside a building due to energy losses to the outside, high temperatures above approximately 60 ºC are known to be detrimental to electrical wiring insulation. Hot air decontamination is therefore considered to be limited to this maximum temperature if used in an occupied building that is expected to be reused without retrofitting the electrical wiring.

1.1 Project Objective

The objective of this project was to determine the impact of temperature and relative humidity (RH) on the dynamic adsorption and desorption performance of activated carbon beds by measurement of the breakthrough and desorption curves of the activated carbon beds at ambient and elevated temperatures to assess the capability of carbon filters in heating, ventilation, and air conditioning (HVAC) applications to capture the CWAs under ambient and elevated temperature conditions. Adsorption characteristics of carbons against chemicals are in most cases measured at room temperature. Less information is available on the impact of temperature and RH, especially for the targeted CWAs.

1.2 Test Facility Description

All testing was performed at the Battelle's Hazardous Materials Research Center (HMRC) located on the Battelle site in West Jefferson, Ohio. Battelle is certified to work with chemical surety materials through its contract with the Defense Threat Reduction Agency (contract number: W81XWH-11-D-0002).

2.0 TECHNICAL APPROACH

2.1 Activated Carbon Products

Four different carbon types/sizes were selected for testing. Properties of these activated carbons are summarized in Table 1. The coarser (lower mesh size numbers) carbons are frequently used in HVAC units or in negative air machines if outfitted with carbon "vapor" filters. The finer (higher mesh size numbers) carbons can be found in e.g., responder masks designed to protect against various toxic industrial chemicals (TICs) and CWAs. In principle, finer carbons provide better protection against TICs or CWAs due to their greater adsorption capacity. However, the flow resistance (measured as the pressure drop across such carbon) would also be higher. Therefore, the finer carbons are not always desirable for standard use in common building HVAC systems due to the higher energy consumption to run such systems. Nevertheless, the finer ASZM-TEDA (12 × 30 mesh) carbon is known to be used in HVAC systems of buildings of high economic, political or historic relevance.

Table 1. Relevant properties of selected carbons.

Carbon	Manufacturer , Location	Type	Mesh Size	Impregnated	Bulk Density (g/mL)
ASZM-TEDA	Calgon Carbon Pittsburgh, PA, USA	Coal	6 × 16 12 × 30	Yes[a]	0.6-0.7
IONEX 03-001	IONEX Research Lafayette, CO, USA	Coconut	8 × 16	No	0.4-0.6
Vapure™ 612	Cabot Norit Act. Carbon Marshall, TX, USA	Coal	6 × 12	No	0.51

[a] Impregnated with copper, silver, zinc, molybdenum and triethylenediamine (TEDA).

The IONEX 03-001 carbon is an activated coconut shell-based activated carbon. This type of carbon usually has greater adsorption capacity than a coal-based (activated) carbon (such as ASZM-TEDA and Vapure 612) because the coconut shell-based carbons typically have more micropores per unit mass and greater surface area. Also, a carbon with a smaller particle size (higher mesh numbers) means better dynamic adsorption performance due to a higher mass transfer rate. Therefore, better adsorption performance is expected for the ASZM-TEDA (12 ×

30 mesh) relative to the other ASZM-TEDA (6 × 16 mesh), IONEX 03-001 (8 × 16 mesh) or Vapure 612 carbon (6 ×12 mesh) carbons.

2.2 Testing Apparatus

The test system, as illustrated schematically in Figure 1, consisted of a temperature (T) - controlled chamber, challenge vapor generator, and upstream and downstream sampling ports.

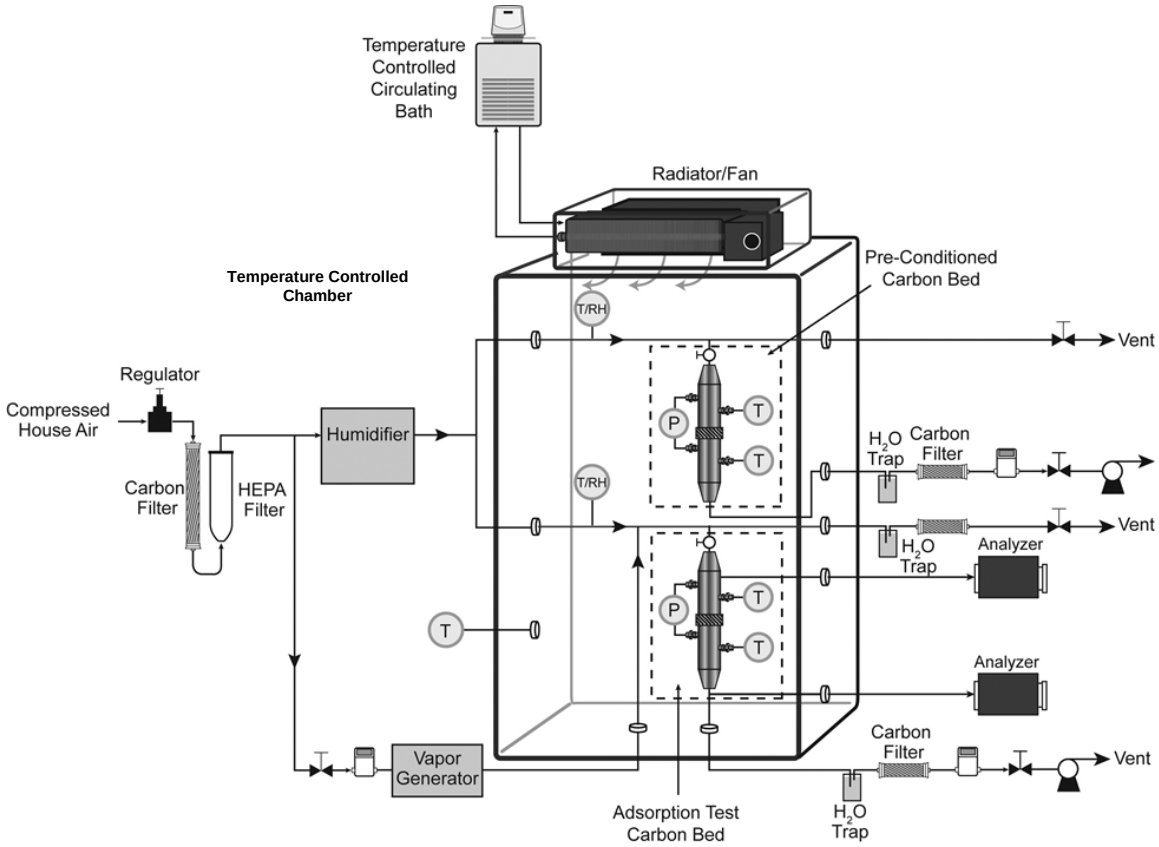

Figure 1. Schematic of the test system used for carbon performance evaluation.

The temperature-controlled chamber housed the carbon bed holders. The chamber was constructed of Lucite® material and had a radiator (Model K84, Beacon Morris, Westfield, MA, USA) mounted to the top that was used to heat or cool the air within the chamber. The radiator was equipped with a blower to circulate air from within the chamber through the radiator. A temperature-controlled water bath (NESLAB RTE 740, Thermo Scientific, Waltham, MA, USA) was used to circulate the heat transfer fluid through the radiator continuously. RH in the

challenge air stream was controlled at the target values, while the RH in the temperature-controlled chamber was not controlled.

2.2.1 Air Flow Handling

Trace amounts of vapor and particulate impurities might exist in the house air supply. Therefore, prior to humidification, the house air was filtered using a carbon filter and a high-efficiency particulate air (HEPA) filter, with the carbon filter removing vapor phase impurities and the HEPA filter removing 99.97 % of particulate impurities. As shown in Figure 1, the challenge vapor produced by the vapor generator was diluted with the humidified, scrubbed house air to obtain the desired challenge vapor concentration and RH prior to entering the temperature-controlled chamber. A Nafion® tube (Perma Pure, Toms River, NJ, USA) was used to add humidity to the challenge atmosphere. The clean air stream was then split into two streams. One stream was passed through the humidifier, and the second remained dry. Needle valves were used to control the flow rates of dry and humidified air. The flow rates were measured using calibrated mass flow meters (MFMs). The ratio of dry to humidified dilution air was adjusted to obtain the target relative humidity. The flow through the carbon bed was set to 9 liters per minute (Lpm). This flow was derived from a 12.0 centimeters/second (cm/s) face velocity through a 4-cm diameter carbon bed. Such flow conditions yield a 0.2 to 0.3 s contact time between the chemical contaminant and the carbon using 2.5 to 3.5 cm bed depths.

2.2.2 Temperature and Relative Humidity

The temperature and RH of the challenge gas were measured before addition of the challenge GB or HD using a T/RH probe at the location shown in Figure 1. The temperature of the challenge gas was also measured after addition of the challenge gas at the indicated locations before and after the carbon bed, as shown in Figure 1. Because agent vapor may foul the RH sensor, the final RH in the challenge gas delivered to the carbon bed was calculated based on the RH-T measurement before agent addition and temperature measurement after the agent addition upstream of the carbon bed.

As shown in Figure 1, the air from the humidifier was split into two streams, referred to as the "conditioning air plenum" and the "challenge plenum". The agent vapor was introduced only into the challenge plenum. Air from the conditioning air plenum was drawn through the carbon bed during carbon bed pre-conditioning. Air was drawn from the challenge plenum during the adsorption test. A two-way valve was installed at the inlet of each carbon bed to allow the challenge concentration to be established and verified prior to challenging the carbon test bed during the adsorption test or pre-conditioning test, respectively.

Flow through the carbon bed was initially controlled by a vacuum pump with an in-line needle valve and measured using a calibrated MFM. Later tests used a calibrated mass flow controller (MFC) in line with a vacuum pump. Sampling ports upstream and downstream of the carbon bed allowed for measurement of the challenge and effluent vapor concentrations, respectively. The flow rate through the carbon bed was monitored and recorded continuously during a test. The temperature, RH and carbon bed pressure drop measurements were captured electronically by a data logger for the duration of the test.

2.2.3 Carbon Bed

The carbon bed holder, as shown in Figure 2, was fabricated with inert anodized aluminum. The inner diameter (ID) of the carbon holder was 4.0 cm, which was determined based on American Society for Testing and Materials (ASTM) D5160, *Standard Guide for Gas-Phase Adsorption Testing of Activated Carbon* (ASTM, 2008). To minimize wall effects, ASTM D5160 requires the carbon bed diameter to be at least 12 times the diameter of the largest carbon granule size. The largest carbon granule size of the three carbon types tested was 3.3 millimeters (mm) (6 mesh), which led to a minimum carbon bed diameter of 4 cm (3.3 mm times 12). Larger bed diameters would further reduce the impact of wall effects. However, the amount of carbon used in these types of studies should be limited to avoid use of significant quantities of CWA during the adsorption phase.

The carbon bed depth was initially set to 2.5 cm, which was expected to be larger than the anticipated critical bed depth. The bed depth was later increased to 3.5 cm to delay breakthrough of agent for some of the carbons tested.

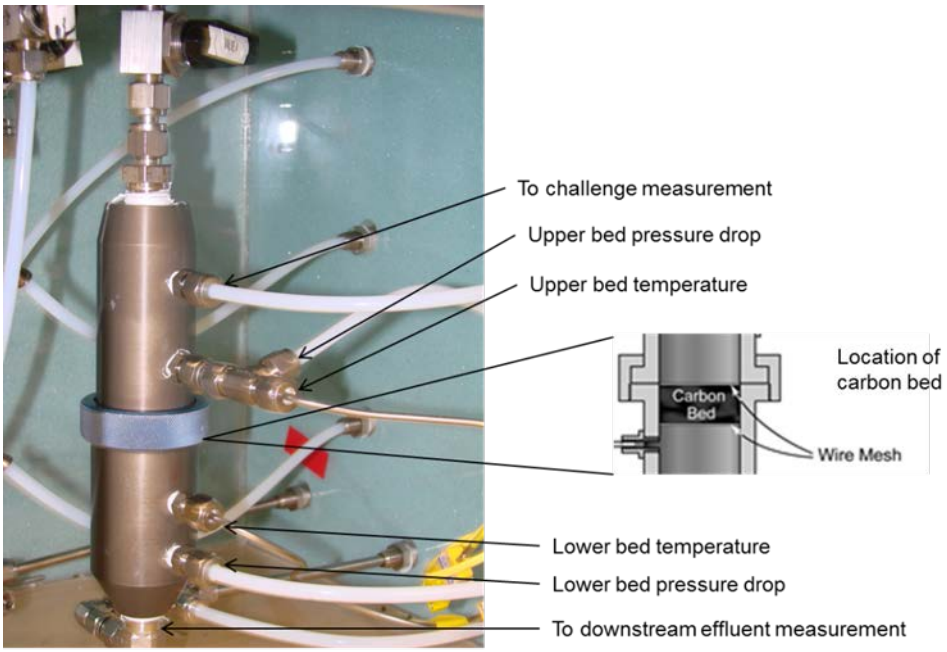

Figure 2. Photograph of the carbon bed holder.

As shown in Figure 2, the inlet of the carbon holder was tapered so that there was a gradual transition to the 4.0 cm ID. The carbon was contained between two stainless steel wire meshes. Temperature and pressure drop measurements were taken at the positions noted above and below the carbon bed. Data were recorded using HOBO pressure transducers/data loggers (Onset Computer Corp., Bourne, MA, USA). This configuration was dictated by the cell design, with only four ports available for five process measurements. The challenge sample port was located 2 cm upstream of the carbon bed. The effluent sample port was located approximately 15 cm downstream of the carbon bed holder. Both sample probes extended beyond the wall of the carbon bed holder so that the sample was collected from the center of the flow stream. The sample lines for monitoring the challenge and effluent gases were 1/8-inch (in) outer diameter (OD) Teflon lines. To minimize the potential for adsorption of agent during transport, the sampling lines were heat-traced.

2.2.4 CWA Vapor Generation

The target test challenge concentration was 1,500 milligrams/cubic meter (mg/m^3) of GB and 500 mg/m^3 HD. The GB concentration was based on a calculated (maximum) GB vapor

concentration following a hypothetical release of 1 liter of liquid GB in a 186 m^2 (2000 ft^2) (office) area. A similar HD amount released would result in a saturated vapor condition (at room temperature), so the HD concentration was set below the saturated vapor pressure (approximately 660 mg/m^3 for HD at room temperature).

Two different chemical vapor generating methods were employed to generate the CWA vapor. A sparging system (Method A) described below was used for all GB testing except for the ASZM-TEDA (12 × 30 mesh) tests while a syringe pump-based infusion system (Method B) was used for all HD testing and the aforementioned GB tests with ASZM-TEDA (12 × 30 mesh). Method A was not suitable to generate the high HD concentration at the 9 Lpm flow rate, hence the agent delivery method was switched. Since the GB and HD challenge concentrations were measured continuously, there is no impact on the effluent concentration results when comparing results obtained with either method.

2.2.4.1 Sparging System (Method A)

As illustrated in Figure 3, the GB challenge gas was generated by sparging dry filtered house air through neat liquid GB. The system consisted of a custom-built glass sparger followed by a custom-built glass droplet trap. The GB-laden air exiting the sparger was passed through the droplet trap to remove any entrained liquid. The droplet trap was filled with glass beads to provide additional surface area for a stable vapor output. Both the sparger and droplet trap were contained in a temperature-controlled circulating bath. Depending on target challenge concentrations, the water bath was operated at a predetermined temperature to generate sufficient agent vapor for subsequent dilution. The vapor stream from the generator was diluted with humidified air to meet the concentration and humidity requirements.

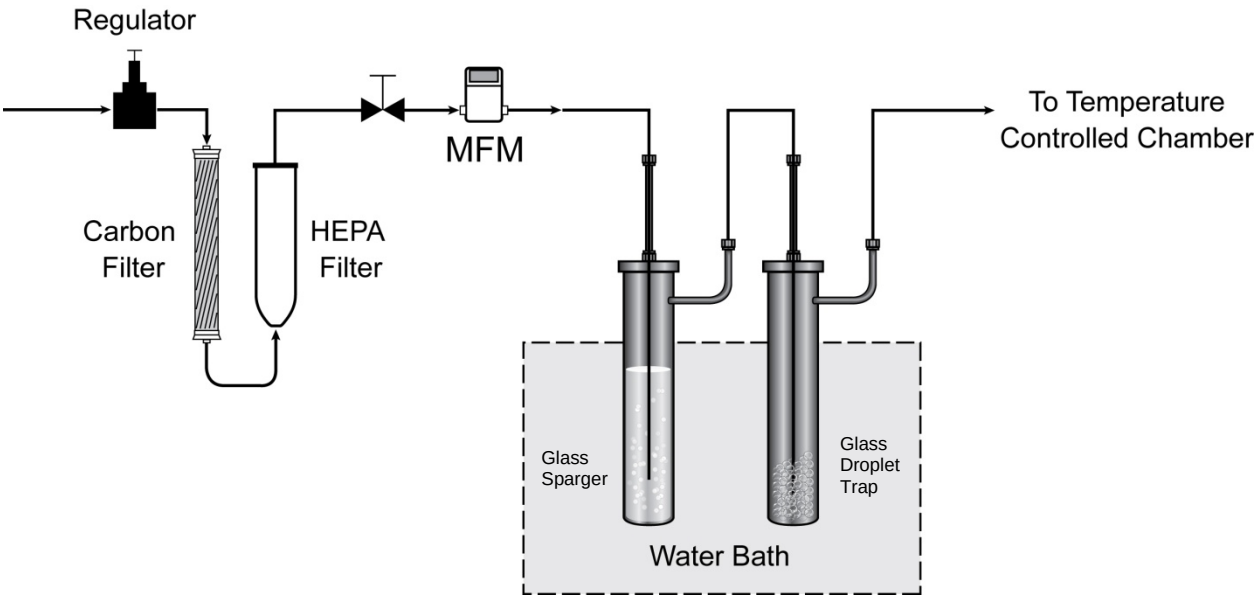

Figure 3. Schematic of vapor generation system.

2.2.4.2 Syringe Pump Vapor Infusion (Method B)

In Method B, HD and GB challenge gases were generated using a liquid infusion vapor generation method requiring a syringe pump (Pump 11 Elite, Harvard Apparatus, Holliston, MA, USA), a heated transfer line, and an air source. A schematic of the vapor infusion challenge generation system and how it interfaces to the test chamber is shown in Figure 4. In this method, the agent vapor was generated by infusing (on the order of several microliters [µL]/minute) of the CWA liquid into a heated transfer line via valve #8. The heated zone, shown as the shaded circle in Figure 4 just upstream from valve #8, consisted of stainless steel tubing wrapped in pressure sensitive heating tape and insulated with a double layer of fiberglass cloth tape. The agent vapor was directed through a three-way valve (valve #7 in Figure 4) into the challenge plenum where it was diluted with conditioned air (depending on the test condition being used) to achieve the target challenge concentration, monitored via gas chromatography (GC) with flame ionization detector (FID) on the back end of the challenge plenum prior to venting the system. Once the target challenge concentration was verified, agent vapor was directed through the test cell using valve #4.

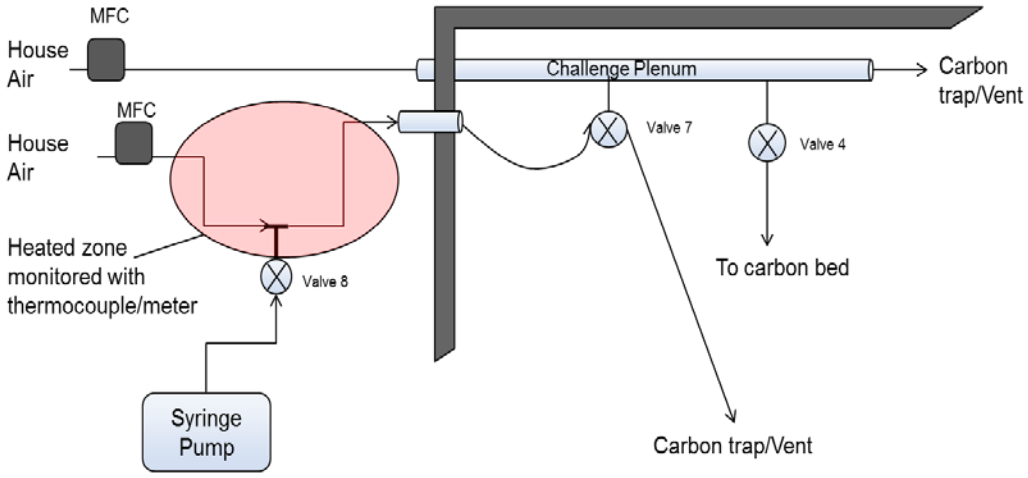

Figure 4. Schematic of the liquid infusion vapor generation system.

Photographs of the syringe pump and heated line interface are shown in Figure 5. Infusion of the CWA liquid into a heated transfer line occurred via valve #8. The temperature was controlled by setting the power supplied to the heating tape. The air temperature within the heated agent transfer line was monitored using a thermocouple inserted prior to the agent introduction point. For HD vapor generation, the temperature of the heated zone was maintained at a temperature below the boiling point (between 140 and 150 degrees Celsius [ºC]). HD begins decomposing near its boiling point of 218 ºC. For GB vapor generated using this method, the temperature was maintained at approximately 130 ºC; the boiling point for GB is 158 ºC.

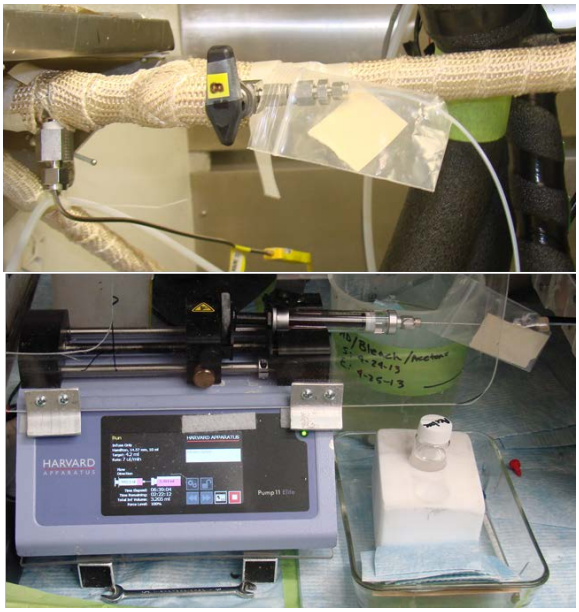

Figure 5. Photographs of the syringe pump vapor infusion apparatus: (lower) programmable syringe pump with loaded syringe, connected to a transfer line, leading to (upper) valve 8 connection to heated transfer line.

2.3 Analytical Methods

Agent vapor in the effluent stream was measured using a MINICAMS® continuous air monitor (OI Analytical, College Station, TX, USA) equipped with a sample loop injector and an FID or a flame photometric detector (FPD). The MINICAMS® is an automatic, near-real-time continuous air monitoring system using gas chromatography and sample collection with a solid-adsorbent pre-concentrator or fixed-volume sample loop. The minimum detection limit for the MINICAMS® is analyte/calibration dependent, with the minimum instrument response at a level of the short term exposure limit (STEL) (GB_{STEL}= 0.0001 mg/m^3).

The agent challenge concentration was measured using an Agilent 5890 GC equipped with an FID (Agilent Technologies, Santa Clara, CA, USA) for HD testing, a 1 milliliter (mL) sample loop, and a heated sample line. The GB challenge concentration was measured using the FPD.

During testing, samples of the challenge and carbon bed effluent were analyzed without dilution. Typical run times for the MINICAMS® and GC were approximately 6 minutes (min) and 8 min, respectively, with both instruments running continuously during the adsorption phase.

Sampling of the challenge concentration by GC was discontinued shortly after the start of desorption phase.

Prior to each test, calibration curves were generated for both the MINICAMS® and the GC using a set of standards of various concentrations. At the conclusion of a test, a one-point calibration check verification (CCV) sample was analyzed for each instrument.

2.4 Test Procedures

Tests were performed following Battelle's Standard Operating Procedure (SOP), entitled *Evaluation of the Activated Carbon Beds with Chemical Agent Vapors (Battelle HMRC SOP X-283)*, which was reviewed and approved by Battelle management and safety representatives.

2.4.1 Carbon Bed Pre-conditioning

Prior to the adsorption/desorption test, each carbon bed was loaded in the test cell as depicted in Figure 6 and placed in the chamber to pre-condition. The purpose of this step was to allow the carbon bed to achieve equilibrium under the environmental conditions (i.e., T/RH) to be used in the agent testing. Appendix A to this report describes the research efforts to determine the minimum equilibrium time based on measurement of weight changes of the carbon bed with time due to change in T and RH. The main outcome of this effort was that a 16 hour (h) equilibrium time ensures equilibrium at all T and RH conditions for all carbon beds tested.

Pre-conditioning was conducted by flowing air from a dedicated clean air source (at the target T and RH) through the carbon bed at the test flow rate overnight (i.e., >16 h).

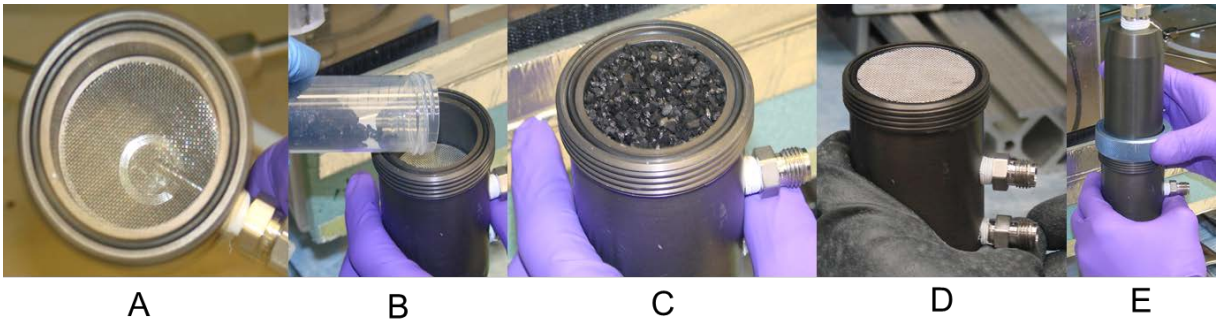

Figure 6. Loading the carbon test cell with IONEX 03-001 carbon (8 × 16 mesh): (A) mesh screen in bottom cell piece and O-ring in the well at the top of the cell, (B) pre-weighed carbon loaded into bottom cell piece, (C) cell bottom with level and packed loaded carbon, (D) mesh screen on top of carbon bed, and (E) top cell piece screwed on using locking ring.

2.4.2 Adsorption and Desorption Testing

After the pre-conditioning phase, the test cell was connected to the agent challenge air source, and the pre-test agent delivery system (Method A or B) was started to ensure that the target challenge concentration was achieved. A photograph of the typical test chamber starting configuration is shown in Figure 7.

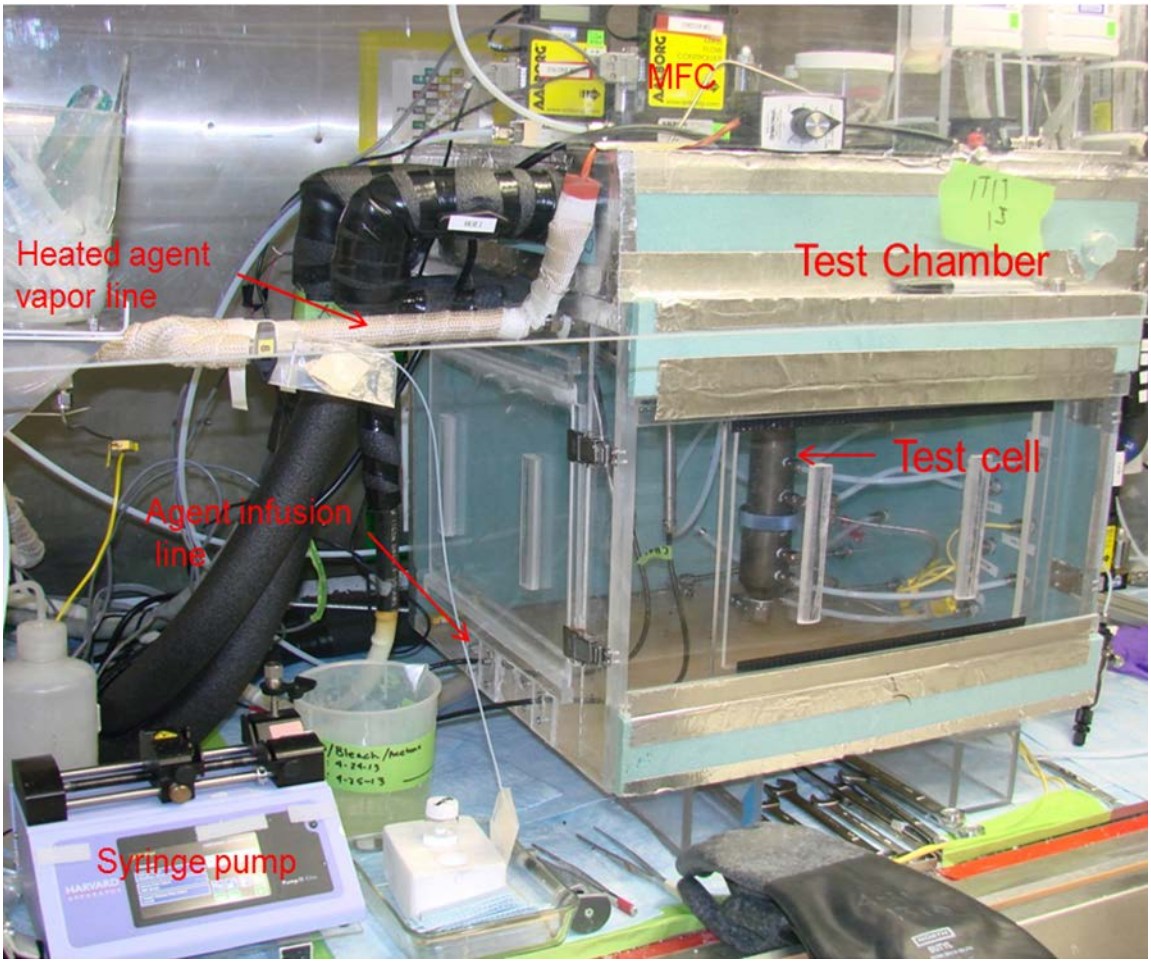

Figure 7. Typical test chamber configuration for carbon bed adsorption and desorption testing.

The challenge concentration, flow rate, and temperature were established and recorded prior to initiating a test. After target conditions were established, challenge flow was introduced to the carbon bed, which defined the start of the test: t = 0 min. All recorded test event times were relative to time t = 0 min. Challenge and carbon bed effluent measurements were made every eight and six minutes, respectively.

An adsorption test proceeded until target breakthrough concentration of the designated chemical agent was reached. At this point, desorption test was started by turning off the agent vapor supply (via Method A or B) while temperature and air flow (no agent) through the carbon bed remained the same as during the adsorption test. The subsequent desorption of chemical agent from the activated carbon bed continued to be monitored until steady state in the agent

effluent concentration was reached. If a steady state had not been achieved within 12 h (or overnight) after the agent vapor challenge ceased, desorption test was stopped.

2.5 Test Matrix

The complete test matrix is presented in Table 2. For each carbon, described in Section 2.1, tests consisted of a reference adsorption / desorption test at 25 ºC and low (< 15 % RH) humidity, a high temperature (55 ºC) and low humidity test, and a high temperature (55 ºC) and high humidity (50 % RH) test. Occasional replicates were included to assess reproducibility of adsorption and desorption results. The inherent difficulty of using CWAs in large quantities (milliliters of agent consumed per test) prevents a more thorough research effort with statistically sufficiently numbers of replicates per test point.

The initial carbon bed depth for all studies was set at 2.5 cm to keep the amount of carbon as low as possible. Results from the first ASZM-TEDA (6 × 16 mesh) were interpreted as signifying that the critical minimum bed depth had not been reached, hence larger bed depths were tested. After two increases in carbon bed depth, a second carbon, IONEX 03-001 (8 × 16 mesh) was tested. All further GB testing was conducted at the thicker 3.5 cm carbon bed depth. A similar approach was used for testing with HD. For HD, no immediate breakthrough occurred for the 2.5 cm carbon bed depth, and the depth was not modified.

Table 2. Complete test matrix.

Carbon Bed	Chemical Agent	Carbon Bed Depth (cm)	Temperature (°C)	RH (%)	Number of Tests
ASZM-TEDA (6 × 16 mesh)	GB	2.5	25 ± 2	Dry (i.e., <15 %)	1
		3.0			1
		3.5			2[a]
IONEX 03-001 (8 × 16 mesh)	GB	3.5	25 ± 2	Dry (i.e., <15 %)	2
			55 ± 2		2
Vapure 612 (6 × 12 mesh)	GB	3.5	25 ± 2	Dry (i.e., <15 %)	2
			55 ± 2		2
ASZM-TEDA (12 × 30 mesh)	GB	2.5	25 ± 2	Dry (i.e., <10 %)	1
			55 ± 2		1
IONEX 03-001 (8 × 16 mesh)	HD	2.5	25 ± 2	Dry (i.e., <10 %)	1
			55 ± 2	Dry (i.e., <10 %)	1
			55 ± 2	Humid (50 ± 10 %)	1
ASZM-TEDA (12 × 30 mesh)	HD	2.5	25 ± 2	Dry (i.e., <10 %)	1
			55 ± 2	Dry (i.e., <10 %)	1
			55 ± 2	Humid (20 ± 10 %)[b]	1
ASZM-TEDA (6 × 16 mesh)	HD	2.5	25 ± 2	Dry (i.e., <10 %)	1

[a] Includes one incomplete test that was truncated due to significant baseline drifting of the MINICAMS®/FID.
[b] For the ASZM-TEDA (12 × 30 mesh) hot/humid test with HD vapor, the target % RH was lowered to 20 % due to condensation observed in the MINICAMS® sampling MFC during the previous testing of IONEX 03-001 carbon under those test conditions.

3.0 QUALITY ASSURANCE AND QUALITY CONTROL

3.1 Data Quality Objectives and Results

The quantitative assessment of the breakthrough curve and the subsequent desorption curve at a given temperature and relative humidity is affected by uncertainty in measurements of challenge and effluent GB and HD concentrations, flow rate through the carbon bed, carbon amount loaded into the carbon bed, and temperature and relative humidity of the system. The uncertainty is defined as relative percentage of difference (%RPD) from the standards. The critical data quality objectives, data quality indicators, and results for these measurements are summarized in Table 3.

GB or HD concentrations in the effluent air stream were measured using the MINICAMS®/FID or the MINICAMS®/FPD. The challenge GB and HD concentrations were measured using GC/FPD and GC/FID, respectively. Prior to or after each test, calibration curves were generated for both the MINICAMS® and GC using a set of standards of various concentrations. At the beginning and the conclusion of a test, a one-point calibration check was performed for each analytical method. The MINICAMS® operational parameters for detection of GB and HD are presented in Appendix B.

As summarized in Table 3, quality control (QC) requirements were met for the measurements of carbon bed weight, flow rate through the carbon bed, temperature, RH, and pressure drop across the carbon bed. For GB challenge concentration measurements, all tests met the QC requirement in pre-test one-point calibration checks (acceptance criterion is RPD ± 25 %). The QC requirement (±25 %) was also met in post-test one-point calibration checks for all tests except one test that showed an RPD of ±30 %. The post-test lower response of this CCV may suggest that the actual challenge concentration may have been 5 % higher than recorded. The breakthrough curve (correction) would therefore have shifted to longer times. This correction is relatively minimal, and its impact is therefore considered to be minimal.

Five tests used the MINICAMS®/FID to measure effluent GB concentration, which included all four tests with the ASZM-TEDA (6 × 16 mesh) carbon, and Run 1 of the IONEX 03-001 carbon test at 25 ºC/dry conditions. For these tests, the QC requirement was met in all pre-test one-point calibration checks. The QC requirement was also met in the post-test one-point calibration checks for two of the five tests. The post-test one-point calibration check was

not conducted with the other three tests due to significant baseline drifting of the MINICAMS®/FID. The impact of these missed checks is relatively low since the data presented are limited to the adsorption phase of the experiment.

Nine tests used the MINICAMS®/FPD to measure effluent GB concentration, which included four tests with the Vapure 612 carbon, three tests with the IONEX 03-001 carbon, and two tests with the ASZM-TEDA (12 × 30 mesh) carbon. QC requirements were met for most of these tests. Two exceptions were: (a) Run 2 with the IONEX 03-001 carbon at 55 ºC/dry conditions, where the RPDs were 44 and 54 % in the pre-test and post-test one-point calibration checks, respectively; and (b) Run 2 with the IONEX 03-001 carbon at 25 ºC/dry conditions, where the pre-test one-point calibration check was not conducted. Results from Run 2 with the IONEX 03-001 carbon at 55 ºC/dry conditions were also confounded by residual GB in the effluent sample line. Results from this Run 2 are presented in Section 4.3.2. However, further interpretation of the IONEX 03-001 carbon at 55 ºC/dry conditions is limited to data observed for Run 1. The impact of the RPD values exceeding 25 % is negligible. The impact of the missing pre-test one-point calibration check for Run 2 with the IONEX 03-001 carbon at 25 ºC/dry conditions on the data quality is also considered to be minimal. The RPD value for the post-test one-point calibration check was reported well within the ±25% range (actual 1 % deviation from expected). The impact of the missed pre-test calibration check is deemed minimal.

All seven tests used the MINICAMS®/FID to measure effluent HD concentration. For these tests, the QC requirement was met in all pre-test one-point calibration checks. The QC requirement was also met in the post-test one-point calibration checks for all HD tests but one. The post-test one-point calibration check for the 55 ºC/humid IONEX 03-001 test was not conducted due to sampling flow failure (condensation in lines). This failure is discussed in Section 4.5.1. Solid sorbent tubes (SSTs) were obtained at the conclusion of the challenge period to determine the effluent concentration.

Table 3. Critical data quality objectives and results.

Parameter	Measurement Method	QC Requirement			Result
		Data Quality Indicator	Acceptable Uncertainty (% RPD)	Frequency of Calibration Check	
Challenge Concentration (mg/m^3)	GC-FPD[(a)] (Agilent 5890)	One-point calibration checks must agree within ±25 % RPD[(d)]	±25 %	Full calibration at the beginning of testing campaign, daily one-point calibration check and a one-point check at the conclusion of the test. Recalibrations made as needed, indicated by one point calibration checks.	• Full calibration before each GB test • GB pre-test one-point check: met QC requirement. • GB post-test one-point check: o RPD ≤ ±30 % for Run 2 with the IONEX 03-001 carbon at 25 °C/dry • All other GB tests met QC requirement
Challenge Concentration (mg/m^3)	GC-FID (Agilent 5890)				• Full calibration prior to HD testing • HD pre-test one-point check: met QC requirement. • HD post-test one-point check: met QC requirement
Effluent Concentration (mg/m^3)	MINICAMS®/FID[(b)] (OI Analytical)				• Full calibration prior to GB and HD testing • GB and HD pre-test one-point check: met QC requirement. • GB and HD post-test one-point check: o Two GB tests met QC requirement: ASZM-TEDA (6 × 16 mesh) carbon with 2.5 cm bed and Run 1 of the IONEX 03-001 carbon at 25 °C/dry o Not conducted for other (3) GB tests due to significant baseline drift o All other GB tests and all HD met QC requirement
Effluent Concentration (mg/m^3)	MINICAMS®/FPD[(c)] (OI Analytical)				• Full calibration prior to GB testing o Pre-test one-point check: Not conducted for Run 2 with the IONEX 03-001 carbon at 25 °C/dry o RPD ≤ ±44 % for Run 2 with the IONEX 03-001 carbon at 55 °C/dry o All other tests met QC requirement • Post-test one-point check: o RPD ≤ ±54 % for Run 2 with the IONEX 03-001 carbon at 55 °C/dry o All other tests met QC requirement
Carbon Bed Weight (g)	Microbalance	Check balance used with standard weight set, agree within ±5 %	±2 %	Semiannually and beginning of testing	• Met QC requirement

Parameter	Measurement Method	QC Requirement			Result
		Data Quality Indicator	Acceptable Uncertainty (% RPD)	Frequency of Calibration Check	
Flow Rate through Carbon Bed (liters per minute, Lpm)	Mass flow controller	Compare against standard dry gas meter reading, must agree within ±5 % of reading	±5 %	Annually and beginning of testing	• Met QC requirement
T (ºC)	Thermocouple	Compare against calibrated thermometer before evaluation testing, must agree within ±2 ºC	±2°C		• Met QC requirement
RH (%)	T/H Probe	Compare against calibrated hygrometer before evaluation testing, must agree within ±10 % of reading, or ±5 % RH, whichever is larger	±5 %		• Met QC requirement
Carbon Bed ΔP (in of H_2O)	Pressure Transducer	Compare against NIST*-traceable calibrated gauge before evaluation testing, must agree within ±10 % of reading	±10 %		• Met QC requirement

[a] Revised from the original GC/FID, as documented in Test/QA Plan Amendment 2.
[b] The MINICAMS®/FID was used to measure effluent concentration for the following tests: GB: all ASZM-TEDA (6 × 16 mesh) carbon tests, Run 1 of the IONEX carbon at 25 ºC /dry conditions; HD: all tests
[c] The MINICAMS®/FPD was used to measure effluent concentration for GB tests, including: all Vapure 612 carbon tests, IONEX 03-001 carbon tests at 55 ºC /dry, Run 2 of the IONEX 03-001 carbon at 25 ºC/dry, and both ASZM-TEDA (12 × 30 mesh).
[d] Revised the original ±15 % RPD, as documented in Test/QA Plan Amendment 2.
*National Institute of Standards and Technology

3.2 Equipment Calibrations

The instrumentation used for the analyses is identified in Section 2.3. The required analytical equipment was maintained and operated according to the quality requirements and documentation of the HMRC. The GC and MINICAMS® systems used for measurement of the agent challenge concentration and effluent stream concentration, respectively, were either calibrated at the beginning of each test condition (multipoint calibration curve) or calibration was verified with a single pre-test standard. Breakthrough tests were concluded with a single post-test check point for each system except as noted in Table 3.

The GC was maintained in calibration such that that the coefficient of determination (r^2) from the linear regression analysis of the calibration curve was more than 0.98. GC calibration curves (3-4 calibration points) were generated around the nominal 1500 and 500 mg/m^3 challenge concentrations for GB and HD, respectively.

The MINICAMS® was calibrated initially at the start of a testing period for a specific chemical agent (GB or HD) and then recalibrated as needed based on the response to the CCV standard prior to each test. MINICAMS® calibration curves (4-8 calibration points) were generated depending on anticipated effluent agent concentrations.

3.3 Technical System Audit

The QA Manager performed two technical systems audits (TSAs) during the performance of the adsorption/desorption testing. The purpose of the TSA was to ensure that testing was performed in accordance with the test/QA plan and applicable SOPs. In the audit, the QA Manager reviewed the sampling and analysis methods used, compared actual test procedures to those specified in the test/QA plan, and reviewed data acquisition and handling procedures. Both audits observed testing of the carbon bed system with GB. Several items were noted during the audit and corrected before additional work was performed.

3.4 Data Quality Audit

For this work, the QA Manager audited at least 10 % of the investigation data and traced the data from initial acquisition, through reduction and statistical comparisons, to final reporting. All data analysis calculations were checked.

4.0 TEST RESULTS

4.1 Equilibrium Time

Prior to the chemical agent adsorption/desorption testing, each carbon bed was preconditioned to achieve equilibrium at the environmental conditions (i.e., temperature and RH) to be used in the agent testing. The preconditioning was conducted by flowing air (at the target temperature and relative humidity) through the carbon bed until water vapor adsorption equilibrium is achieved. To determine the time required to achieve water vapor adsorption equilibrium, a set of equilibrium tests was conducted for all carbon beds at three test conditions of 55 ± 2 °C and 50 ± 5 % RH, 55 ± 2 °C and dry (<15 % RH) and 25 ± 2 °C and dry. Those results are presented in Appendix A.

4.2 Preliminary Testing with GB Surrogate

Before the test matrix in Table 2 was implemented, preliminary testing was conducted to ensure system safety and operation. A safety dry run (no carbon present) was conducted with dimethyl methylphosphonate (DMMP) at an average challenge concentration of 1,570 mg/m^3. Immediate DMMP breakthrough was detected in the test. To ensure that the immediate DMMP breakthrough was not due to any bias with the test system, a test was conducted with a carbon (ASZM-TEDA 12 × 30 mesh) that was expected to have a longer breakthrough time due to much smaller particle size. No breakthrough of DMMP was detected during the 70 min exposure at a challenge concentration of 1,220 mg/m^3. The result verified that the test system was functional.

4.3 Results for GB

In initial GB tests, the effluent concentrations were measured by the MINICAMS®/FID. After several tests, the MINICAMS®/FID baseline started drifting off scale, especially during overnight desorption. The effluent concentration measurement was then switched to the MINICAMS®/FPD. No baseline drift was observed with the MINICAMS®/FPD, indicating that

whatever in the carbon bed effluent that had interfered with the FID baseline did not affect FPD analysis.

4.3.1 ASZM-TEDA (6 × 16 Mesh) Carbon Tests

Four GB tests were conducted with ASZM-TEDA carbon at 25 °C/dry conditions and a target challenge concentration of 1,500 mg/m^3. Immediate breakthrough was measured with a 2.5 cm depth ASZM-TEDA (6 × 16 mesh) carbon bed at target challenge of 1,500 mg/m^3 and 25 °C/dry conditions. This result implied that the critical bed depth at the test conditions was deeper than the anticipated 2.5 cm bed depth. The bed depth was enhanced to 3.0 cm and finally 3.5 cm to generate data meaningful to the project.

The GB challenge concentrations measured in the four tests are presented in Appendix C (Figures C-1 to C-4). Steady challenge concentrations were achieved in the tests, with standard deviations less than 10 % of the averages. The flow rate, temperature, and RH recorded during the tests were plotted versus time, and the plots are presented in Appendix C. As demonstrated in the plots (Figures C-1 to C-4), the flow rate, temperature, and RH were steady throughout the adsorption/desorption tests of the ASZM-TEDA carbon. Pressure drop across the carbon bed was not recorded during these tests because the pressure transducer was not operating properly. The lack of pressure measurement does not have a direct impact on the measurements of the breakthrough and desorption curves.

The measured breakthrough and desorption curves at different bed depths are presented in Figure 8. The adsorption time plotted in Figure 8 was normalized to the target challenge concentration of 1,500 mg/m^3, so that the breakthrough curve from each individual test could be compared directly, even if there were small (< ± 20 %) variations in the average challenge concentrations among the tests. For example, if the measured average challenge concentration for a test was 1,350 mg/m^3, the target was 1,500 mg/m^3, and the actual adsorption time was t (min), then the normalized (plotted) adsorption time would be t (min) × 1,350 mg/m^3/1,500 mg/m^3 = 0.9 × t (min). The effluent concentrations presented in Figure 8 were measured by the MINICAMS®/FID. Two tests were conducted at a 3.5 cm bed depth. The first run was stopped at 78 min into adsorption, due to significant baseline drifting of the MINICAMS®/FID (data not shown).

As expected, the breakthrough time increased greatly with the breakthrough curve shifted to the right (i.e., longer times) as bed depth increased from 2.5 to 3.0 cm. Further increased bed depth to 3.5 cm, however, did not shift the breakthrough curve, with the breakthrough curves of the 3.5 cm beds overlapping with the breakthrough curves of the 3.0 cm bed. Overlapping breakthrough curves were not expected because the 17 % extra carbon in the 3.5 cm bed should generate longer breakthrough times. The test system and the recorded testing parameters, including flow rate, temperature, RH, and challenge/effluent concentrations, were checked, and no problems were identified. The reason for the unexpected behavior remains unknown.

Desorption of GB was observed after the challenge GB was ceased, and clean air was introduced through the carbon beds at the flow rate and T/RH conditions equivalent to the adsorption test. As shown in Figure 8, the desorption concentrations initially decreased quickly, reaching approximately 10 to 16 % of the peak concentration (i.e., the final breakthrough concentration before switching to desorption) within the first 30 min. The desorption concentration then decreased gradually and finally leveled off (with a slightly decreasing trend). The leveled off values appeared to be increasing with increased GB loading (or exposure period) during adsorption, with leveled off values of 0.5, 0.7, and 3 mg/m^3 measured, respectively, for the tests with 2.5, 3.5, and 3.0 cm carbon beds that had been exposed to GB for 60, 153, 196 min, respectively.

The desorption process persisted at a concentration three to four orders of magnitude higher than the STEL of GB (i.e., 0.0001 mg/m^3 for GB) for hours. For example, after 9 h of desorption, the effluent concentration was still at a level of approximately 3 mg/m^3 for the test with the 3.0 cm carbon bed.

Only small quantities of adsorbed GB, however, were desorbed. For example, for the test with the 3.0 cm carbon bed, the amount of GB adsorbed was estimated to be 2.6 grams (g), based on measured challenge and breakthrough curves, flow rate, and adsorption period (196 min). The amount of GB desorbed after 5.5 h of desorption was estimated to be 0.016 g, based on desorption curves and flow rate. Therefore, only 0.6 % of adsorbed GB was desorbed in the 5.5 h desorption.

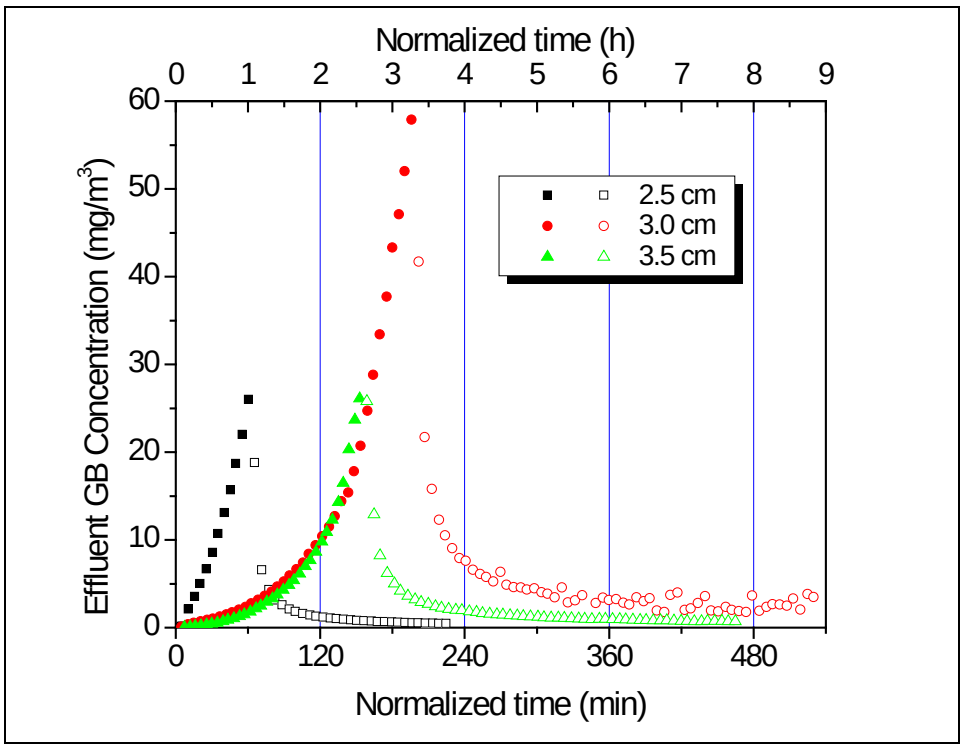

Figure 8. Breakthrough and desorption curves at 25 °C/dry and varying bed depth for ASZM-TEDA (6 × 16 mesh) carbon. Desorption phase starts at the transition from solid to open symbols.

4.3.2 IONEX 03-001 (8 × 16 Mesh) Carbon Tests

All four tests with the IONEX 03-001 carbon were conducted with bed depth of 3.5 cm. Duplicate tests were conducted at 25 °C/dry and 55 °C/dry conditions and target challenge concentration of 1,500 mg/m^3. The GB challenge concentrations measured in the tests are presented in Appendix C (Figures C-5 to C-10). As shown in Appendix C, steady challenge concentrations were achieved for two tests, Run 2 at 25 °C/dry (Figure C-6) and Run 1 at 55 °C/dry (Figure C-7). For these two tests, the standard deviations of the challenge were less than 10 % of the averages. For the first run at 25°C/dry, as shown in Figure C-5, the challenge concentration began to decrease at 240 min as the GB source in the vapor generator was depleted, and the concentration reduced to 150 mg/m^3 at 330 min. Airflow through the carbon bed was stopped and the test restarted the next morning with a replenished vapor generator. During the second run at 55 °C/dry, as shown in Figure C-8, significant variation in the challenge concentration was observed, with the standard deviation over 40 % of the average.

As demonstrated in Figures C-5 to C-10, the flow rate, temperature, and RH were steady throughout the adsorption/desorption tests of the IONEX 03-001 carbon. Pressure drop across the carbon bed was not recorded during the two tests at 25 °C/dry conditions because the pressure transducer was not operating properly. As shown in Figures C-8 and C-10, the pressure drop was stable during the tests at 55 °C/dry conditions, with average pressure drop of 0.23 inches of water and standard deviation less than 1.5 % of the average.

The measured breakthrough and desorption curves for the IONEX 03-001 carbon at 25 ºC/dry conditions are presented in Figure 9. The effluent GB concentration was measured by the MINICAMS®/FID for the first run and by the MINICAMS®/FPD for the second run. The breakthrough curve of Run 1 shifted to the right, most likely due to suspending of the adsorption test overnight. Results from Run 1 were therefore not considered to be representative of a single, continuous, adsorption GB test. Only the results from Run 2 at the 25 °C/dry conditions were used for further comparison. Note that the initial breakthrough after approximately 180 min occurred for both runs.

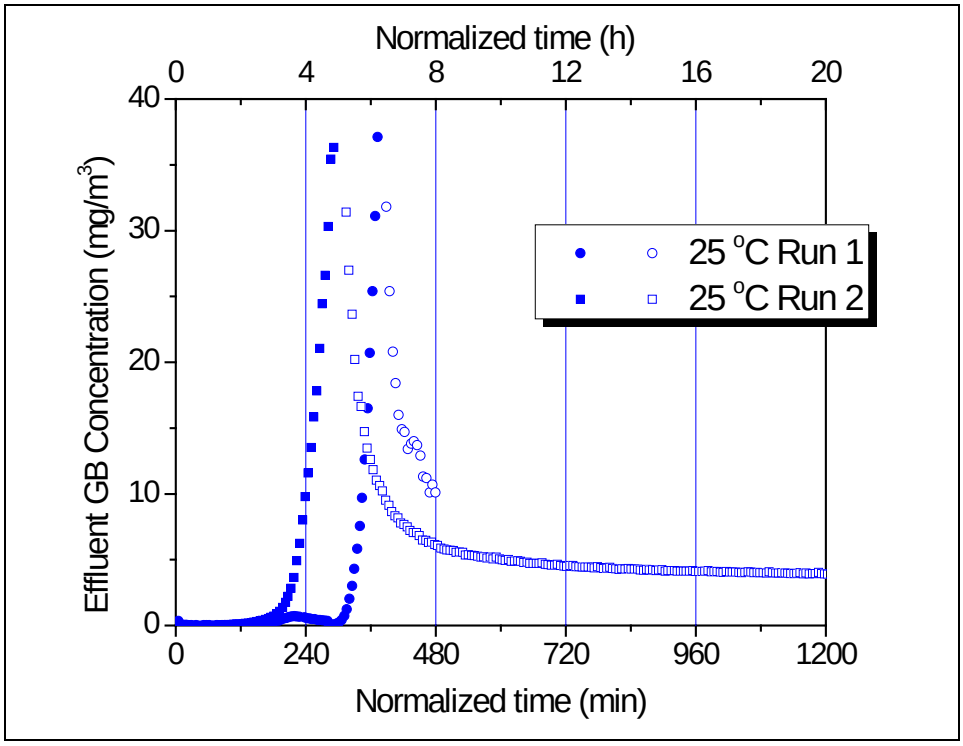

Figure 9. Breakthrough and desorption curves of the IONEX 03-001 carbon at 25 °C/dry. Desorption phase starts at the transition from solid to open symbols.

The IONEX 03-001 (8 × 16 mesh) carbon demonstrated significantly better adsorption performance than the ASZM-TEDA (6 × 16 mesh) carbon. For example, as measured in the Run 2 at 25 °C/dry conditions, the effluent GB concentration held at <0.04 mg/m^3 until t = 80 min while for the ASZM-TEDA (6 × 16 mesh) carbon the effluent concentration reached 0.04 mg/m^3 after only 10 min into the adsorption test.

Similar to the results observed in the ASZM-TEDA tests, a quick reduction in desorption concentration occurred in the initial stage of desorption. The desorption concentration then leveled off (with a slightly decreasing trend), with a desorption concentration of approximately 4 mg/m^3 after desorption for over ten hours.

Figure 10 presents the breakthrough and desorption curves for IONEX 03-001 carbon at 55 °C/dry conditions. As shown in Figure 10, for Run 2, the measured effluent concentration reduced constantly during the first 250 min of adsorption, with concentration reduced from approximately 1.0 to 0.02 mg/m^3. The effluent GB concentration measured during the period was believed to be artificial and due to residual GB in the downstream pipelines. Prior to this test, the system was tested with a shallow carbon bed at 55 °C/50 % RH to investigate the potential formation of HF, and some GB may have remained in the downstream pipeline after the test. Results from this duplicate run were considered to be biased and were not used in the comparison with other GB IONEX adsorption data.

At 55 °C/dry conditions, the IONEX 03-001 carbon demonstrated good adsorption performance. For example, during Run 1, the effluent GB concentration remained at <0.04 mg/m^3 for the first 170 min. The effluent concentration then increased slowly to 0.8 mg/m^3 at 340 min when the adsorption test was stopped.

Different from desorption at 25 °C/dry, the desorption concentration increased slowly and constantly during the desorption test, with the concentration increased from 0.8 mg/m^3 at the startup of desorption to 1.4 mg/m^3 after 10 hours of desorption (Run 1).

Similar to the tests with the ASZM-TEDA carbon, only a small quantity of the adsorbed GB was desorbed. For example, only 1 % and 0.1 % of the adsorbed GB was estimated to be desorbed over ten h of desorption for the tests at 25 °C/dry (Run 2) and 55 °C/dry (Run 1) conditions, respectively.

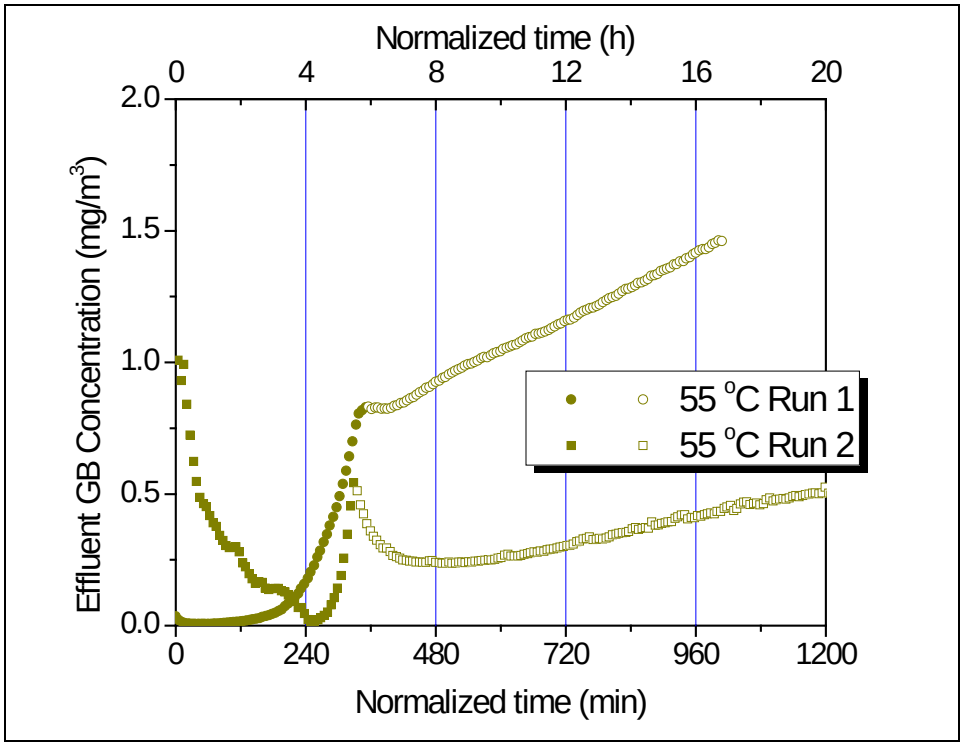

Figure 10. Breakthrough and desorption curves of the IONEX 03-001 carbon at 55 °C/dry. Desorption phase starts at the transition from solid to open symbols.

The performance of the IONEX 03-001 carbon at 25 °C/dry (Run 2 only) and 55 °C/dry (Run 1 only) is compared in Figure 11. Significantly better adsorption performance was demonstrated for the carbon bed tested at 55 °C/dry. The observation contradicts the expectation, because for physisorption like GB, the adsorption capacity is expected to reduce with increasing temperature. One factor that might contribute to the result is that the carbon beds were pre-conditioned overnight at 25 °C/dry or 55°C/dry prior to testing. Prolonged pre-conditioning (>16 h) at 55 °C/dry might desorb more contaminants or water vapor from the carbon pores which enhances the carbon adsorption capacity. According to the carbon bed water equilibrium tests conducted (see Appendix A), the carbon bed lost approximately 4 % of the weight at 55 °C/dry versus 3 % of the weight at 25 °C/dry when pre-conditioned for 3 h.

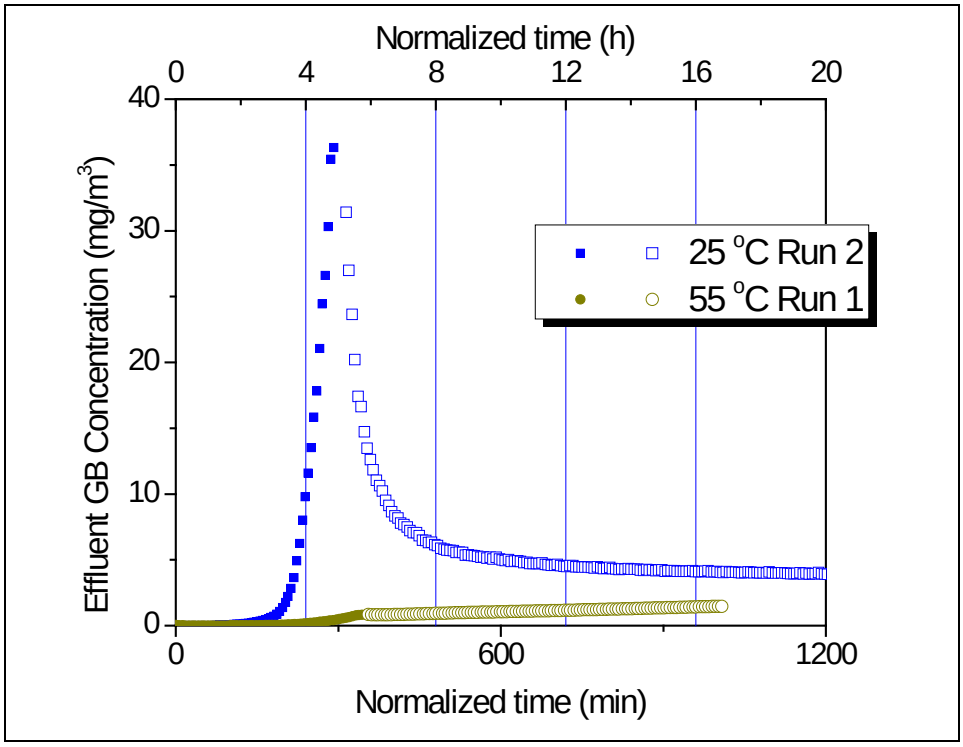

Figure 11. A comparison of the IONEX 03-001 carbon performance at 25 °C/dry and 55 °C/dry. Desorption phase starts at the transition from solid to open symbols.

4.3.3 Vapure 612 Carbon Tests

Four tests were conducted with the Vapure 612 carbon at a bed depth of 3.5 cm. Duplicate tests were conducted at 25 °C/dry and 55 °C/dry conditions and a target challenge concentration of 1,500 mg/m^3. The GB challenge concentrations measured in the tests are presented in Appendix C (Figures C-11 to C-16). Steady challenge concentrations were achieved for the tests, with standard deviations less than 10 % of the averages.

The flow rate, temperature, and RH were steady throughout three of the four tests with the Vapure 612 carbon (as shown in Figures C-11, C-13, and C-15). The exception was Run 2 with the Vapure 612 carbon at 25 °C/dry conditions. As shown in Figure C-12, the flow rate and temperature were steady during the test, while RH spiked from <1 to 9.5 % at about 2 min after switching from adsorption to desorption mode. The RH spike lasted approximately 18 min and was due to an operation error when the air supply from the humidifier was interrupted. The flow through the carbon bed during the incident was maintained at 9 Lpm (Figure C-12), with the air pulled through the vent line to the carbon bed. Because the incident period was short (<20 min),

the target flow rate of 9 L/min was maintained, and the spiked RH (i.e., <9.5 %) was still within the range of the target RH for the dry condition (i.e., RH <15 %, as defined in Table 3); the impact of the incident on the measurement of the desorption curve was believed to be negligible.

Pressure drop across the carbon bed was not recorded during the two tests at 25 °C/dry conditions because the pressure transducer was not operating properly. Pressure drop was stable during the tests at 55 °C/dry conditions. As shown in Figures C-14 and C-16, the average pressure drop was approximately 0.14 inches of water with standard deviation less than 1.5 % of the average. Lower pressure drop (~0.14 inches of water) was measured across a Vapure 612 carbon bed (3.5 cm) than across an IONEX 03-001 carbon bed (~0.23 inches of H_2O). This result is expected, considering the larger carbon particle size of the Vapure 612 carbon: 6 × 12 mesh for the Vapure 612 versus 8 × 12 mesh for the IONEX 03-001 carbon.

Measured breakthrough and desorption curves of the Vapure 612 carbon at 25 °C/dry conditions are presented in Figure 12. As shown in Figure 12, the duplicate tests provided rationally consistent results. Immediate breakthrough was measured with the Vapure 612 carbon beds, which is similar to the tests with the ASZM-TEDA carbon. The effluent concentrations increased from 0.2 mg/m^3 at t = 0 min to 3.5 to 6.5 mg/m^3 at the end of the adsorption test (i.e., 350 min). Desorption concentrations decreased quickly at the initial stage and then leveled off. After ten hours of desorption, the effluent concentration was approximately 0.4 to 0.7 mg/m^3.

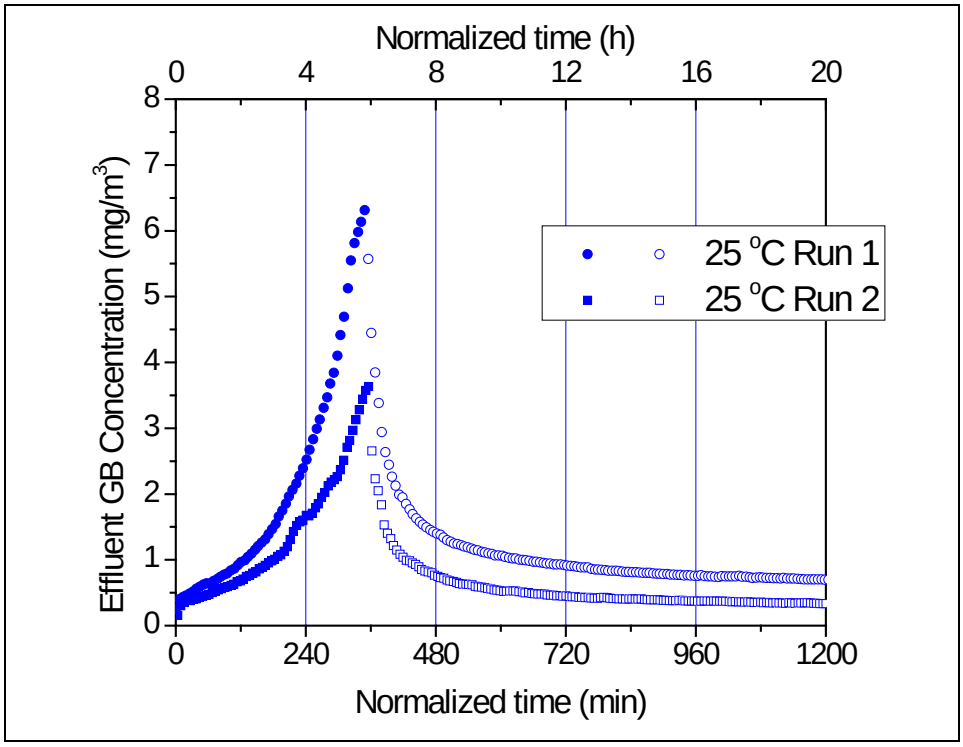

Figure 12. Breakthrough and desorption curves of the Vapure 612 carbon at 25 °C/dry. Desorption phase starts at the transition from solid to open symbols.

Figure 13 presents the breakthrough and desorption curves of the Vapure 612 carbon at 55 °C/dry conditions. Immediate breakthrough occurred under these conditions, and the effluent concentration increased steadily during the adsorption period. For example, during the first run, the effluent concentrations increased to 5.8 mg/m^3 at the end of adsorption (i.e., 270 min). Desorption concentration decreased quickly at the initial stage and then increased gradually for both runs. After ten h of desorption, the desorption concentration was 3.6 mg/m^3 during Run 1 and approximately 4.5 mg/m^3 during Run 2.

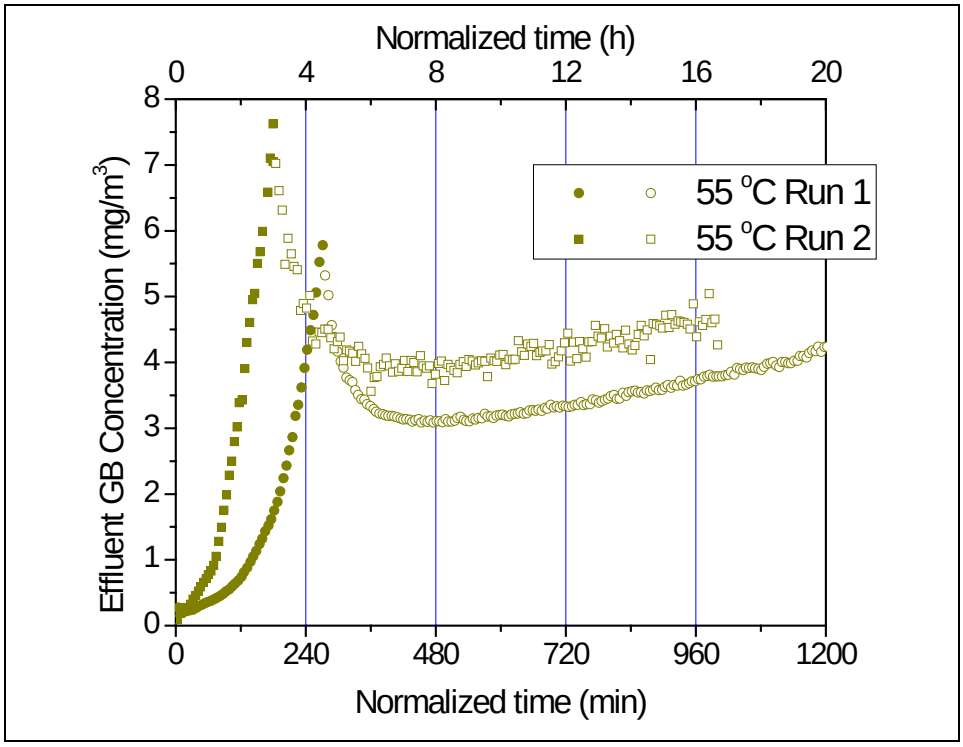

Figure 13. Breakthrough and desorption curves of the Vapure 612 carbon at 55 °C/dry. Desorption phase starts at the transition from solid to open symbols.

Only small quantities of the adsorbed GB were desorbed, which was consistent with the tests using the ASZM-TEDA carbon and IONEX 03-001 carbon. For example, only 0.1 % and 0.5 % of the adsorbed GB was estimated to be desorbed after over 10 h of desorption for the tests at 25°C/dry (Run 1) and 55 °C/dry (Run 1) conditions, respectively.

The performance of the Vapure 612 carbon at conditions of 25 °C/dry and 55 °C/dry is compared in Figure 14. As shown in Figure 14, at the initial stage, the adsorption performance at 55 °C/dry was slightly better than the adsorption performance measured at 25 °C/dry, with lower effluent concentration at 55 °C/dry until t = 100 and 30 min, respectively, for Run 1 and Run 2. The breakthrough curves at 55 °C/dry condition then shifted to the left of the curves at 25 °C/dry and behaved as expected at higher temperature. Initial better performance observed at 55 °C/dry was consistent with the performance observed in the IONEX 03-001 carbon tests. According to the carbon bed water equilibrium tests conducted (see Appendix A), the Vapure 612 carbon bed lost approximately 4.2 % of the weight at 55 °C/dry versus 3.6 % at 25 °C/dry when pre-conditioned for 3 h. Prolonged pre-conditioning at 55 °C/dry might be a factor contributing to the results by desorbing more contaminants or water vapor out of the carbon pores.

Desorption trends at 25 °C/dry and 55 °C/dry were also different. After passing the initial desorption stage, the desorption concentration slowly decreased at 25 °C/dry, while constantly increasing at 55 °C/dry.

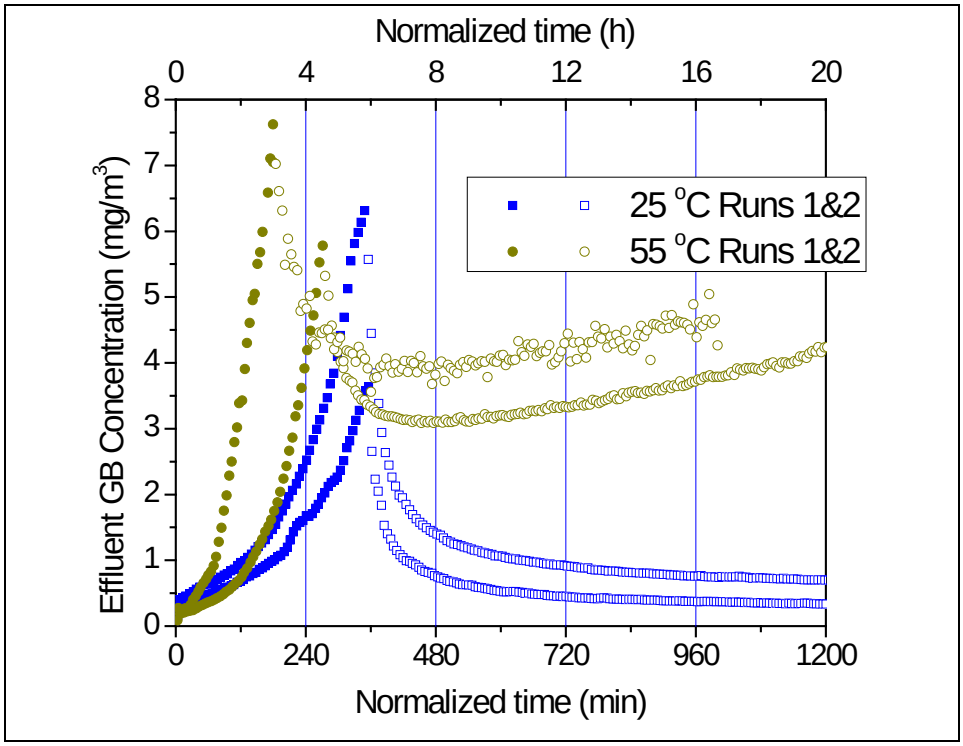

Figure 14. A comparison of the Vapure 612 carbon performance at 25 °C/dry and 55 °C/dry. Desorption phase starts at the transition from solid to open symbols.

4.3.4 ASZM-TEDA (12 × 30 Mesh) Carbon Tests

Two tests were conducted with the ASZM-TEDA (12 × 30 mesh) carbon: one trial each at 25 °C/dry and 55 °C/dry conditions, both at a target challenge concentration of 1,500 mg/m^3. These tests were performed using a 2.5 cm bed depth and used the infusion vapor generation method (described in Section 2.2.4.2) to generate the GB vapor challenge. Graphs depicting the adsorption and desorption behavior under each test condition are shown in Figures 15 and 16. Graphs summarizing the environmental conditions for each test are given in Appendix C (Figures C-17 and C18 for ambient/dry conditions and Figures C-19 and C-20 for the hot/dry conditions).

In Figure 15, the adsorption and desorption behavior of the ASZM-TEDA (12 × 30 mesh) carbon at 25 ºC/dry conditions is shown, overlaid with the measured challenge concentration.

After confirming the challenge concentration at the target value (pre-test values were approximately 1580 mg/m^3), the challenge flow was switched through the test cell. The measured GB challenge concentration was observed to drop to near 200 mg/m^3 upon introduction into the carbon bed. The measured challenge never returned to pre-test values. Nevertheless, breakthrough of GB was detected within 100 to 120 minutes. The indicated drop in challenge concentration was likely due to a leak in the system, though a leak was never confirmed during testing. The plot of the pressure drop (Appendix C, Figure C-18) indicates a gradual increase in upper cell pressure drop from 0.15 in H_2O to 0.25 in H_2O during the agent exposure test. (Subsequent testing with the ASZM-TEDA (12 × 30 mesh) carbon with HD showed that 0.25 in H_2O was typical for this carbon type.) If there were imperfections in the packed test bed allowing channeling of the challenge vapor, this channeling would have been accompanied by an immediate challenge breakthrough observed in the effluent. This type of breakthrough did not occur, as the effluent concentration remained at a baseline level (near the detection limit) throughout the initial phase of the test. During the vapor infusion period, the total volume of GB delivered during the challenge period was 2.2 mL, and this total volume is consistent with the calculations for agent vapor generated at ca. 1500 mg/m^3. The challenge exposure was stopped at 143 min.

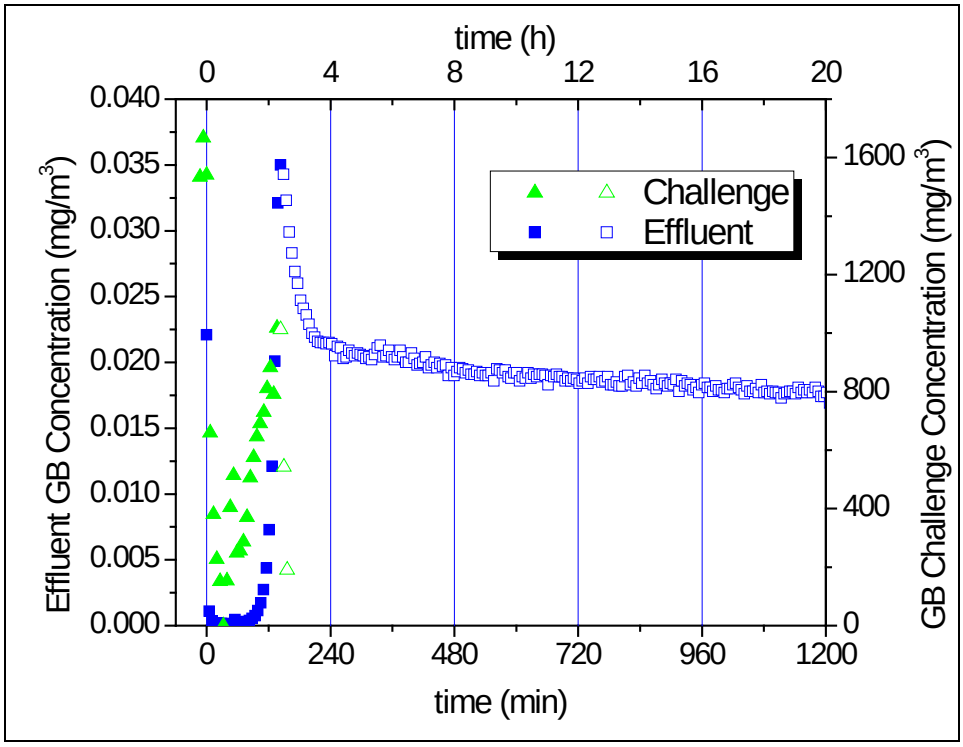

Figure 15. Summary graph of ASZM-TEDA (12 × 30 mesh) carbon challenged with GB vapor at 25 °C /dry conditions. Desorption phase starts at the transition from solid to open symbols.

At the conclusion of the adsorption period, clean air was introduced through the test bed and desorption phase was started. The desorption curve, shown in Figure 15, indicates that GB desorption persisted throughout desorption period at a concentration of approximately one half of the peak effluent concentration when the GB challenge was stopped at 143 min.

Figure 16 shows the adsorption and desorption behavior of GB at 55 ºC/dry conditions on the ASZM-TEDA (12 × 30 mesh) carbon at a 2.5 cm bed depth. The MINICAMS® effluent data are overlaid with the challenge concentration data points. After an initial spike in the challenge concentration, the GB vapor settled to near the target of 1500 mg/m^3 (average = 1496 ± 256 mg/m^3). Pre-testing system checks had ensured all connections in the vapor generation and sampling lines were tightened. Environmental data for this test are shown in Appendix C, Figures C-19 and C-20. Temperature and RH (Figure C-19) were stable throughout testing. The pressure drop measurement (shown in Figure C-20) was also stable at approximately 0.26 in H_2O throughout the test. Challenge breakthrough was beginning to occur after approximately 100 min in the adsorption phase. After concluding the challenge exposure at 149 min, the desorption

curve was monitored overnight. The desorption phase also displayed the persistent off-gassing of GB (dropping from 0.85 mg/m^3 to 0.40 mg/m^3 during the overnight desorption test) observed in the ambient test using this same carbon type.

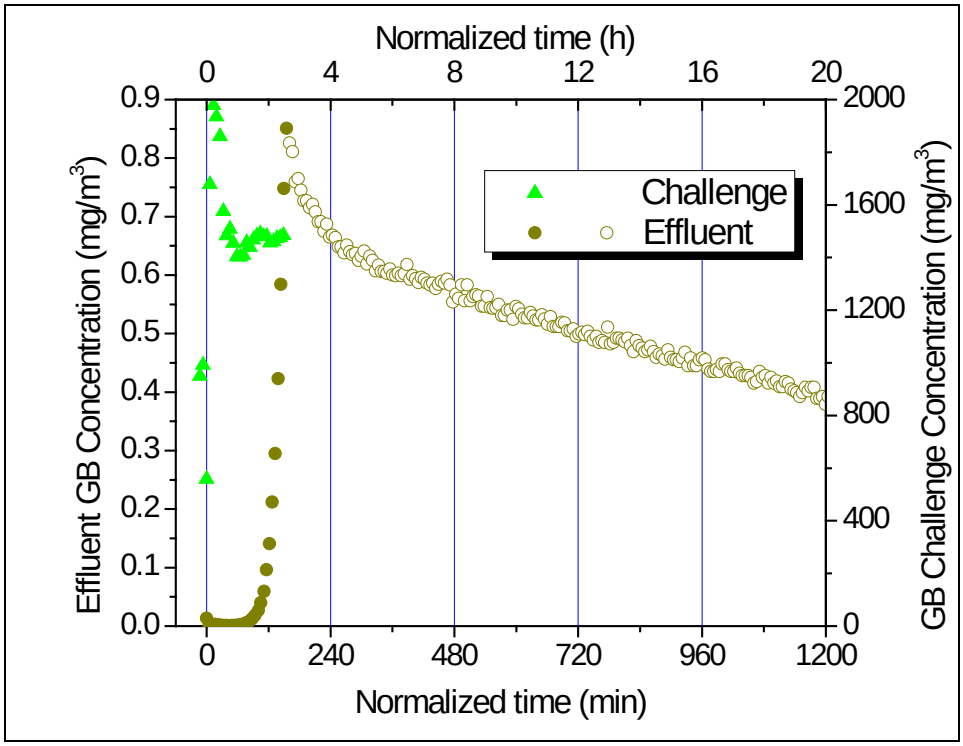

Figure 16. Summary graph of ASZM-TEDA (12 × 30 mesh) carbon challenged with GB vapor at 55 °C/dry conditions. Desorption phase starts at the transition from solid to open symbols.

The performance of the ASZM-TEDA (12 × 30 mesh) carbon at conditions of 25 °C/dry and 55 °C/dry is compared in Figure 17. As shown in Figure 17, with a focus on the first six hours of the test, significantly better adsorption performance was demonstrated for the carbon bed tested at 25 °C/dry. This behavior is in line with the expectation that a higher temperature leads to reduced adsorption capacity. Desorption trends were similar. After passing the initial fast desorption stage, the desorption concentration slowly decreased for both temperatures at approximately the same rate.

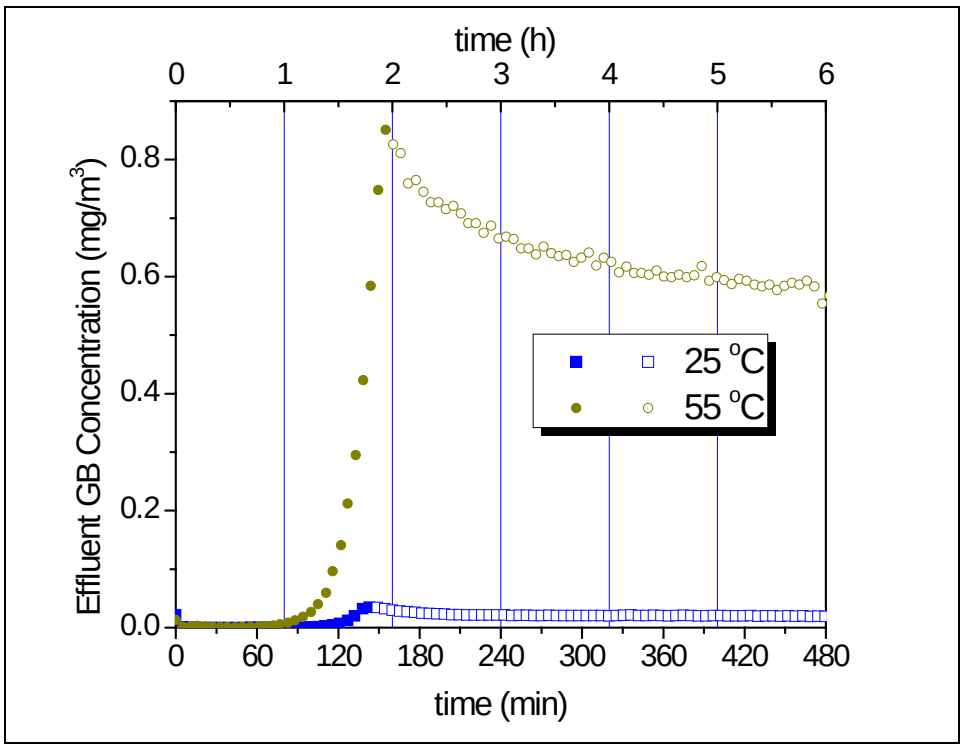

Figure 17. Summary graph of ASZM-TEDA (12 × 30 mesh) carbon challenged with GB vapor at 55 °C/dry conditions. Desorption phase starts at the transition from solid to open symbols.

4.3.5. High Humidity Adsorption and Desorption Studies

The initial test plan called for additional tests for all carbons at high temperature and high humidity (55 ºC/50 % T/RH values). HF was detected in the effluent of a preliminary test at this 55 ºC/50 % RH condition. Consequently, adsorption tests originally planned under this condition were not executed for any of the carbon beds. HF is highly corrosive, and its presence posed a serious hazard to the analysis equipment in this study. At high temperature and humidity, HF is believed to form as a GB decomposition/hydrolysis product. Although adsorption of HF onto activated carbon may be feasible, such investigation was beyond the scope of this study and was not investigated further. Nevertheless, HF formation due to hydrolysis of GB at elevated RH would still pose a risk to, e.g., the duct work of an HVAC system through which the hot air is transported. Using the aforementioned release scenario and assuming complete hydrolysis of GB, the HF concentration could be as high as 260 parts per million (ppm). This concentration is at the lower end of laboratory studies that investigate the impact of HF on (electronic)

equipment. A further assessment of the impact, i.e., corrosion that HF may have on metal ductwork was beyond the scope of this study.

4.4 Results for HD

HD adsorption and desorption tests were performed using the IONEX 03-001 carbon and both ASZM-TEDA carbons at a bed depth of 2.5 cm. Single tests were conducted at 25°C/dry, 55 °C/dry and 55 °C/humid conditions with a target challenge concentration of 500 mg/m^3. In addition, a single test was performed using the ASZM-TEDA (6 × 16 mesh) carbon at 25 ºC/dry condition. The HD environmental conditions measured in the tests are presented in Appendix C (Figures C-21 to C-27 for IONEX 03-001 [8 × 16 mesh], Figures C-28 to C-33 for ASZM-TEDA [12 × 30 mesh], and Figures C-34 and C-35 for ASZM-TEDA [6 × 16 mesh]).

An HD shakedown test was completed with the IONEX 03-001 carbon using a 2.5 cm bed depth at 25 °C/dry conditions and a target challenge concentration of 500 mg/m^3. The test confirmed that the target challenge could be achieved and maintained and that immediate breakthrough did not occur using the 2.5 cm bed depth.

4.4.1 IONEX 03-001 (8 × 16 Mesh) Carbon Tests with HD

Three HD tests were conducted with the IONEX 03-001 carbon using a bed depth of 2.5 cm. Single tests were conducted at 25 °C/dry, 55 °C/dry, and 55°C/humid conditions and a target challenge concentration of 500 mg/m^3. The HD challenge concentrations measured in the tests are overlaid with the MINICAMS® effluent results in subsequent graphs. Steady challenge concentrations were generally achieved during the tests, though the generation system was shown to be sensitive and produced unexpected changes in concentration. The test cell temperature, RH and pressure drop across the test bed were monitored throughout the IONEX 03-001 carbon tests (as shown in Appendix C, Figures C-21 through C-27). The temperature and RH were steady throughout testing.

The summary graph shown in Figure 18 depicts the challenge, adsorption and desorption results of the IONEX 03-001 carbon at 25 ºC/dry conditions. The HD challenge concentration, shown in the upper left, averaged 547 mg/m^3 over the duration of the challenge period (381 min).

Once the desorption phase started, the HD effluent decreased at a rate comparable to the adsorption curve. HD desorption returned to low baseline values (detection limit of the MINICAMS®) after approximately 400 min desorption time. Figures C-21 and C-22 in Appendix C show the temperature, humidity and pressure drop measurements made during the duration of the adsorption and desorption at 25 ºC/dry conditions. The graphs indicate that the environmental conditions were stable throughout testing.

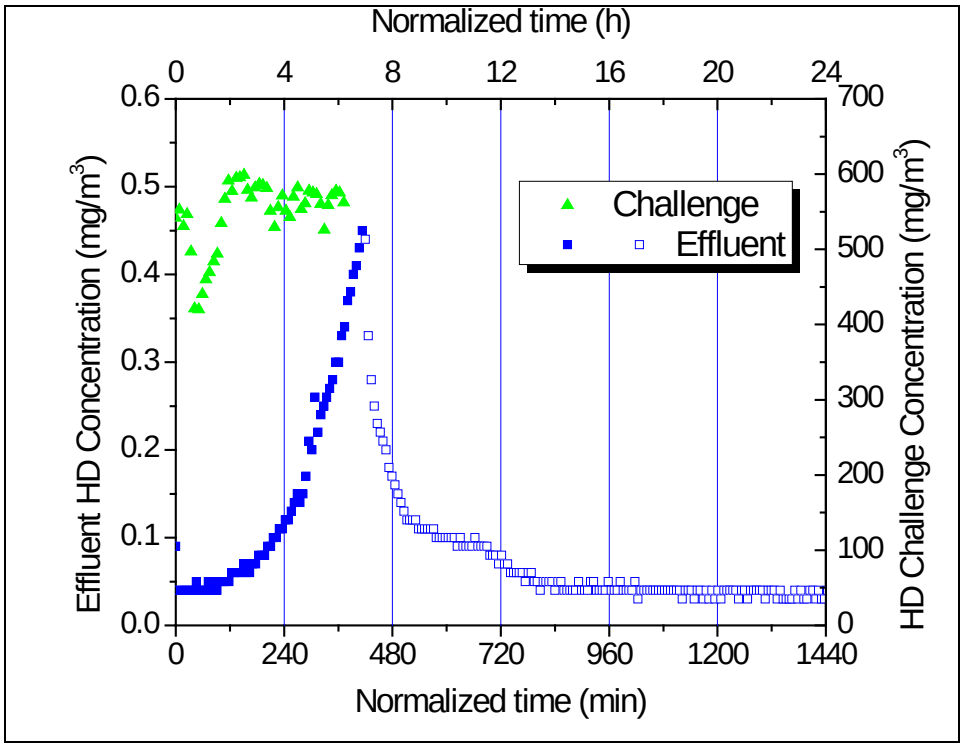

Figure 18. Summary graph of IONEX 03-001 carbon challenged with HD vapor at 25 °C/dry conditions. Desorption phase starts at the transition from solid to open symbols.

In Figure 19, the combined results of the adsorption and desorption testing of the IONEX 03-001 carbon at 55 ºC/dry conditions are shown. During this test, the HD vapor challenge started higher (approximately 700 mg/m^3) than the target concentration, but ultimately was brought into the target range after approximately 150 min of system troubleshooting (which included shutting off the syringe pump feed to allow the system to clear to lower vapor concentrations). The average HD vapor challenge concentration over the duration of adsorption testing was 508 ± 170 mg/m^3. The initial phase of the effluent curve during the adsorption test corresponded to the fluctuations observed while attempting to troubleshoot the challenge

generation. The effluent HD data in Figure 19 were not corrected for the fluctuations in the vapor challenge. A numerical approach to adjust the adsorption time using the actual vapor challenge concentration profile (as opposed to a correction based on the mean of the vapor challenge concentrations across the adsorption phase) shows that the impact of the irregular delivery is very minimal with the last data point prior to the end of the adsorption phase shifting to a shorter time by only 8 minutes. After observing breakthrough behavior in the adsorption curve, the HD challenge vapor was stopped after 390 min, and the system was placed in desorption mode. The HD effluent vapor concentration dropped to near baseline levels after approximately 100 min.

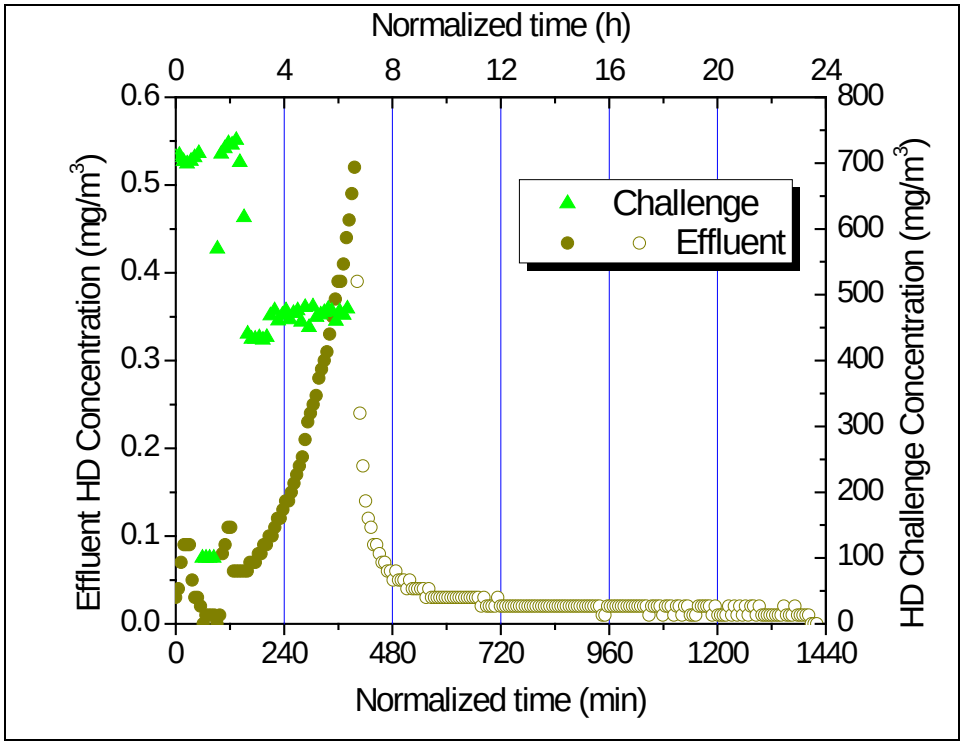

Figure 19. Summary graph of IONEX 03-001 carbon challenged with HD vapor at 55 °C/dry conditions. Desorption phase starts at the transition from solid to open symbols.

The environmental conditions for this challenge at 55 ºC/dry conditions are shown in Figures C-23 and C-24 in Appendix C. The temperature and RH for the test (Figure C-23) were steady throughout the testing period just like the measured pressure drop (Figure C-24), indicating stable flow conditions.

A comparison of the 25 °C/dry and 55 °C/dry adsorption/desorption curve results is shown in Figure 20. Both sets of data were obtained using FID detection. The adsorption performance of this carbon is similar between the two test conditions, while a slight difference in the desorption behavior is noted between the two test conditions. The desorption in the 25 ºC/dry test occurred less rapidly than the 55 ºC/dry desorption over the first five hours of the desorption period.

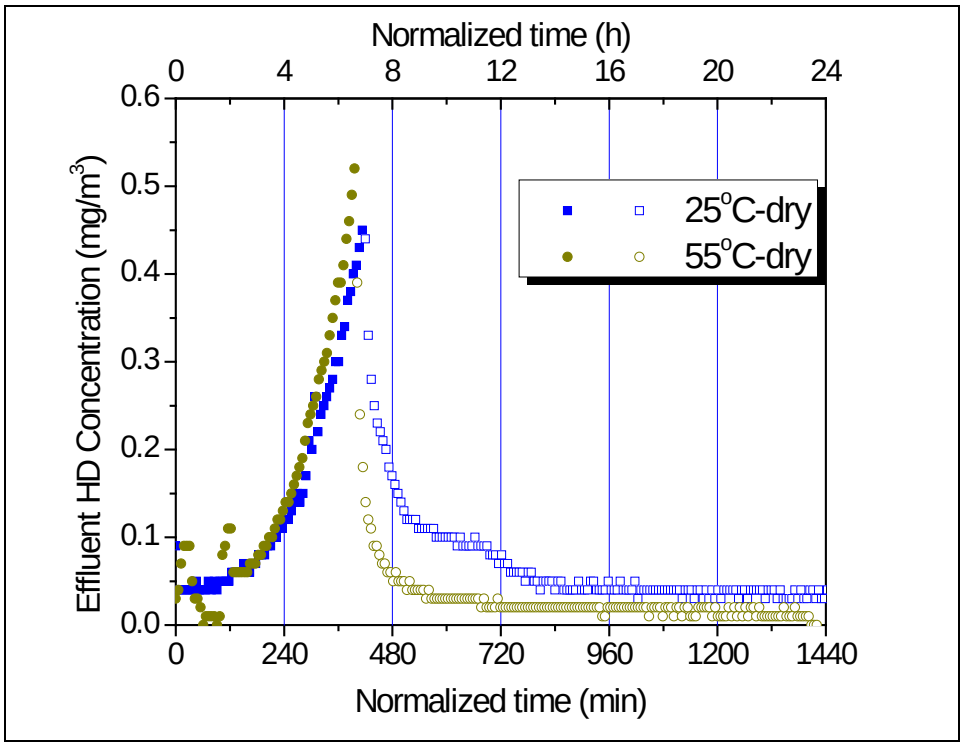

Figure 20. Summary of HD adsorption and desorption for IONEX 03-001 carbon at 25 °C/dry and 55 °C/dry conditions. Desorption phase starts at the transition from solid to open symbols.

The graphical summary of the IONEX 03-001 carbon at 55 ºC/humid conditions is shown in Figure 21. Environmental conditions (temperature and humidity) for this test are shown in Appendix C (Figures C-25 and C-26). The humidity target for this test was 50 %. The RH plot in Figure C-25 showed that the humidity dropped to an average of 35 % upon addition of the HD vapor to the challenge air stream and displayed large variations throughout testing under these conditions. This drop in humidity could not be compensated, despite repeated attempts to adjust air flow and humidity bath temperatures during the test. The plot of pressure drop in Figure

C-26 shows a decreasing trend in pressure drop across the test bed during adsorption testing from 0.15 in H_2O to 0.075 in H_2O (plot shows both the upper and lower bed pressure readings, relative to ambient pressure). In addition, condensation formed in the downstream sampling line (MINICAMS®) after a period of time, causing the MINICAMS® MFC to fail after 258 min. This behavior is observed in the MINICAMS® flow vs. time plot, shown in Appendix C, Figure C-27. The formation of condensation was caused by temperature gradients in the sampling system. Dew point calculations suggested that the entire test system should be above 41 ºC to prevent condensation. While the test cell was conditioned to 55 ºC and the sample line prior to the MINICAMS® was heated, and the MINICAMS® itself has heated zones that pertain to chromatography, the MINICAMS® sampling MFC and post-instrument exhaust lines were not heated (and, in the case of the MFC, should not be). Prior to this flow issue, the MINICAMS® did not indicate evidence of HD breakthrough. Both the FID and FPD detectors were monitored during this test to ensure possible detection of effluent breakthrough. The average HD vapor challenge concentration was 482 ± 98 mg/m^3 for the duration of the adsorption test. At 350 min, the adsorption test was halted (due to the MINICAMS® sampling malfunction). The desorption phase could not be completed due to lack of response by the MINICAMS®. To verify an ending effluent concentration for the adsorption phase of testing, two SSTs were acquired downstream of the carbon bed at t = 350 min, extracted with acetone, and analyzed for HD using GC-FID. The resulting concentration was ~ 0.04 mg/m^3 HD, a low concentration typical of pre-breakthrough “baseline” behavior (the detection limit, based on previous testing).

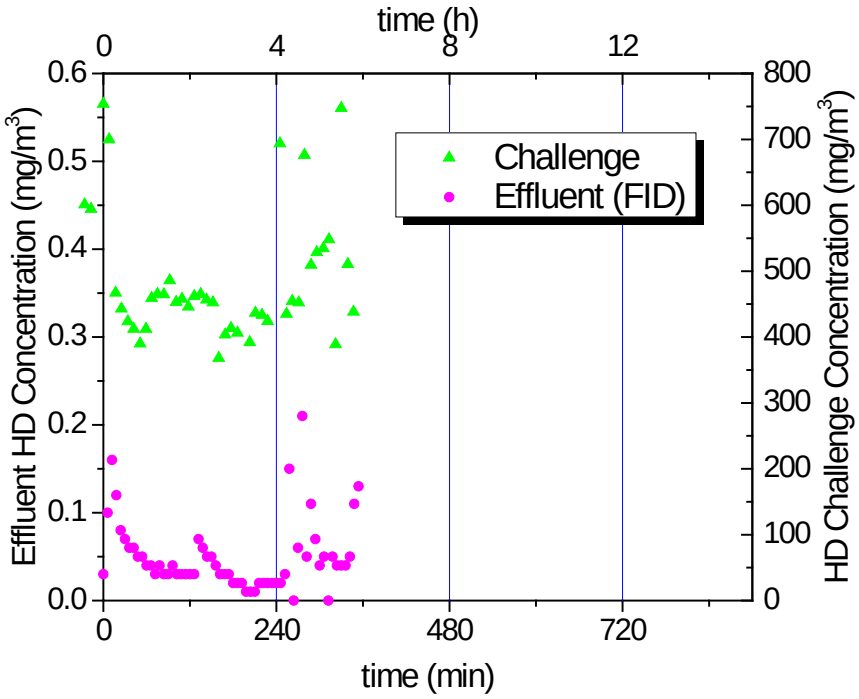

Figure 21. Summary graph of IONEX 03-001 carbon challenged with HD vapor at 55 °C/humid conditions.

In addition, SST samples were analyzed for thiodiglycol (TDG) to determine the potential degradation of HD under the hot/humid test conditions. TDG is the primary degradation product of HD due to hydrolysis. The presence of TDG under these test conditions should not be unexpected; however, it is unclear whether TDG specifically forms on the carbon bed during adsorption.

Qualitative analysis of the SST samples indicated the presence of TDG in the effluent. Two potential sources may result in TDG formation during this test. Under these test conditions (55 ºC/50 % RH), HD hydrolysis should be facile. The half-life of HD in distilled water at 50 ºC has been reported to be 1.1 min (Clark, 1989). HD hydrolysis at 50 ºC/humid conditions on bituminous pulverized low (BPL) ash carbon was determined to be 40 % hydrolysis in six hours and 100 % hydrolysis at 24 hours (McGarvey et al., 2003). For HD adsorbed to carbon at 55 ºC/ humid conditions, formation of TDG is likely. As mentioned previously, the high temperature of the vapor infusion system can induce some HD decomposition. The vaporization of TDG itself is slightly more difficult to achieve. The boiling point of TDG is higher (160 ºC) than the set-point temperature of the vaporization system (~ 140 ºC), so any TDG present would be more

likely to condense than be vaporized. After performing maintenance on the system at the conclusion of HD testing, a soft, polymeric material was collected from the agent injection inlet on the heated transfer line. This material was analyzed and determined to contain TDG.

4.4.2 ASZM-TEDA (12 × 30 Mesh) Carbon Tests with HD

A graphic summary of the ASZM-TEDA (12 × 30 mesh) carbon, exposed to HD at 25 ºC and dry conditions, is given in Figure 22. The plot shows the challenge HD concentration (average of 576 ± 180 mg/m^3), along with both the FID and FPD MINICAMS® data, showing the effluent HD concentration. Responses from both MINICAMS® detectors were undistinguishable at this low concentration. Environmental conditions are given in Appendix C, Figures C-28 and C-29. The test bed was challenged for 355 min, during which no evidence of breakthrough was observed in the effluent data. Some instability was noted in the challenge concentration, where the concentration increased to saturation levels during the final 100 min of exposure. This instability did not impact the effluent breakthrough curve. After the agent exposure period, the test bed was exposed to clean air overnight, during which no evidence of desorption was observed. Changes observed in the MINICAMS® plot were all below the detection limit and are considered noise.

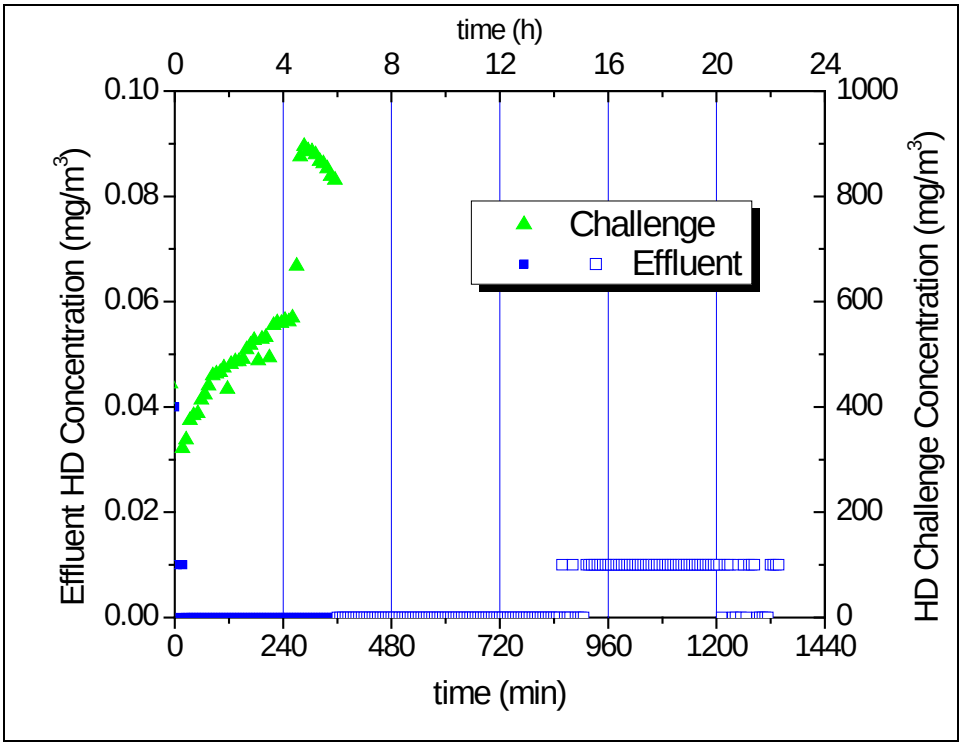

Figure 22. Summary graph of ASZM-TEDA (12 × 30 mesh) carbon challenged with HD vapor at 25 °C/dry conditions. Desorption phase starts at the transition from solid to open symbols.

Examination of the test carbon after testing revealed an ash gray coloring on the normally jet-black carbon. A photograph of the carbon before and after testing is shown in Figure 23. This discoloration was not observed with the IONEX 03-001 carbon or during GB testing with the ASZM-TEDA (12 × 30 mesh) carbon.

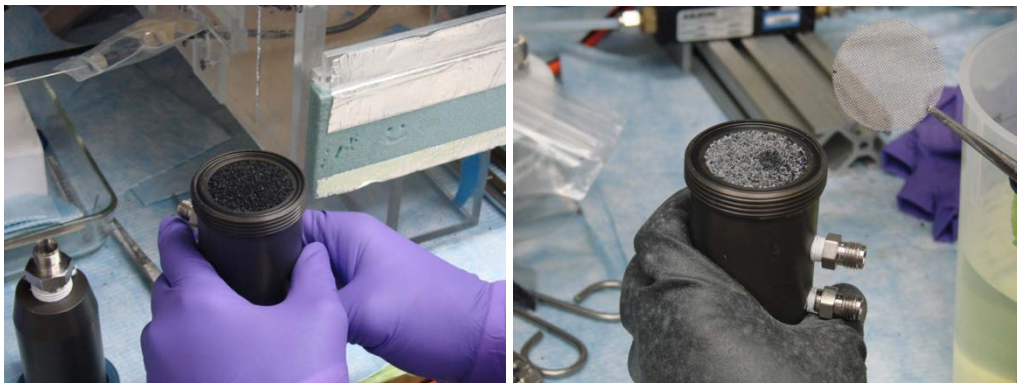

Figure 23. Photographs of ASZM-TEDA (12 × 30 mesh) carbon before (left) and after (right) exposure to HD vapor at 25 °C/dry conditions.

A graphical summary of the ASZM-TEDA (12 × 30 mesh) carbon, exposed to HD at 55 ºC and dry conditions, is shown in Figure 24. The plot shows the challenge HD concentration (average of 527 ± 60 mg/m^3), along with both the FID and FPD MINICAMS® data, showing the effluent HD concentration. Responses from both MINICAMS® detectors were undistinguishable at this low concentration. Graphs showing the environmental conditions are given in Appendix C, Figures C-30 and C-31. The test bed was challenged for 346 minutes, during which no evidence of breakthrough was observed in the effluent data. After the agent exposure period, the test bed was exposed to non-agent laden air overnight, during which no evidence of desorption was observed.

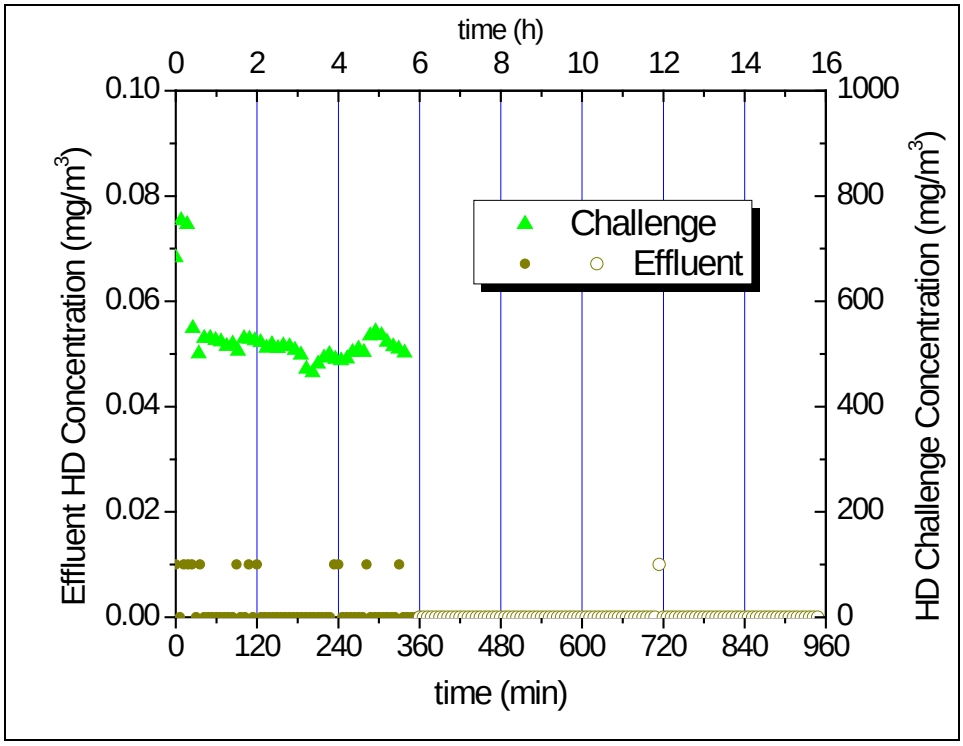

Figure 24. Summary graph of ASZM-TEDA (12 × 30 mesh) carbon challenged with HD vapor at 55 °C/dry conditions. Desorption phase starts at the transition from solid to open symbols.

A summary graph of the ASZM-TEDA (12 × 30 mesh) carbon adsorption and desorption curves, after exposure to HD vapor at 55 ºC and humid conditions, is shown in Figure 25. After completing the IONEX 03-001 test at 55 ºC/50 % RH, the humidity in this test (20 %) was chosen on the basis of the potential for dew point condensation at room temperature that caused the MINICAMS® MFC to fail. Environmental conditions are shown in Appendix C, Figures C-

32 and C-33. The plot in Figure 25 shows the average HD vapor challenge concentration (514 ± 24 mg/m^3), along with both the FID and FPD MINICAMS® data, showing the effluent HD concentration. The test bed was challenged for 366 min, during which no evidence of breakthrough was observed in the effluent data. After the agent exposure period, the test bed was exposed to clean air overnight, during which no evidence of desorption was observed. Despite the lower humidity, problems with condensation still occurred during the overnight desorption test, resulting in the MINICAMS® sampling MFC failure after 300 min of desorption time (Appendix C, Figure C-34). Observed peaks in the effluent as observed by MINICAMS® in FID mode after 480 minutes are presumably due to condensation and injection of water into system. These responses do not reflect actual breakthrough of agent.

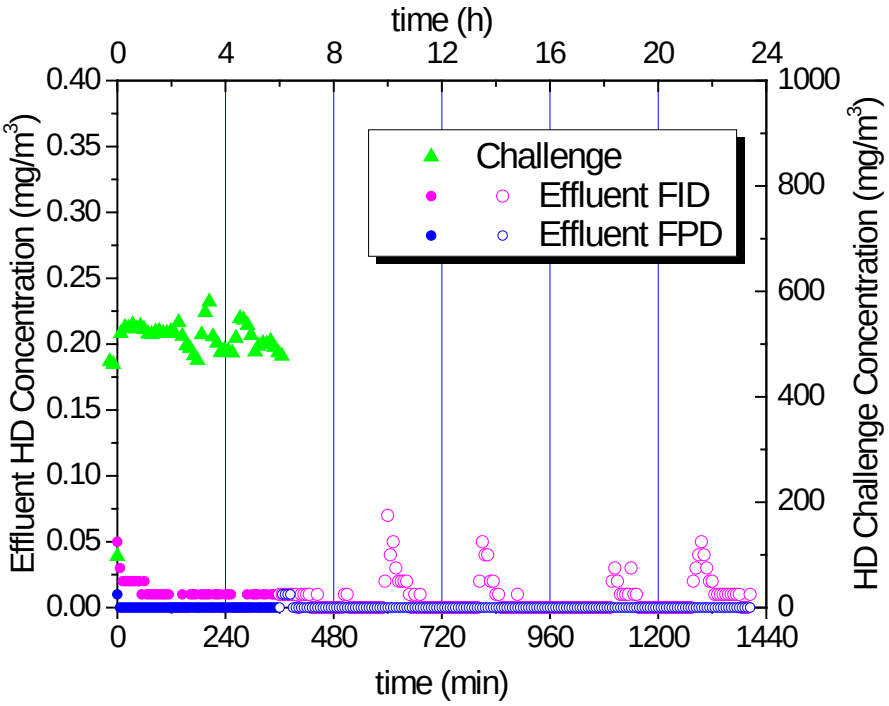

Figure 25. Summary graph of ASZM-TEDA (12 × 30 mesh) carbon challenged with HD vapor at 55 °C/humid conditions. Desorption phase starts at the transition from solid to open symbols.

Because the ASZM-TEDA (12 × 30 mesh) carbon did not exhibit any breakthrough characteristics after six h with HD vapor under dry test conditions, no breakthrough was anticipated under humid conditions. Sorbent tubes were not sampled at the conclusion of the test; however, a sample of the exposed carbon from the test bed was extracted with acetone after

the test was completed and found to contain both HD and TDG. TDG was also found at the injection point of the agent vapor infusion system while performing system maintenance at the conclusion of HD testing. The temperature of the generation system was not high enough to induce bulk TDG vaporization (thus, the material must have collected at the injection point as it formed over a period of time). In addition, continued decomposition of HD to TDG while HD was adsorbed to the carbon bed is not an unreasonable decomposition route under these test conditions.

4.4.3 ASZM-TEDA (6 × 16 Mesh) Carbon Test with HD

As a single point of comparison to confirm the effects of ASZM-TEDA carbon particle mesh size on adsorption behavior (relevant in comparison to the 12 × 30 mesh carbon performance), the ASZM-TEDA (6 × 16 mesh) carbon was tested against an HD vapor challenge under ambient conditions using a 2.5 cm bed depth. A graphical summary of the ASZM-TEDA (6 × 16 mesh) carbon exposed to HD at 25 ºC and dry conditions is shown in Figure 26. The plot shows the average HD vapor challenge concentration (534 ± 70 mg/m^3), along with the FID MINICAMS® data, showing the effluent HD concentration. Environmental data from this test are shown in Appendix C, Figure C-35 and C-36. The test bed was challenged for 337 min, and evidence of breakthrough was notable during this test. Some instability was noted in the challenge concentration, where the concentration increased to nearly 600 mg/m^3 after 150 min of testing. This increase in the challenge concentration appears to correlate with a sudden increase in the effluent concentration. After the agent exposure period, the test bed was exposed to clean air overnight, resulting in rapid desorption as observed in previous GB testing using this carbon.

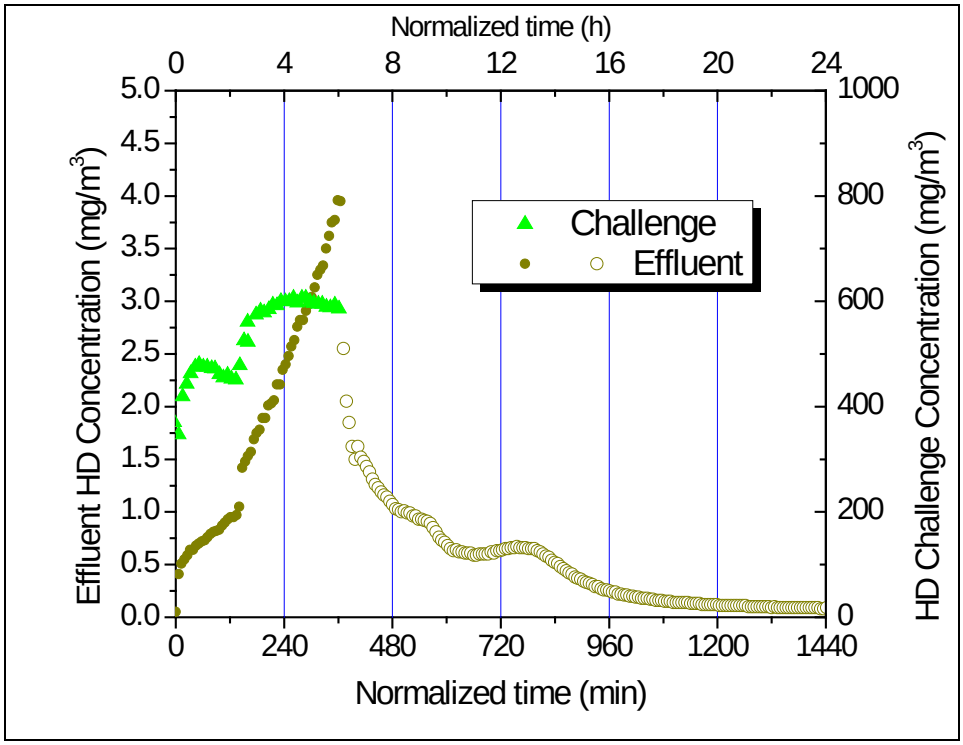

Figure 26. Summary graph of ASZM-TEDA (6 × 16 mesh) carbon challenged with HD vapor at 25 °C/dry conditions. Desorption phase starts at the transition from solid to open symbols.

5.0 SUMMARY

5.1 Sarin, GB

Four types of activated carbons (ASZM-TEDA [6 × 16 mesh and 12 × 30 mesh], IONEX 03-001 [8 × 16 mesh], and Vapure 612 [6 × 12 mesh]) were tested against a GB vapor challenge for adsorption and desorption performance. The target test challenge concentration was 1,500 mg/m^3 of GB. The ASZM-TEDA (6 × 16 mesh) carbon was tested at 25 °C/dry conditions at three carbon bed depths of 2.5, 3.0, and 3.5 cm. The IONEX 03-001 and Vapure 612 carbons were tested at a carbon bed depth of 3.5 cm and two temperature/RH conditions (25 °C/dry and 55 °C/dry). Lastly, the ASZM-TEDA (12 × 30 mesh) was tested at a carbon bed depth of 2.5 cm and two temperature/RH conditions (25 °C/dry and 55 °C/dry). A total of 14 GB adsorption and desorption tests were performed.

Among the coarser carbons tested (i.e., excluding the ASZM-TEDA (12 × 30 mesh) carbon results), the IONEX 03-001 carbon demonstrated the best GB adsorption performance, with carbon bed effluent concentration held at <0.04 mg/m^3 for 85 and 170 min, respectively, at 25 °C/dry and 55 °C/dry conditions for a 3.5 cm bed depth. Immediate breakthrough occurred with both the ASZM-TEDA (6 × 16 mesh) and Vapure 612 carbon beds, as the GB concentration in the effluent steadily increased, albeit initially very gradually. Comparable adsorption curves were obtained for the GB vapor on the ASZM-TEDA (12 × 30 mesh) carbon bed relative to the IONEX 03-001 carbon, and the effluent concentration was held at < 0.04 mg/m^3 for 100 min at 55 ºC/dry conditions. The thinner 2.5 cm carbon bed depth was specified for this carbon due to a primary focus on HD testing at the time of the last two GB tests. Initial estimates for HD vapor breakthrough (see Section 4.5) indicated longer breakthrough times for most carbons than observed for GB vapor, hence a shorter bed depth was used. Increasing temperature from 25 °C to 55 °C (at dry RH) shifted the onset of GB adsorption slightly to shorter times, e.g., better adsorption performance measured for the ASZM-TEDA (12 × 30 mesh) in the initial stage of adsorption under 25 ºC/dry test conditions (< 0.04 mg/m^3 for 140 min at 25 ºC/dry conditions).

Contrary to anticipated results, increasing temperature from 25 °C/dry to 55 °C/dry did not appear to affect the carbon bed adsorption performance adversely, with significantly better

adsorption performance measured for the IONEX 03-001 carbon and better adsorption performance observed for the Vapure 612 carbon at the initial stage of adsorption. There is no definitive explanation for this result. Prolonged (>16 h) pre-conditioning at 55 °C/dry was believed to be a factor, since the pre-conditioning might desorb contaminants or water vapor from carbon pores to increase the adsorption capacity (pre-conditioning the IONEX 03-001 and Vapure 612 carbon at 55 °C/dry conditions yielded 4 and 4.6 % weight loss, respectively).

The breakthrough curve measurements were used to calculate the dynamic adsorption capacity of each of the tested carbons for GB at various temperatures. These values were based on the measured carbon mass (see Appendix C) from which the carbon density was derived for the tested carbons except for the ASZM-TEDA (12 × 30 mesh) carbon density for which a literature value was used. To obtain comparable results across all carbons, the breakthrough time was defined here as the time to reach the immediately dangerous to life or health (IDLH) concentration (0.1 mg/m^3 for GB [NIOSH 2013]) in the effluent. Note that under real conditions, the effluent should not be allowed to reach this concentration unless that effluent is captured in a second carbon bed of equal or larger/thicker size. Table 4 summarizes the calculated dynamic adsorption capacity. Values for the ASZM-TEDA (6 × 16 mesh) and Vapure 612 carbon are upper values because breakthrough as defined here occurred nearly immediately following exposure of the carbon to the 1500 mg/m^3 GB challenge concentration.

Table 4. Dynamic desorption capacities for GB of tested carbons based on 3.5 cm bed depth measurements.

Carbon Type	Mesh Size	Dynamic Desorption Capacity (g GB/g carbon)	
		25 ºC	55 ºC
Calgon Carbon ASZM-TEDA™	6 × 16	0.006	NA
Calgon Carbon ASZM-TEDA™	12 × 30	0.095	0.081
IONEX Research IONEX 03-001	8 × 16	0.076[a]	0.148[b]
Cabot Norit® Vapure™ 612	6 × 12	0.004	0.004

NA: Not Attempted
[a]: Run #2
[b]: Run #1

GB desorption from the carbon bed was observed for all three types of carbons, after the GB challenge was stopped and clean air was pulled through the carbon bed at the flow and T/RH conditions equivalent to the adsorption test. In general, the GB concentration downstream of the carbon bed, as a result of GB desorbing from the carbon, decreased quickly at the initial stage of desorption, and then leveled off. The desorption behavior was dependent on temperature. After an initial drop in GB concentration downstream of the carbon (effluent stream), the GB concentration continued to *decrease* with time as 25 ºC dry clean air continued to flow through the carbon bed. Conversely, after an initial decrease in GB concentration, the GB concentration in the effluent gradually *increased* with time as 55 ºC, dry, clean air continued to flow through the carbon bed. Consequently, GB desorption may pose more risk at the higher temperature of 55 ºC because of the slowly increasing trend of the desorption concentration with time.

GB desorption from the carbon beds was persistent for each of the carbons tested, with desorption concentrations sustained at levels of three to four order of magnitude higher than the STEL (i.e., 0.0001 mg/m^3 for GB) after ten hours of desorption. Only a small quantity of the adsorbed GB, however, was desorbed. After desorption for up to ten hours, less than 1 % of the adsorbed GB was desorbed at both 25 ºC/dry and 55 ºC/dry conditions for all types of carbons tested.

GB adsorption at high temperature (55 ºC) and high humidity (~50 %) was not performed due to the observation of HF in a preliminary test at this condition. HF is highly corrosive and is believed to form as a GB decomposition/hydrolysis product. Such tests were not run due to the potential damage to analytical equipment.

5.2 Sulfur Mustard, HD

Three types of activated carbon (ASZM-TEDA [6 × 16 mesh], ASZM-TEDA [12 × 30 mesh], and IONEX 03-001 [8 × 16 mesh]) were tested successfully against an HD vapor challenge for adsorption and desorption performance. The target test challenge concentration was 500 mg/m^3 for HD. The three carbons used in HD testing were tested at 25 ºC/dry, 55 ºC/dry, and 55 ºC/humid conditions. A total of seven HD adsorption and desorption tests were performed.

In the HD vapor challenge tests, the ASZM-TEDA (12 × 30 mesh) carbon out-performed the IONEX 03-001 carbon. No evidence of breakthrough was observed after nearly six h of HD vapor exposure under all test conditions using the ASZM-TEDA (12 × 30 mesh) carbon. The IONEX 03-001 carbon began exhibiting breakthrough behavior at approximately three to four h of HD vapor exposure. Comparison of the ASZM-TEDA (12 × 30 mesh) carbon test result to the ASZM-TEDA (6 × 16 mesh) carbon test result under the 25 ºC/dry conditions indicates that the difference in granule size is the primary reason for this difference in breakthrough behavior. Such a result is consistent with adsorption theory. The larger mesh (smaller granule sizes) enhances mass transfer and can adsorb the incoming vapor much more rapidly. Similar to the observation made in GB testing, increasing the test temperature from 25 ºC to 55 ºC did not appear to impact the adsorption behavior of the IONEX 03-001 carbon towards HD vapor significantly. The lack of replicates for each test condition does not allow to conduct a more statistical evaluation to determine whether this observation is (statistically) significant.

Like the GB data, the breakthrough curve measurements were used to calculate the dynamic adsorption capacity of each of the tested carbons for HD. As before, the breakthrough time was defined here as the time to reach the IDLH concentration (0.7 mg/m^3 for HD, [NIOSH 2013]) in the effluent. Table 5 summarizes the calculated dynamic adsorption capacity. Values for the ASZM-TEDA (12 × 30 mesh) represent low estimates as no breakthroughs were observed for this carbon when exposed to the 500 mg/m^3 HD challenge concentration.

Table 5. Dynamic desorption capacities for HD of tested carbons based on 2.5 cm bed depth measurements under dry (< 15% RH) conditions.

Carbon Type	Mesh Size	Dynamic Desorption Capacity (g HD/g carbon)	
		25 ºC	55 ºC
IONEX Research IONEX 03-001	8 × 16	0.148	0.137
Calgon Carbon ASZM-TEDA™	12 × 30	> 0.090	> 0.080
Calgon Carbon ASZM-TEDA™	6 × 16	0.010	NA

NA: Not Attempted

Desorption of HD from the IONEX 03-001 carbon was more rapid at 55 ºC compared to the 25 ºC test condition. Testing HD vapor adsorption and desorption at 55 ºC/humid conditions was complicated by condensation in the MINICAMS® sample flow system. For the IONEX 03-

001 carbon, sorbent tubes collected at the conclusion of the challenge period (350 min) confirmed a low concentration (~0.04 mg/m^3) of HD. Analysis of post-challenge sorbent tubes indicated the presence of TDG in the effluent. Continued decomposition of HD to TDG while adsorbed to the carbon bed is not an unreasonable decomposition route under these test conditions.

6.0 GENERAL CONCLUSIONS

Consideration of both the adsorption and desorption characteristics of a carbon under different environmental conditions should be critical to the choice of carbon in filtration systems. Table 6 summarizes the trends in breakthrough times when compared to the 25 °C/dry breakthrough time of the same carbon. Different CWAs appear to behave differently on the carbon beds as shown here for GB and HD. GB adsorbs well to the IONEX 03-001 carbon but also significantly desorbs from the carbon, particularly under high temperatures. The ASZM-TEDA (12 × 30 mesh) carbon performed comparably with regard to both adsorption and desorption characteristics (although differences in bed depth preclude a direct comparison with the IONEX 03-001 carbon). Further, HF formation from the degradation of GB under humid conditions is a significant concern for human safety and infrastructure integrity. HD adsorbs best to the ASZM-TEDA (12 × 30 mesh) carbon, with no evidence of breakthrough up to six h of exposure to 500 mg/m^3 of HD. Decomposition of HD is also evident on both the IONEX 03-001 carbon and the ASZM-TEDA (12 × 30 mesh) carbon under humid conditions, but the decomposition product (TDG) does not appear to pose a significant threat to infrastructure integrity or human safety.

Breakthrough time comparisons made in this report assume that the impacts of temperature, bed thickness and RH are independent. Any interaction effects among these parameters could not have been estimated in this study because of the lack of replicates for most of the experimental test conditions. The inherent difficulty of using CWAs in large quantities (milliliters of agent consumed per test) limits a more thorough research effort with sufficient replicates.

This research provides information on the impact of temperature and RH on the performance of activated carbon beds as to capture chemical warfare agent vapors. The observed changes in breakthrough times for GB and HD at elevated temperatures and RH will provide decision makers with information for the use of these activated carbon to capture the effluent air flow. This information will facilitate their use as part of a hot air decontamination approach to remediate an indoor facility.

Table 6. Summary of trends in breakthrough times with respect to 25 °C adsorption results.

Agent, concentration (mg/m^3)		GB, 1500		HD, 500	
Carbon Type	**Mesh Size**	**55 °C/dry**	**55 °C/humid**	**55 °C/dry**	**55 °C/humid**
Calgon Carbon ASZM-TEDA™	6 × 16	ND	NA[a]	NA	NA
Calgon Carbon ASZM-TEDA™	12 × 30	--	NA[a]	+/-	+/-
IONEX Research IONEX 03-001	8 × 16	++	ND[a]	=	++[b]
Cabot Norit® Vapure™ 612	6 × 12	--	NA[a]	NA	NA

++: longer breakthrough time
=: equal breakthrough time; no discernable impact
- -: shorter breakthrough times
+/-: no breakthrough observed for any condition
ND: Not Determined
NA: Not Attempted
[a] Not determined due to formation of HF.
[b] Enhanced HD hydrolysis extends breakthrough time.

7.0 REFERENCES

ASTM Standard Guide for Gas-Phase Adsorption Testing of Activated Carbon, D5160-95 (Reapproved 2008).

Battelle SOP HMRC X-283, "Evaluation of the Activated Carbon Beds with Chemical Agent Vapors". *SOP available upon request; see Disclaimer.*

Clark, D. N., "Review of Reactions of Chemical Agents in Water", AD-A213, Defense Technical Information Center, September 1989.

EPA 2009 Report. Decontamination of Toxic Industrial Chemicals and Chemical Warfare Agents on Building Materials Using Chlorine Dioxide Fumigant and Liquid Oxidant Technologies.
U.S. Environmental Protection Agency, Washington, DC, EPA/600/R-09/012, 2009

EPA 2010 Report. Assessment of Fumigants for Decontamination of Surfaces Contaminated with Chemical Warfare Agents. U.S. Environmental Protection Agency, Research Triangle Park, NC, EPA/600/R-10/035, 2010.

EPA 2011 Report. Decontamination of Sulfur Mustard and Thickened Sulfur Mustard Using Chlorine Dioxide Fumigation. U.S. Environmental Protection Agency, Research Triangle Park, NC, EPA/600/R-11/051, 2011.

McGarvey, D., Mahle, J., and Wagner, G. Chemical Agent Hydrolysis on Dry and Humidified Adsorbents (No. ECBC-TR-334), Edgewood Chemical Biological Center, Aberdeen Proving Ground, MD, 2003.

National Institute for Occupational Safety and Health (NIOSH) Education and Information Division, http://www.cdc.gov/niosh/ershdb/AgentListCategory.html. Page last updated June 18, 2013. Last access May 2014.

Wagner, G., Sorrick, D. C., Procell, L. R., Brickhouse, M. D., Mcvey, I. F., and Schwartz, L. I. Decontamination of VX, GD, and HD on a Surface Using Modified Vaporized Hydrogen Peroxide, Langmuir 2007, 23, 1178-1186.

APPENDIX A: CARBON BED EQUILIBRIUM TESTS

A.1 INTRODUCTION

Prior to the chemical agent adsorption/desorption testing, each carbon bed was preconditioned to achieve equilibrium at the environmental conditions (i.e., temperature and RH) to be used in the agent testing. Preconditioning was included to ensure that breakthrough data were obtained with the carbon bed in the same state as the conditions under which the agent was added. This approach avoids that breakthrough data were collected in which the environmental conditions of the challenge air flow were changing the local carbon bed temperature and RH until equilibrium would be reached

The preconditioning process was conducted by flowing air (at the target temperature and relative humidity) through the carbon bed until water vapor adsorption equilibrium was achieved. To determine the time required to achieve water vapor adsorption equilibrium, a set of equilibrium tests was conducted at three test conditions of 55 ± 2 °C and 50 ± 5 % RH, 55 ± 2 °C and dry (<15 % RH) and 25 ± 2 °C and dry. Those results are presented in Section A.3.

The test system and approach to precondition the carbon is described briefly in Section A.2. The test system described is the same system that is used to test the chemical warfare agent adsorption characteristics of the carbon at the target environmental conditions.

A.2 TEST METHOD

During the water vapor equilibrium test, carbon was loaded into the carbon holder in the same manner that was used for the agent adsorption tests. Three carbon types were selected: (1) ASZM-TEDA carbon (6 × 16 mesh) from Calgon Carbon, (2) IONEX 03-001 (8 × 16 mesh) from IONEX Research Corporation, and (3) Norit® Vapure™ 612 (6 × 12 mesh) from Cabot Norit Activated Carbon. The carbon bed depth for each carbon was 2.5 cm with a 4.0 cm cross section, corresponding to carbon weights of 20.6, 14.3, and 16.0 grams (g), respectively, for the ASZM-TEDA (6 × 16 mesh) carbon, IONEX 03-001 carbon, and Vapure 612 carbon. The filtered air stream flowing through the carbon bed was maintained at the target condition of temperature (55 or 25 °C), RH (50 % or <15 %), and 9 L/min, corresponding to a face velocity of 12 cm/s (the same as the velocity required for the chemical agent adsorption test). Every hour, the air flow was stopped; the carbon holder was disconnected from the test system and weighed.

The carbon holder was then returned to the test system, and air flowed through the carbon bed for another hour. This process was repeated until the carbon weight did not increase for two consecutive measurements, or until ten h of preconditioning testing. If the carbon weight still increased after ten h of testing, the preconditioning test was continued overnight without the hourly weight measurement. The carbon weight was measured next morning after about 24 h of the preconditioning.

A schematic of the test system is depicted in Figure A-1; details are described in the main body of this report.

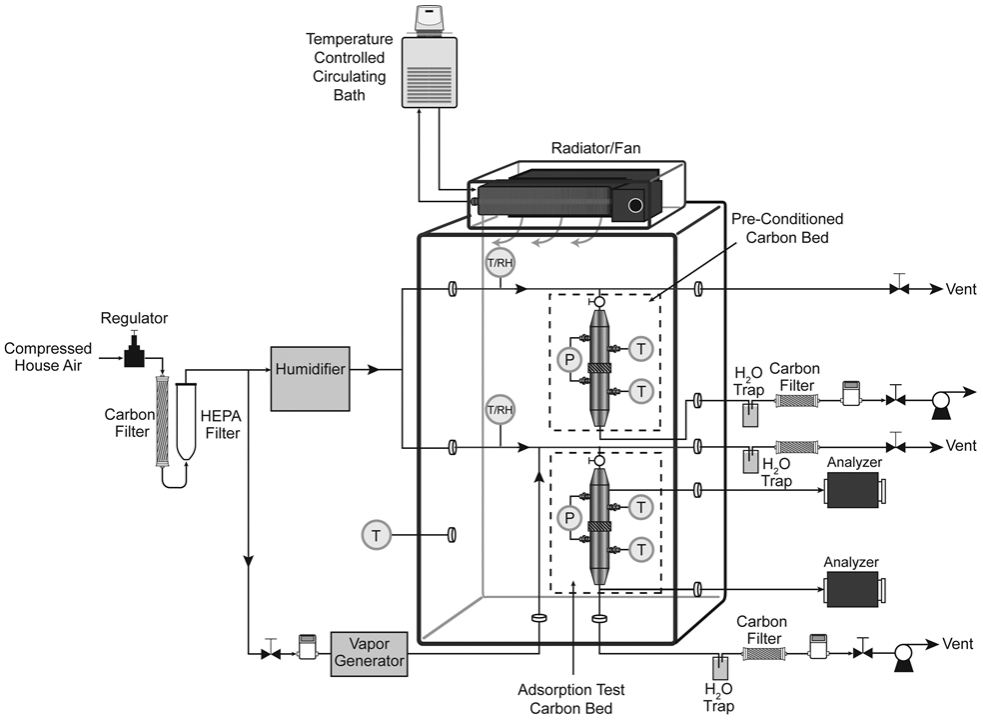

Figure A-1. Schematic of the test system used for carbon performance evaluation.

The flow rate through the carbon bed was controlled by a mass flow controller from AALBORG Instruments and Control (Series No. GFC17; Orangeburg, NY, USA). The temperature and RH in the system challenge were monitored continuously by a T-RH probe from Vaisala (Model No. HMT338, Helsinki, Finland). Air stream temperatures at the top and bottom of the carbon bed were monitored by two thermocouples. All temperature, relative humidity, and flow rate data were recorded throughout the test by a data acquisition system from Yokogawa (Houston, TX, USA). The relative humidity at the carbon bed was not measured. Instead, the RH was calculated based on the RH and temperature measured in the system influent and the

average temperature measured at the top and bottom of the carbon bed using the following equations:

$$RH_{Carbon\_Bed} = \frac{P_{sat}(T_{inlet}) \text{ X } RH_{inlet}\,\%}{P_{sat}(T_{Average\_Bed})} \quad (1)$$

where RH_{Carbon_Bed} is the relative humidity at the carbon bed, T_{inlet} is the temperature in the system influent, $T_{Average\_Bed}$ is the average of the temperatures measured at the top and bottom of the carbon bed, $P_{sat}(T_{inlet})$ is the saturation water vapor pressure at T_{inlet}, RH_{inlet} is the relative humidity measured in system influent, and $P_{sat}(T_{Average\_Bed})$ is the saturation water vapor pressure at $T_{Average\_Bed}$.

A.3 TEST RESULTS

A.3.1 Carbon Bed Equilibrium Time at 55 ± 2 °C and 50 ± 5 % RH

The measured plots of weight gain versus preconditioning time at 55 ± 2 °C and 50 ± 5 % RH are presented in Figures A-2, A-3, and A-4, respectively, for the ASZM-TEDA (6 × 16 mesh), the IONEX 03-001, and the Vapure 612 carbon.

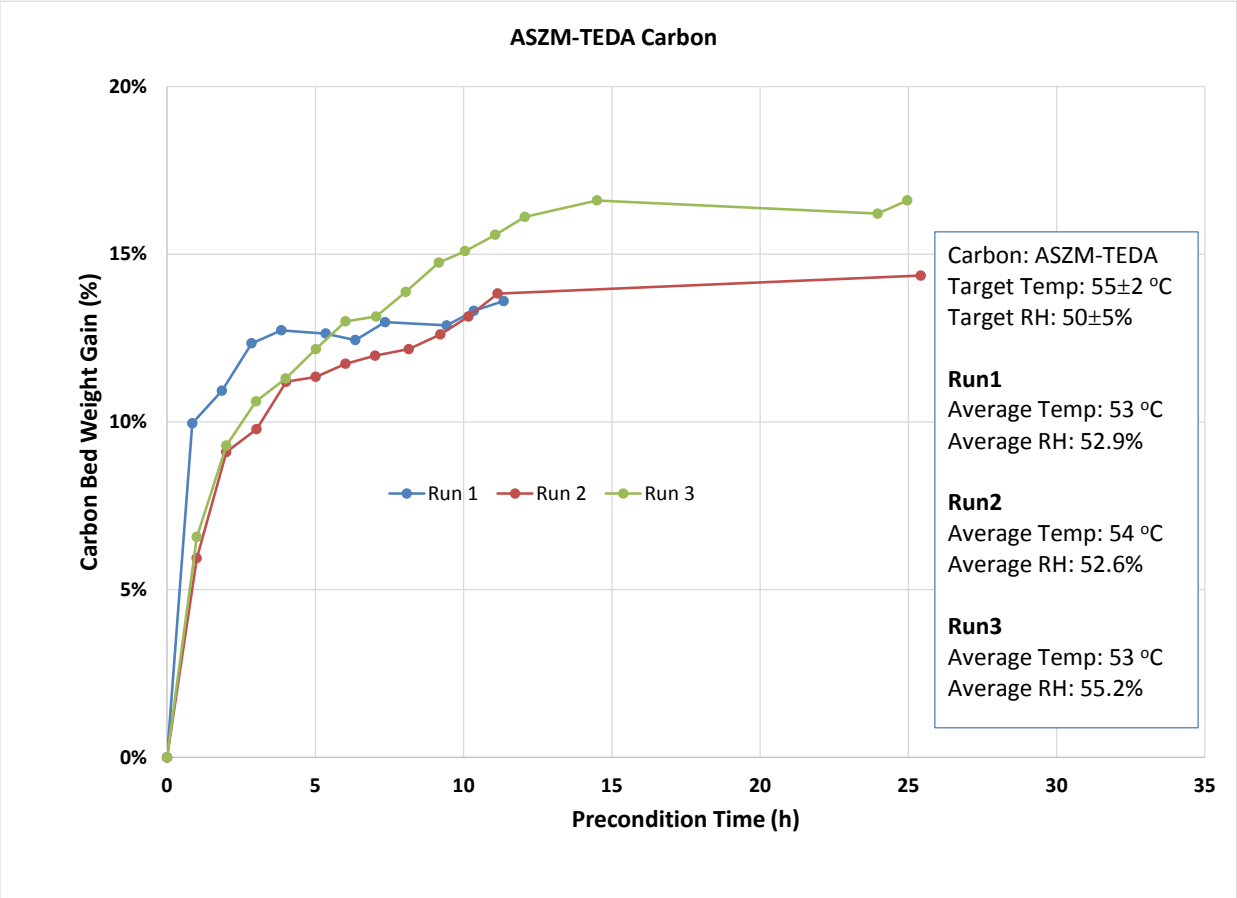

Figure A-2. ASZM-TEDA (6 × 16 mesh) carbon bed weight gain versus preconditioning time at 55 ± 2 °C and 50 ± 5% RH.

For ASZM-TEDA carbon, approximately 14 to 17 % of the weight gain was achieved during the 25 h of preconditioning, corresponding to a water vapor adsorption capacity of 0.14 to 0.17 g water/g of carbon. As shown in Figure A-2, the carbon bed gained weight quickly within the first four h of preconditioning, then the weight gain slowed dramatically. In the first run, the test was stopped after 11 h of preconditioning as the weight gain, on average, had ceased indicating saturation of the carbon bed. In the second and third runs, there was a consistent upward drift in the weight gain, so the test was continued overnight and the weight gain was measured at t = 25 h in the second run, and at t = 12, 14.5, 24, and 25 h in the third run. As shown in Figure A-2, the carbon bed approached equilibrium after approximately 12 h of preconditioning, evidenced by the fact that only 0.5 % of the weight gain was achieved in the last 13 h of preconditioning from 12 to 25 h during Run 3, which corresponds to only 3 % of the overall weight gain.

The test results show that the final weight gain or water adsorption capacity of ASZM-TEDA carbon was very sensitive to operation temperature and RH. Slight variation in temperature

and RH within the target ranges could cause measurable change in water adsorption capacity. For example, during Run 3, the temperature was 1 °C lower and RH was 2.6 % higher than in Run 2, which led to approximately a 13 % increase in water adsorption capacity. Based on these results, preconditioning of the ASZM-TEDA carbon bed for (at least) 12 h at 55 ± 2 °C and 50 ± 5% RH is considered sufficient.

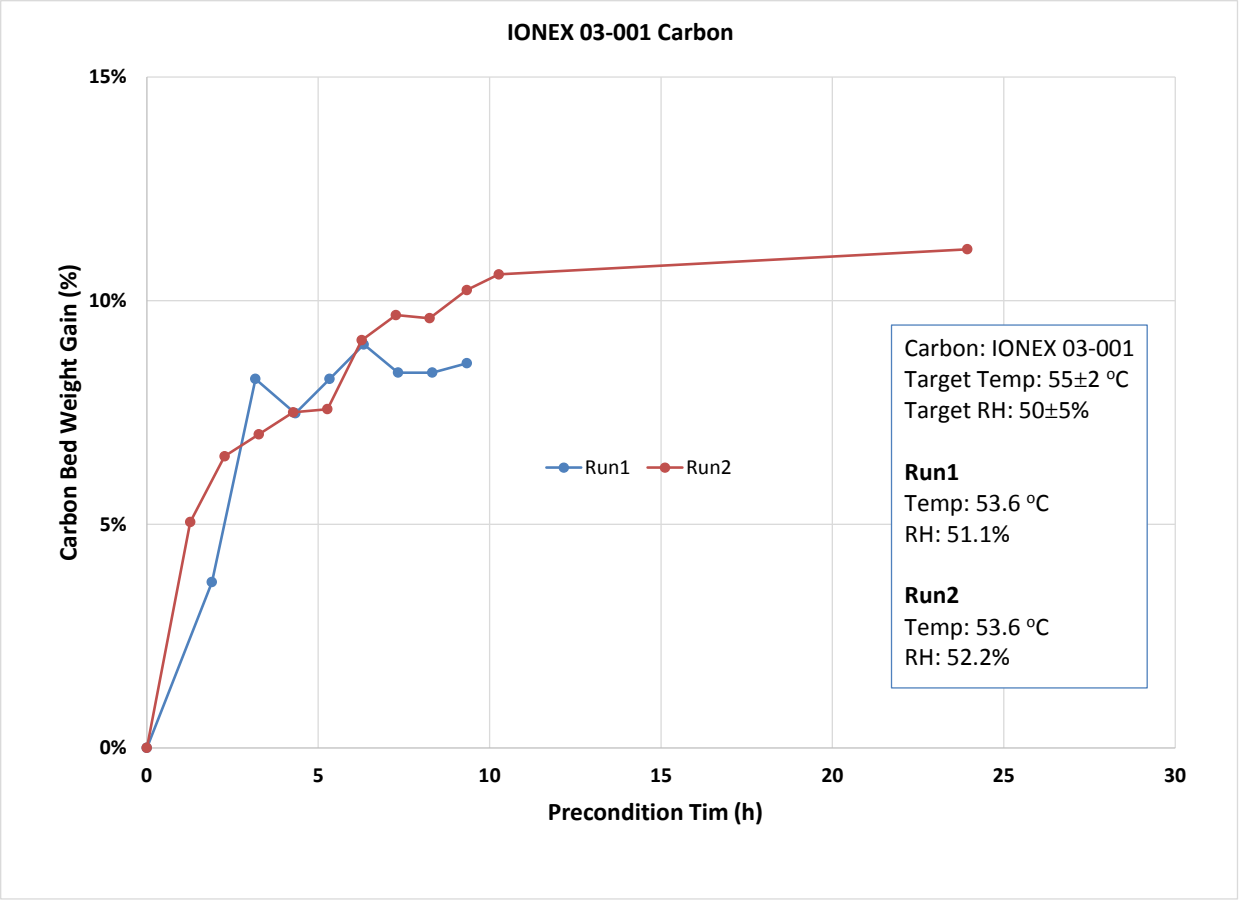

Figure A-3. IONEX 03-001 (8 × 16 mesh) carbon bed weight gain versus preconditioning time at 55 ± 2 °C and 50 ± 5% RH.

For IONEX 03-001 carbon, approximately 11 % of the weight gain was achieved during the 24 h of preconditioning, corresponding to a water vapor adsorption capacity of 0.11 g water/g of carbon. Rapid weight gain was observed in the first two to three hours in both Runs 1 and 2, thereafter the weight gain slowed significantly. In the first run, the test was stopped after approximately nine h of preconditioning as the weight gain had ceased, on average, indicating saturation of the carbon bed. In the second run, the upward trend in the weight gain was consistent, therefore the test was continued overnight, and weight gain was measured at t = 24 h. As shown in Figure A-3, the weight gain approached equilibrium after ten h of preconditioning.

The preconditioning test was continued for another 14 h from 10 to 24 h but the carbon only achieved 0.6 % of additional weight gain, which corresponds to only 5 % of the overall weight gain.

Based on the test results, preconditioning of the IONEX 03-001 carbon bed for (at least) ten h is considered sufficient.

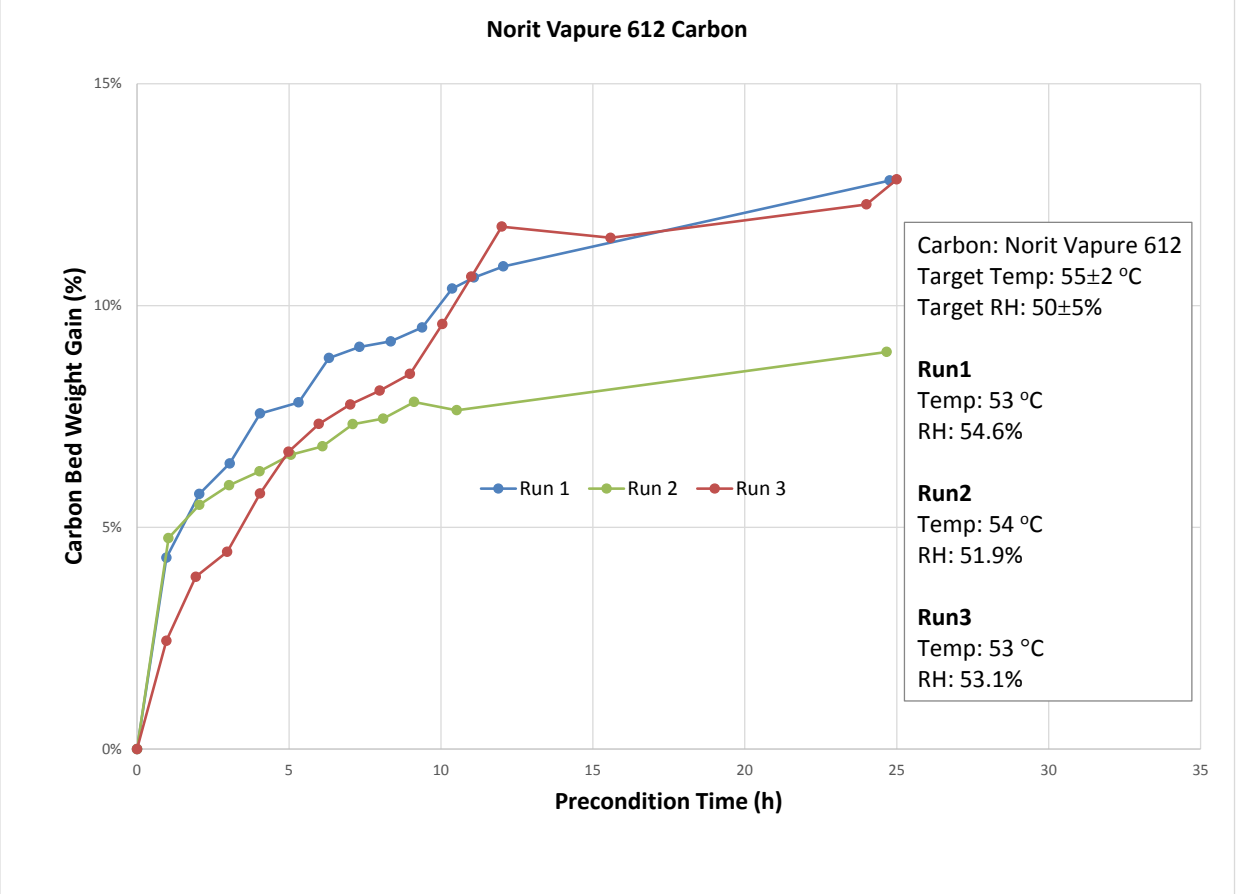

Figure A-4. Vapure 612 (6 × 12 mesh) carbon bed weight gain versus preconditioning time at 55 ± 2 °C and 50 ± 5% RH.

For Vapure 612 carbon, after 24 h of preconditioning, approximately 13 % and 9 % weight gains were achieved, respectively, in Runs 1 and 3, and Run 2, which correspond to water vapor adsorption capacities of 0.13 and 0.09 g water/g of carbon, respectively. The higher weight gain obtained in Runs 1 and 3 was attributed to the slightly higher average RH (i.e., 54.6 % and 53.1 % in Runs 1 and 3 versus 51.9 % in Run 2) and slightly lower temperature (i.e., 53 °C in Runs 1 and 3 versus 54 °C in Run 2) during Runs 1 and 3. Unlike the ASZM-TEDA carbon and the IONEX 03-001 carbon, the weight gain continued to increase after ten h of preconditioning for Runs 1 and 3. Continued preconditioning from 10 to 24 h achieved 2.4 %

and 1.3 % of additional weight gains, respectively, in Runs 1 and 3, which corresponds to more than 15 % of the overall weight gain for all three runs. Therefore, as shown in Figure A-4 for Vapure 612 carbon, it is necessary to precondition the carbon bed for (at least) 24 h.

In summary, the water adsorption capacities measured at 55 ± 2 °C and 50 ± 5 % RH averaged 0.15, 0.11, and 0.11 g/g, respectively, for the ASZM-TEDA carbon, the IONEX 03-001 carbon, and the Vapure 612 carbon. For the ASZM-TEDA and IONEX 03-001 carbon, the carbon bed approached equilibrium after 12 h of preconditioning. The Vapure 612 carbon needed longer than 12 h to approach equilibrium. Based on the test results, it is recommended a preconditioning time of at least 12 h for the ASZM-TEDA and the IONEX 03-001 carbons and a preconditioning time of at least 24 h for the Vapure 612 carbon at the conditions of 55 ± 2 °C and 50 ± 5 % RH.

A.3.2 Carbon Bed Equilibrium Time at Dry Conditions (RH<15 %)

The measured plots of weight change of the ASZM-TEDA carbon versus preconditioning time are presented in Figures A-5 to A-6, respectively, for the tests conducted at 55 °C and dry conditions and 25 °C and dry conditions. As shown in Figures A-5 and A-6, the carbon bed reached equilibrium within one hour at both test conditions. The carbon bed lost approximately 2 % of weight at 55 °C and 1 % of weight at 25 °C due to drying.

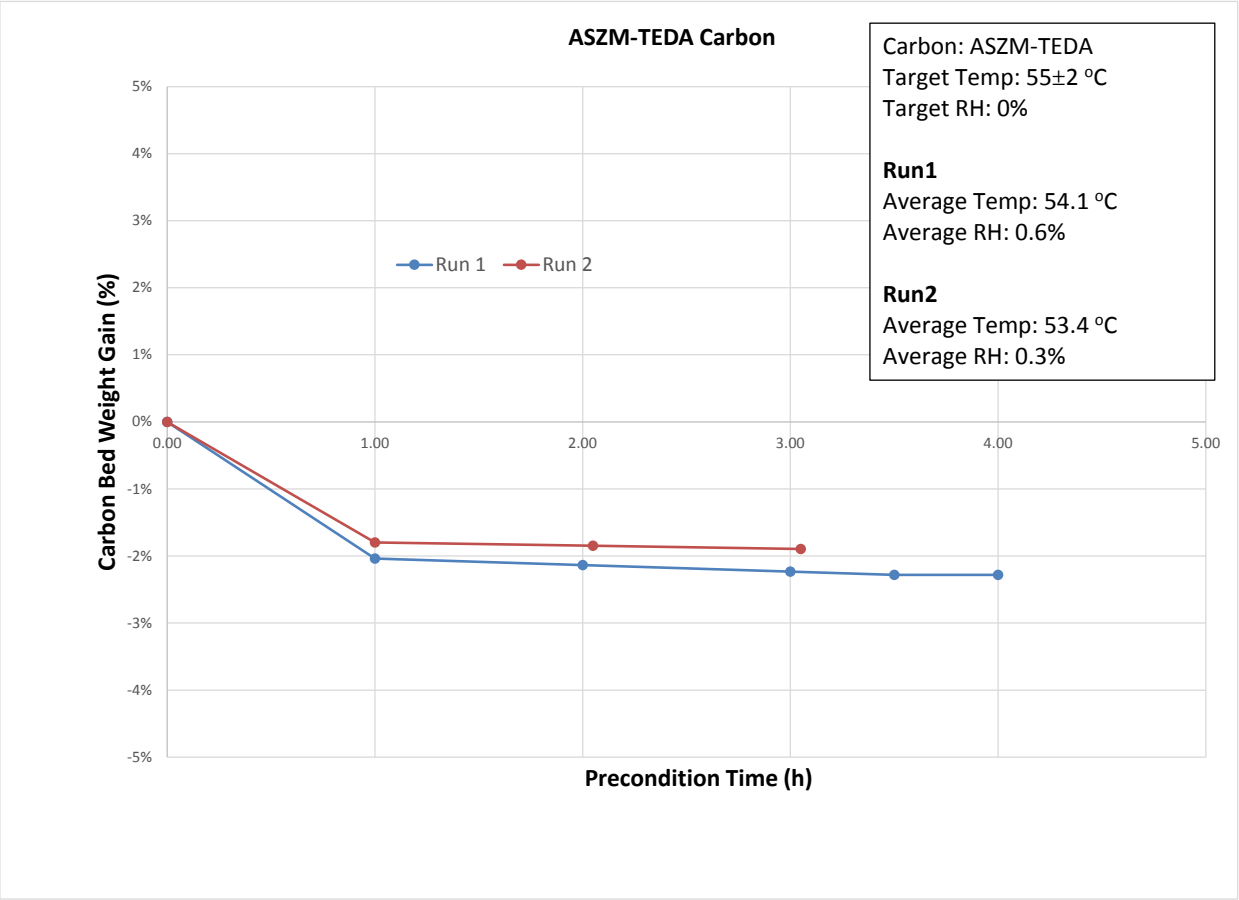

Figure A-5. ASZM-TEDA (6 × 16 mesh) carbon bed weight change versus preconditioning time at 55 ± 2 °C and dry.

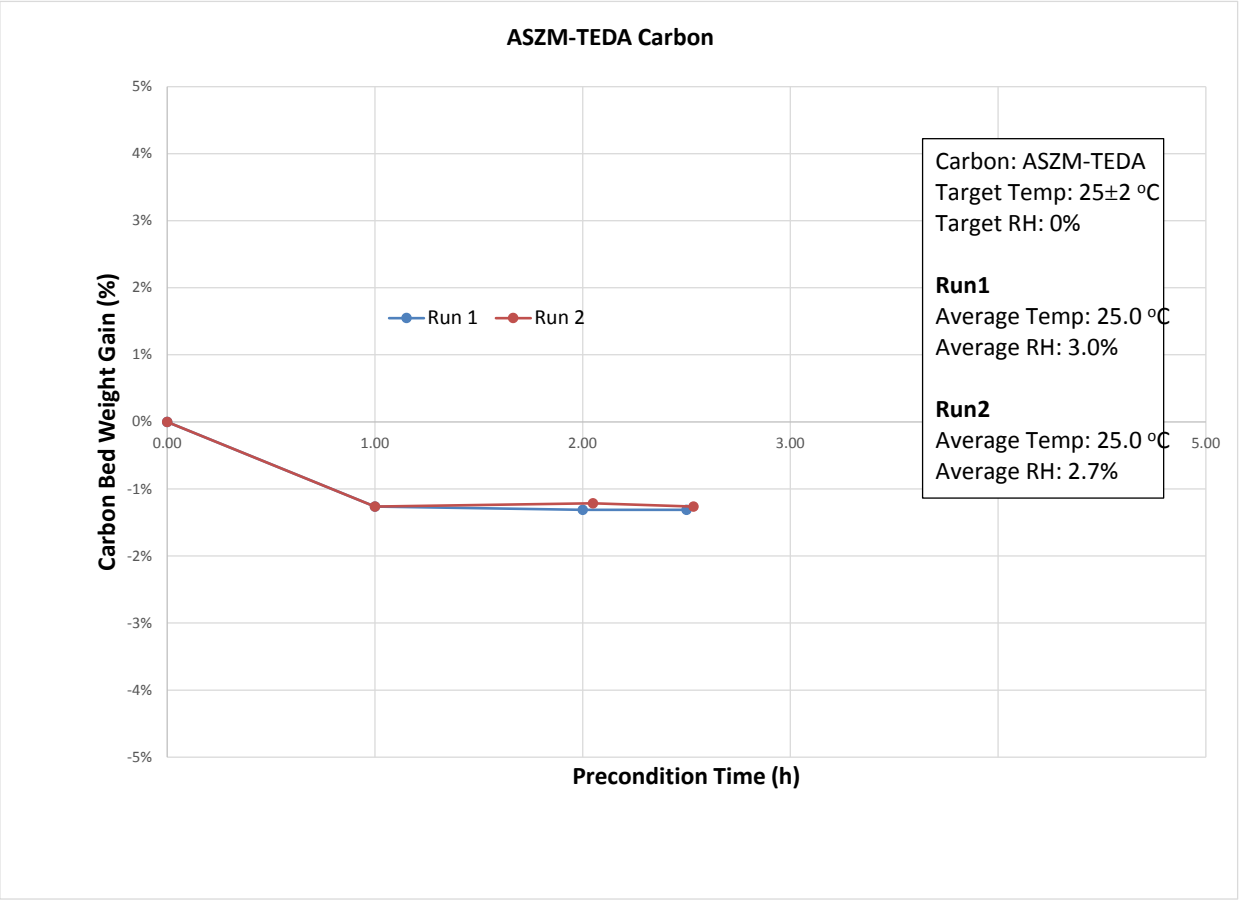

Figure A-6. ASZM-TEDA (6 × 16 mesh) carbon bed weight change versus preconditioning time at 25 ± 2 °C and dry.

The measured plots of weight change of the IONEX 03-001 carbon versus preconditioning time are presented in Figures A-7 to A-8, respectively, for the tests conducted at 55 °C and dry conditions and 25 °C and dry conditions. As shown in Figures A-7 and A-8, the carbon bed reached equilibrium within one hour at both test conditions. The carbon bed lost approximately 4 % of weight at 55 °C and 3 % of weight at 25 °C due to drying.

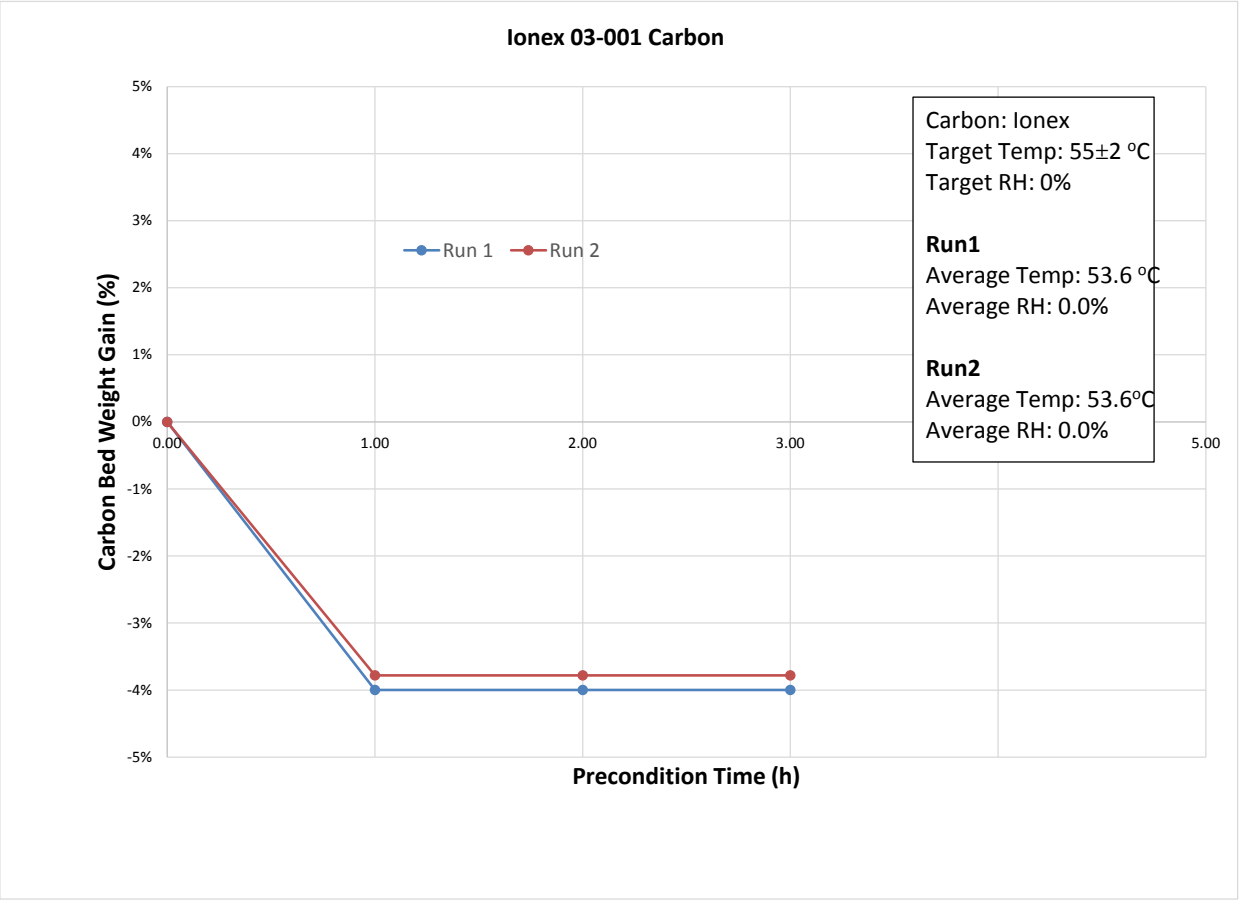

Figure A-7. IONEX 03-001 (8 × 16 mesh) carbon bed weight change versus preconditioning time at 55 ± 2 °C and dry.

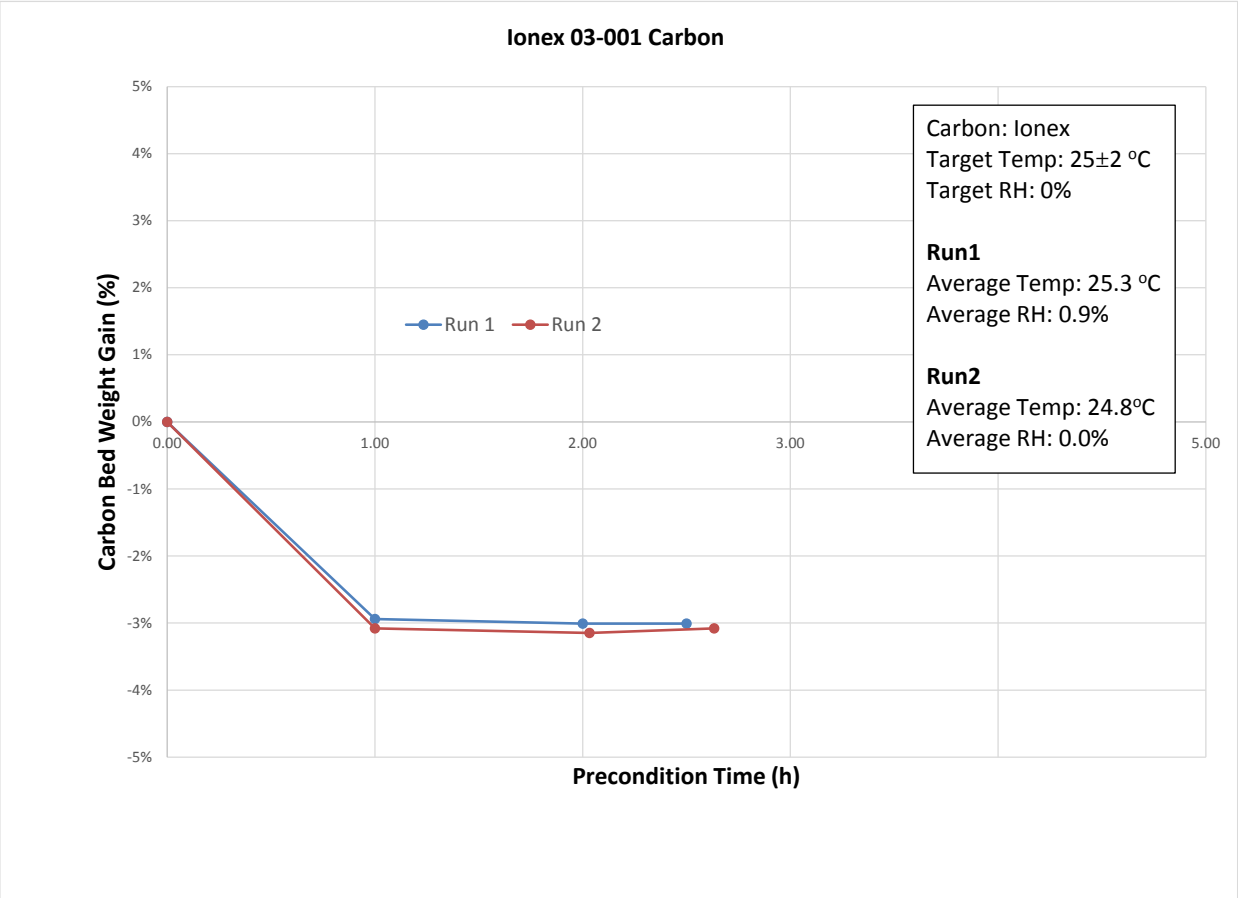

Figure A-8. IONEX 03-001 (8 × 16 mesh) carbon bed weight change versus preconditioning time at 25 ± 2 °C and dry.

The measured plots of weight change of the Vapure 612 carbon versus preconditioning time are presented in Figures A-9 to A-10, respectively, for the tests conducted at 55 °C and dry conditions and 25 °C and dry conditions. As shown in Figures A-9 and A-10, the carbon bed reached equilibrium within one hour at both test conditions. The carbon bed lost about 4.2 % of weight at 55 °C and 3.6 % of weight at 25 °C due to drying.

Based on the test results, at conditions of 55 °C and dry and 25 °C and dry, preconditioning of the ASZM-TEDA, IONEX 03-001, and Vapure 612 carbon beds for one h is sufficient.

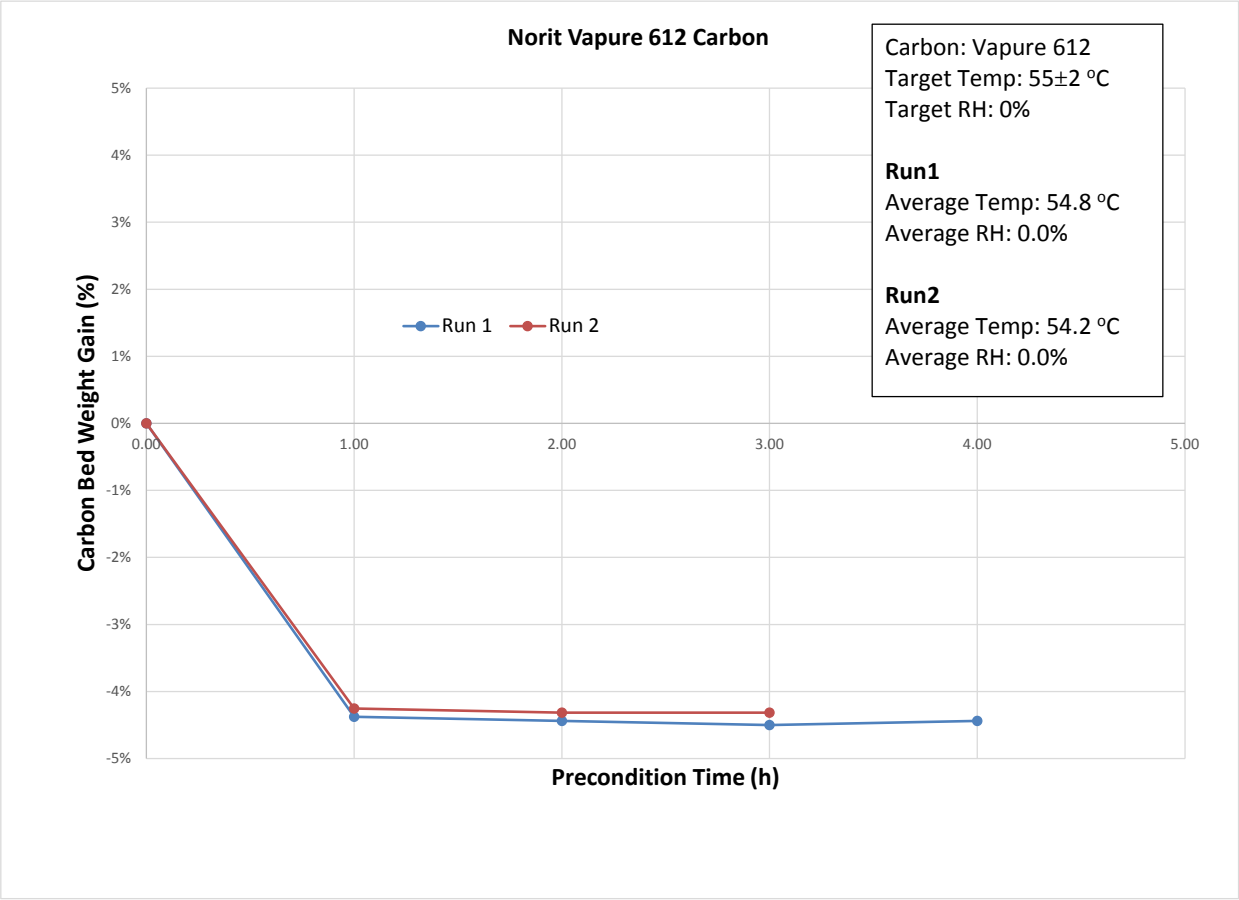

Figure A-9. Vapure 612 (6 × 12 mesh) carbon bed weight change versus preconditioning time at 55 ± 2 °C and dry.

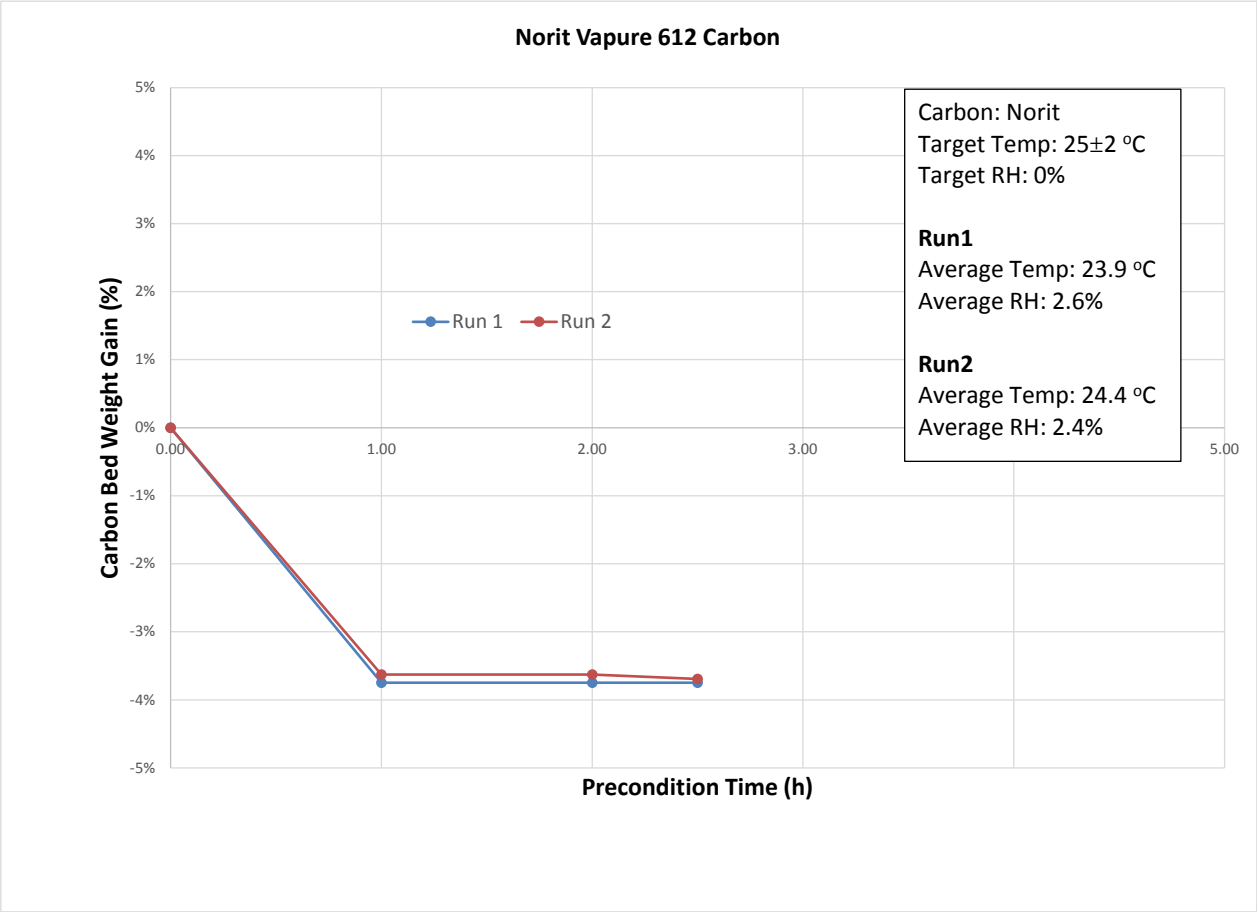

Figure A-10. Vapure 612 (6 × 12 mesh) carbon bed weight change versus preconditioning time at 25 ± 2 °C and dry.

APPENDIX B: OPERATIONAL PARAMETERS FOR THE MINICAMS®

O·I·Analytical — CMS Field Products

Operating Conditions — CMS-7, - — 16:59 08/09/2012

S/N 2078 — RUN NO ALARM

Method: NGS	Parameter	Setpoint	Actual	Limit
TEMPERATURES, °C:	Ambient	40	39	± 25
	Inlet	75	76	± 15
	Detector Block	150	150	± 15
	Detector Flame	315	321	± 99
	Column		200	
	Column 1, Low	50	51	± 15
	Column 1, High	200	200	± 15
	Column 1, Rate, °C/min	200	201	± 20
	Column 2, High	200		
	Column 2, Rate, °C/min	0		
	PCT Heater		137	
	PCT Heater, Low	40	42	± 15
	PCT Heater, High	235	237	± 20
PRESSURES, psig:	Air	25	25	± 5
	Carrier (Nitrogen)	40	39	± 5
	Hydrogen	25	26	± 5
SAMPLE (2 L/min LMF):	Flow Rate, ccm	170	-44	± 50
	Avg. Flow Rate, ccm		199	
	Volume, L @ 21°C, 0 feet		0.598	
VOLTAGE, VDC:	FPD Photomultiplier	600	600	± 50
ELECTROMETER:	FPD Signal, nA	77	FPD Zero, nA	0
	FID Signal, nA	55884	FID Zero, nA	0
TIMED EVENTS, sec:	Purge	0 - 160	Sample	160 - 340
	Desorb	5 - 50	Column 1	40 - 160
	Column 2	160 - 160		

CONCENTRATION REPORTS: — Alarm Setpoint, % ng 0

Cmpd	Status	Concn, mg/m3	Amount, ng	Height,* nA	Area, nA-sec	RT, sec	Width, sec	Gate On	Gate Off
GB	RUN	141	84259	50854	0	60.5	0.0	52	61
GX	RUN	0	0.00	5793	22007	56.8	3.3	52	61

* Concentration readings are based on peak height

CALIBRATION INFORMATION:

Cmpd	Det	ng Level	Date	Time	Height,* nA	Area, nA-sec	RT, sec	Width, sec	Gate On	Gate Off
GB	FID	1200.0	08/07/2012	14:57	724	2716	57.0	3.2	52	61
GX	FPD	1200.0	01/01/2000	00:00	0	0	0.0	0.0	52	61

SAMPLING SEQUENCE: — SOFTWARE: 07022007 — ELAPSED TIME: 85 sec

Figure B-1. Operational parameters of the MINICAMS® for GB detection.

O·I·Analytical — CMS Field Products

Operating Conditions — **CMS-7, -** — **11:19 05/01/2013**

S/N 2078 — **RUN NO ALARM**

Method: MGM3	Parameter	Setpoint	Actual	Limit
TEMPERATURES, ºC:	Ambient	40	41	± 25
	Inlet	75	76	± 15
	Detector Block	150	151	± 15
	Detector Flame	315	306	± 99
	Column		186	
	Column 1, Low	50	51	± 15
	Column 1, High	200	200	± 15
	Column 1, Rate, ºC/min	200	201	± 20
	Column 2, High	200		
	Column 2, Rate, ºC/min	0		
	PCT Heater		63	
	PCT Heater, Low	60	61	± 15
	PCT Heater, High	235	236	± 20
PRESSURES, psig:	Air	25	23	± 5
	Carrier (Nitrogen)	40	38	± 5
	Hydrogen	25	24	± 5
SAMPLE (2 L/min LMF):	Flow Rate, ccm	100	126	± 50
	Avg. Flow Rate, ccm		107	
	Volume, L @ 21°C, 0 feet		0.321	
VOLTAGE, VDC:	FPD Photomultiplier	600	599	± 50
ELECTROMETER:	FPD Signal, nA	29	FPD Zero, nA	0
	FID Signal, nA	71	FID Zero, nA	0
TIMED EVENTS, sec:	Purge	0 - 180	Sample	180 - 360
	Desorb	5 - 60	Column 1	60 - 150
	Column 2	150 - 150		

CONCENTRATION REPORTS: — **Alarm Setpoint, % MGM3** 0

Cmpd	Status	Concn, mg/m3	Concn, MGM3	Height,* nA	Area, nA-sec	RT, sec	Width, sec	Gate On	Gate Off
HD	RUN	0	0.00	0	0	0.0	0.0	143	152
H2	RUN	0	0.00	0	0	0.0	0.0	143	152

* Concentration readings are based on peak height

CALIBRATION INFORMATION:

Cmpd	Det	MGM3 Level	Date	Time	Height,* nA	Area, nA-sec	RT, sec	Width, sec	Gate On	Gate Off
HD	FPD	1.0	04/29/2013	12:05	1059922	3301759	148.7	2.8	143	152
H2	FID	1.0	04/29/2013	12:06	116	340	147.6	2.9	143	152

SAMPLING SEQUENCE: — **SOFTWARE:** 07022007 — **ELAPSED TIME:** 154 sec

Printed : 5/2/2013 11:25 AM — Facility: HMRC (Host 3) — Station: Station 7 — Analysis : 60493

Figure B-2. Operational parameters of the MINICAMS® for HD detection.

APPENDIX C: PLOTS OF GB AND HD CHALLENGE CONCENTRATIONS, TEMPERATURE, RH, FLOW RATE, AND ΔP

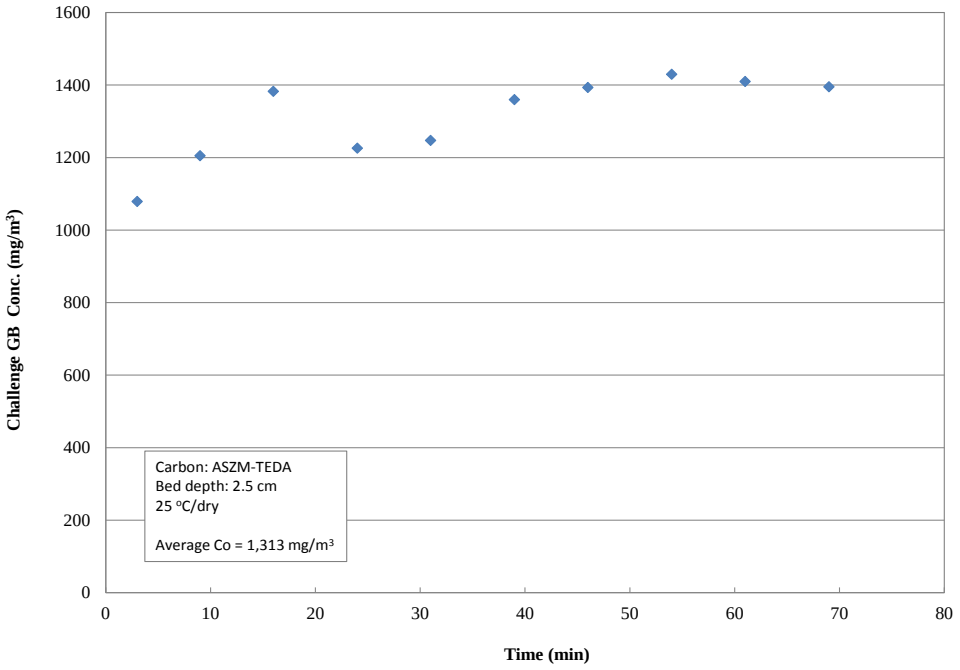

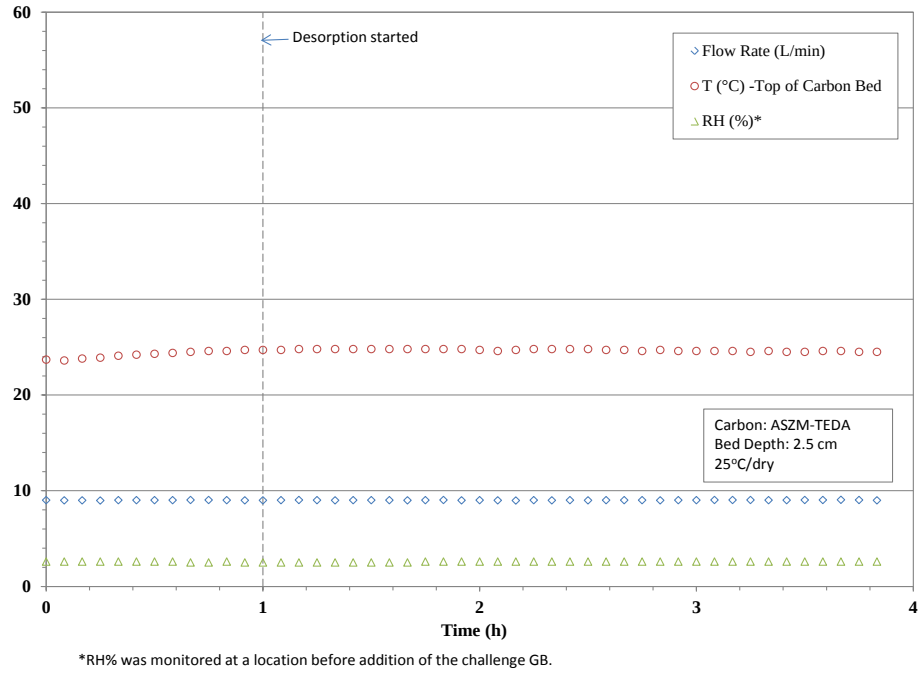

*RH% was monitored at a location before addition of the challenge GB.

Figure C-1. ASZM-TEDA (6 × 16 mesh) carbon, 2.5 cm bed depth, 25 °C/dry.

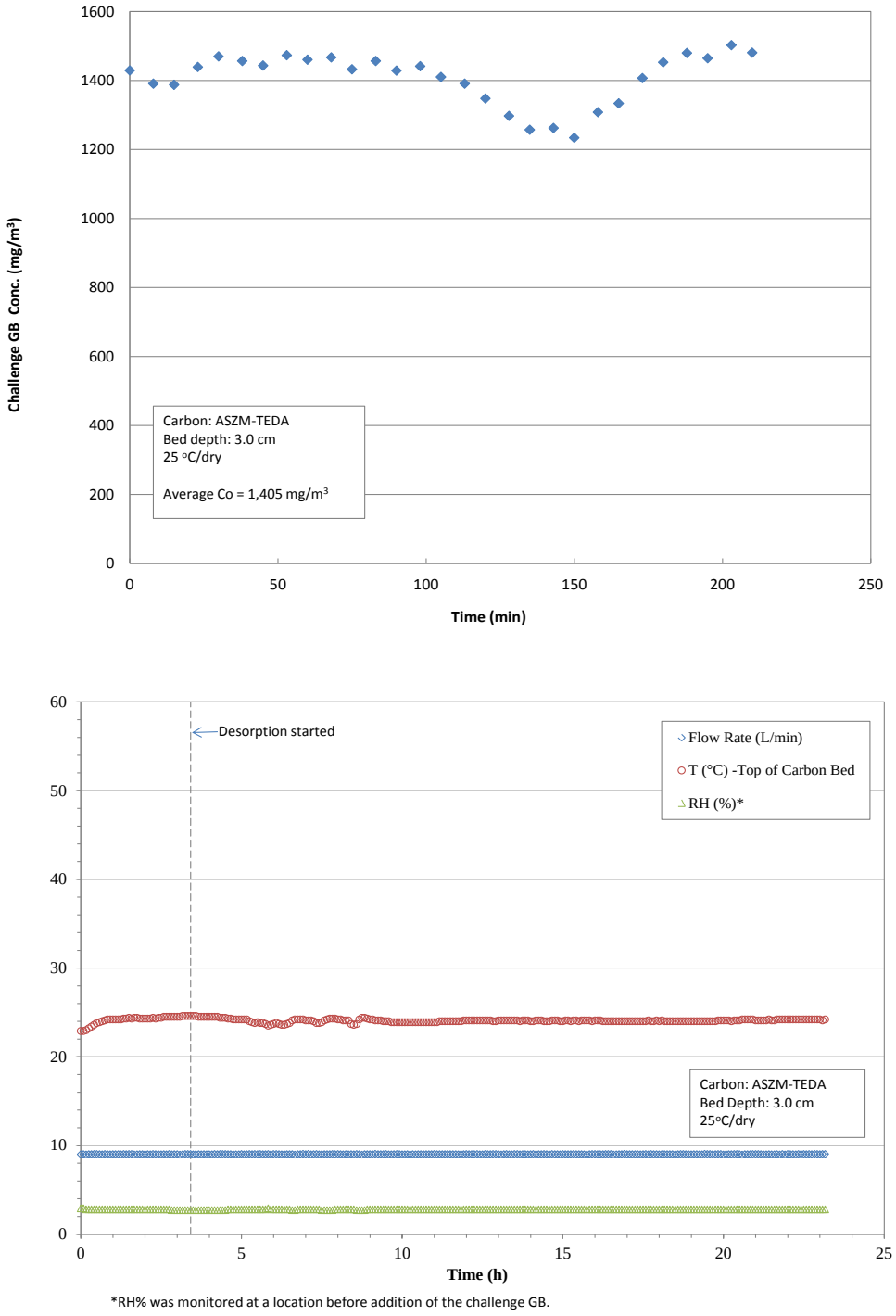

Figure C-2. ASZM-TEDA (6 × 16 mesh) carbon, 3.0 cm bed depth, 25 °C/dry.

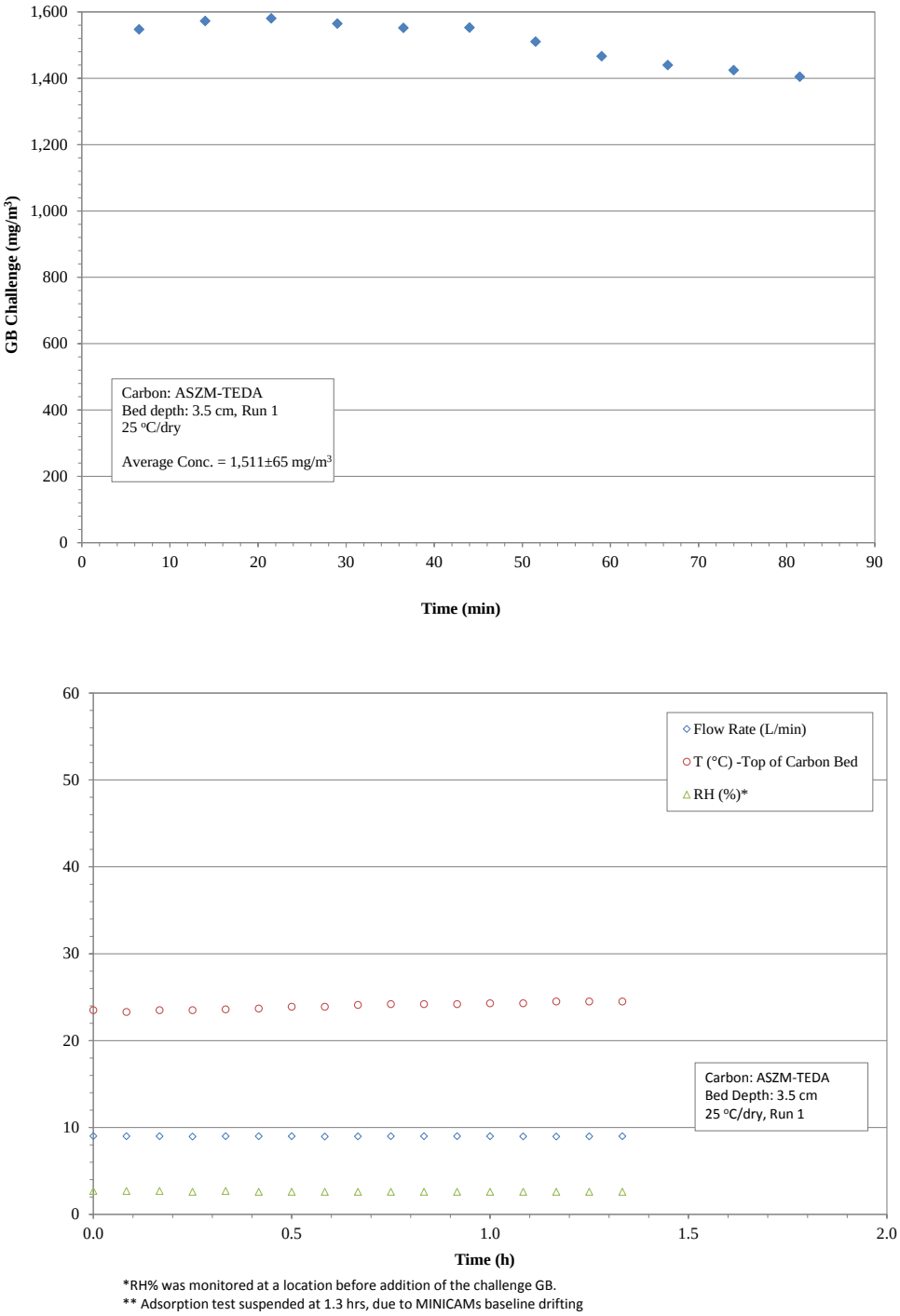

Figure C-3. ASZM-TEDA (6 × 16 mesh) carbon, 3.5 cm bed depth, 25 °C/dry, Run 1.

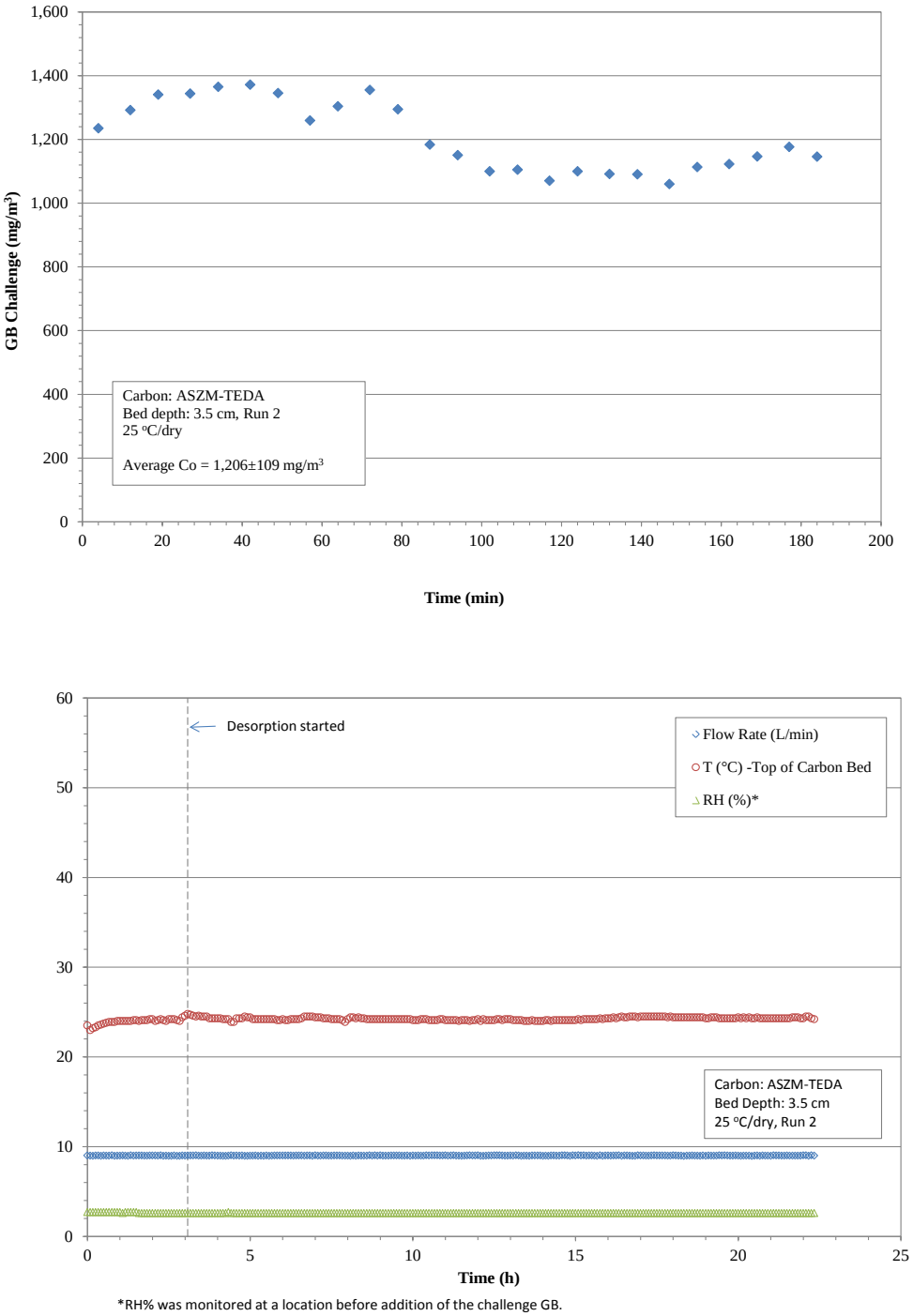

Figure C-4. ASZM-TEDA (6 × 16 mesh) carbon, 3.5 cm bed depth, 25 °C/dry, Run 2.

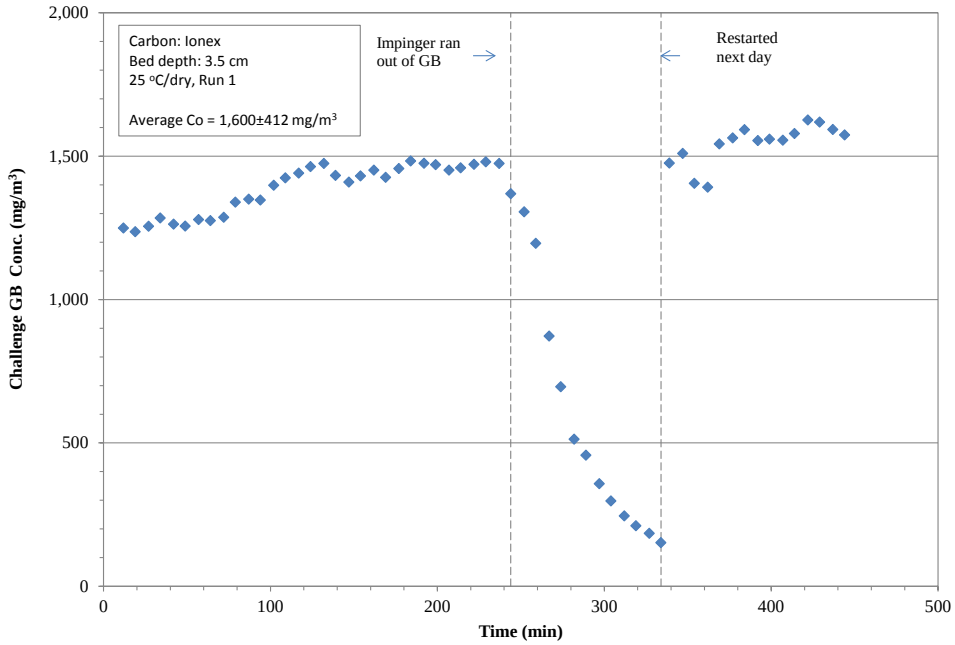

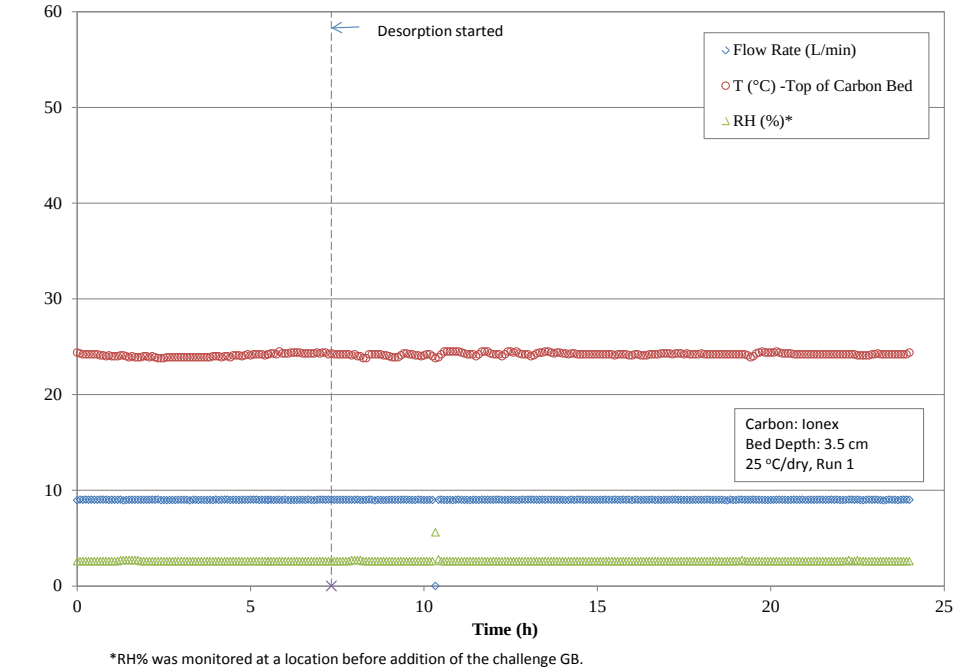

*RH% was monitored at a location before addition of the challenge GB.

Figure C-5. IONEX 03-001 carbon, 3.5 cm bed depth, 25 °C/dry, Run 1.

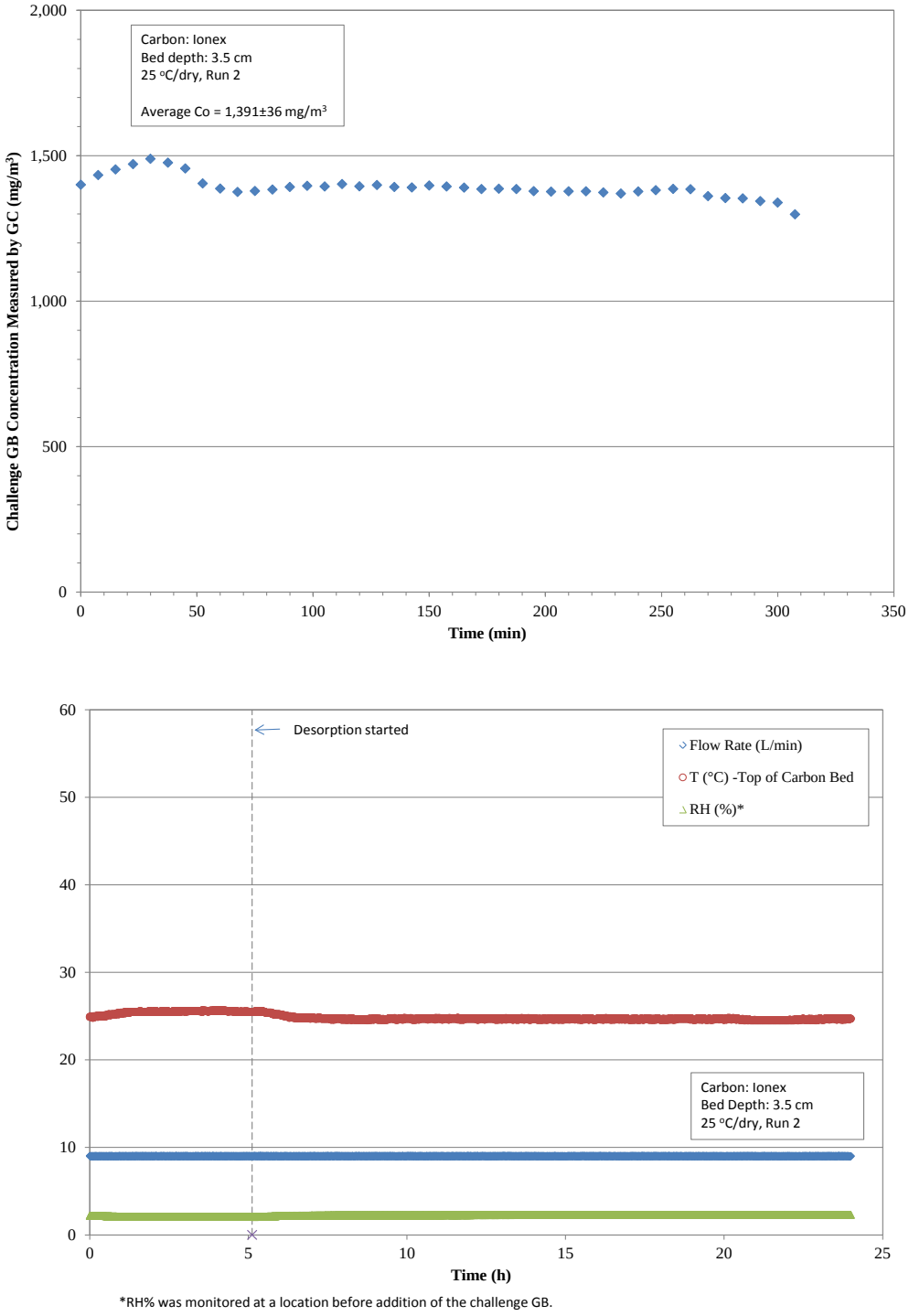

Figure C-6. IONEX 03-001 carbon, 3.5 cm bed depth, 25 °C/dry, Run 2.

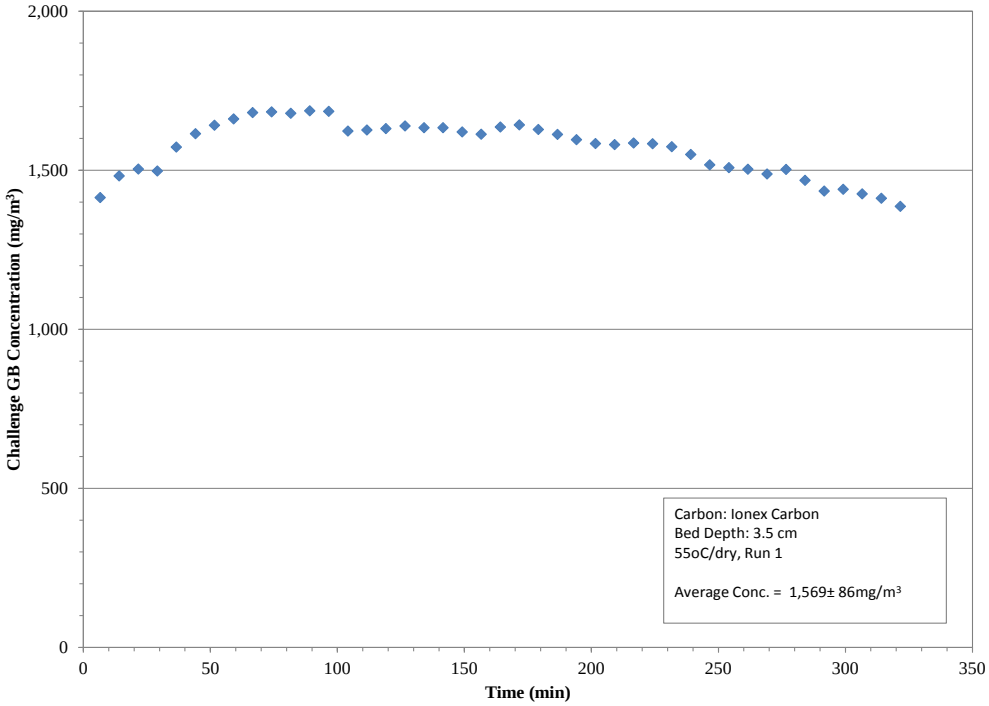

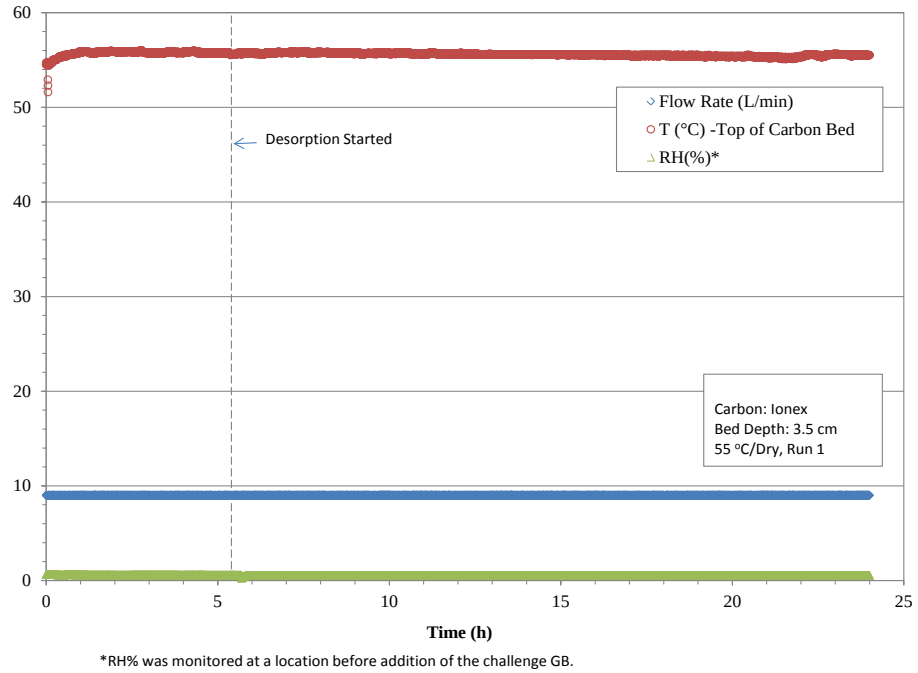

*RH% was monitored at a location before addition of the challenge GB.

Figure C-7. IONEX 03-001 carbon, 3.5 cm bed depth, 55 °C/dry, Run 1.

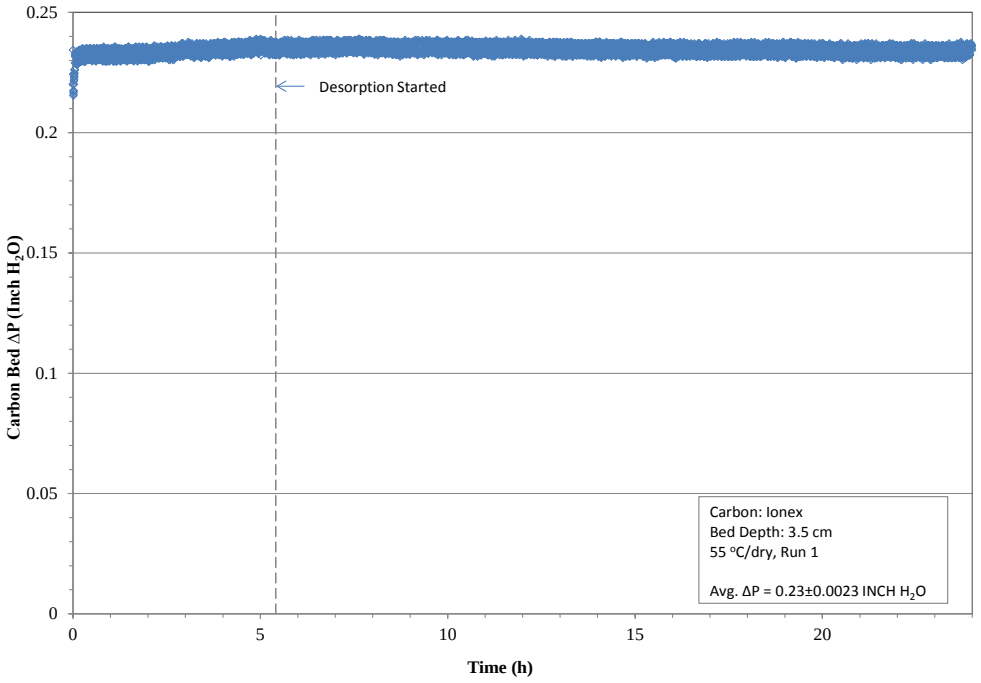

Figure C-8. IONEX 03-001 carbon, 3.5 cm bed depth, 55 °C/dry, Run 1 (Continued).

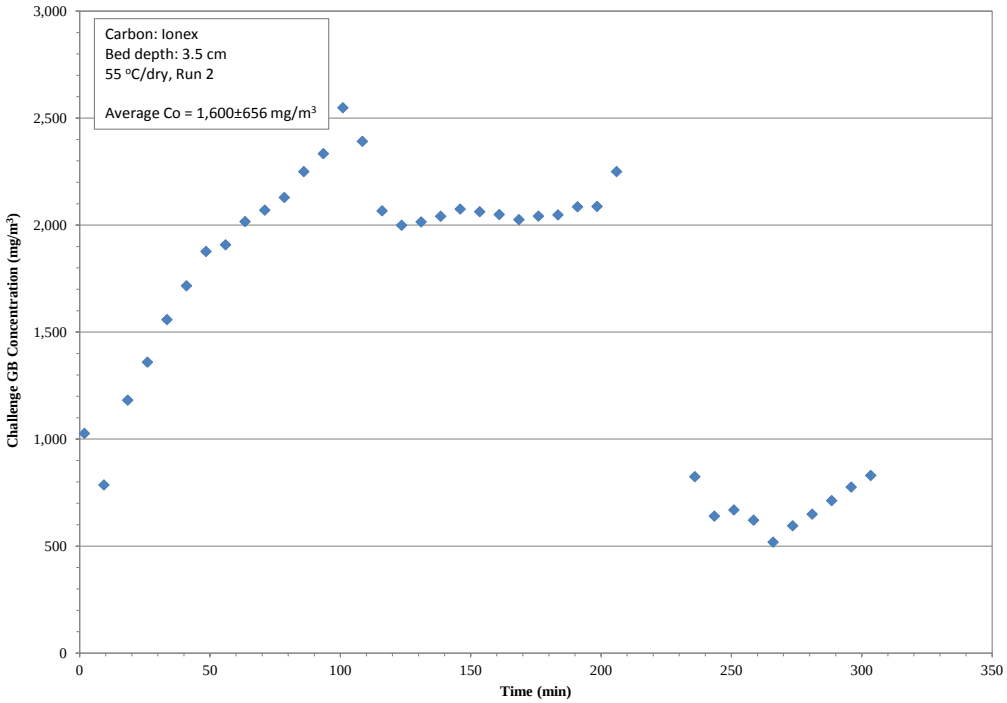

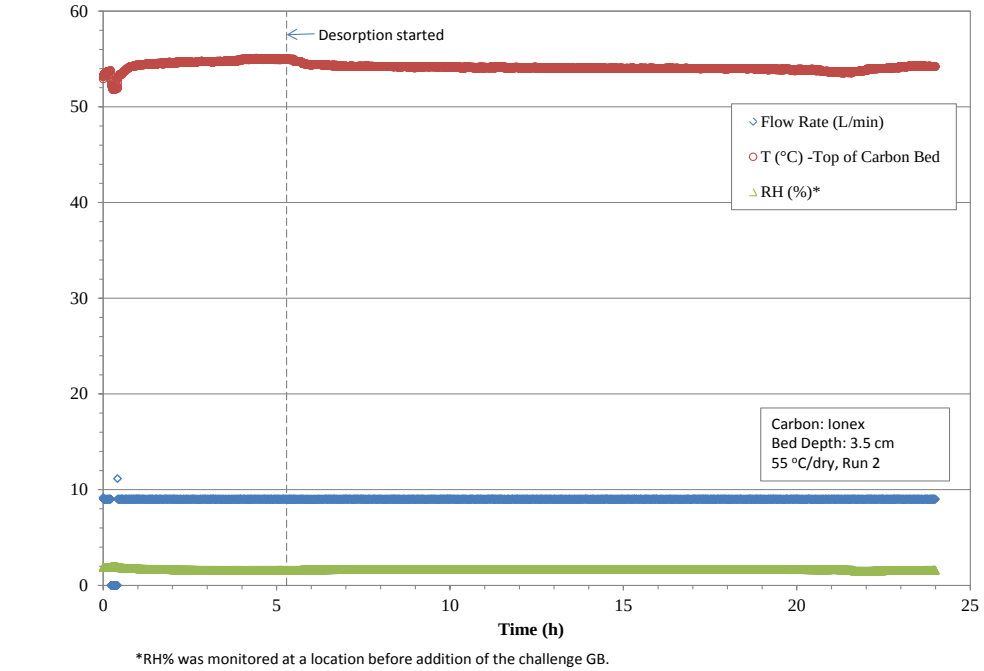

*RH% was monitored at a location before addition of the challenge GB.

Figure C-9. IONEX 03-001 carbon, 3.5 cm bed depth, 55 °C/dry, Run 2.

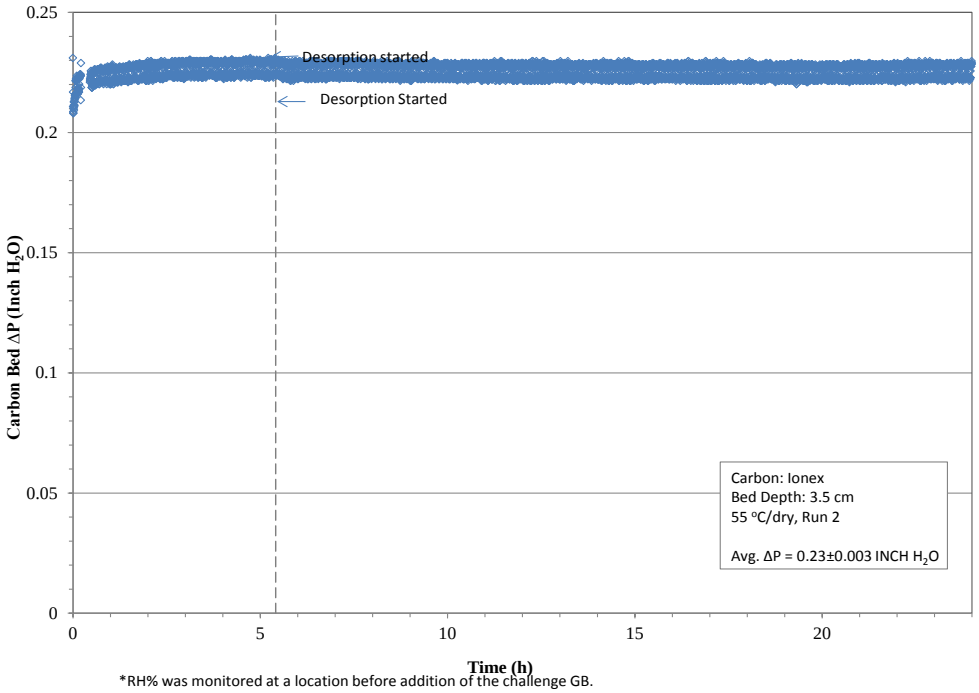

Figure C-10. IONEX 03-001 carbon, 3.5 cm bed depth, 55 °C/dry, Run 2 (continued).

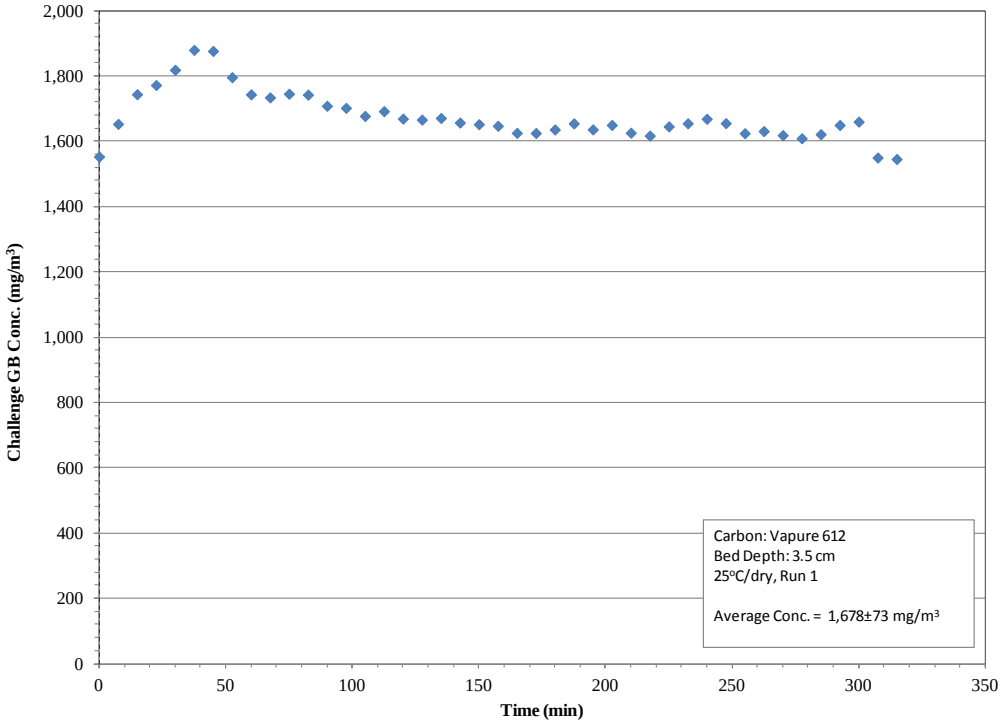

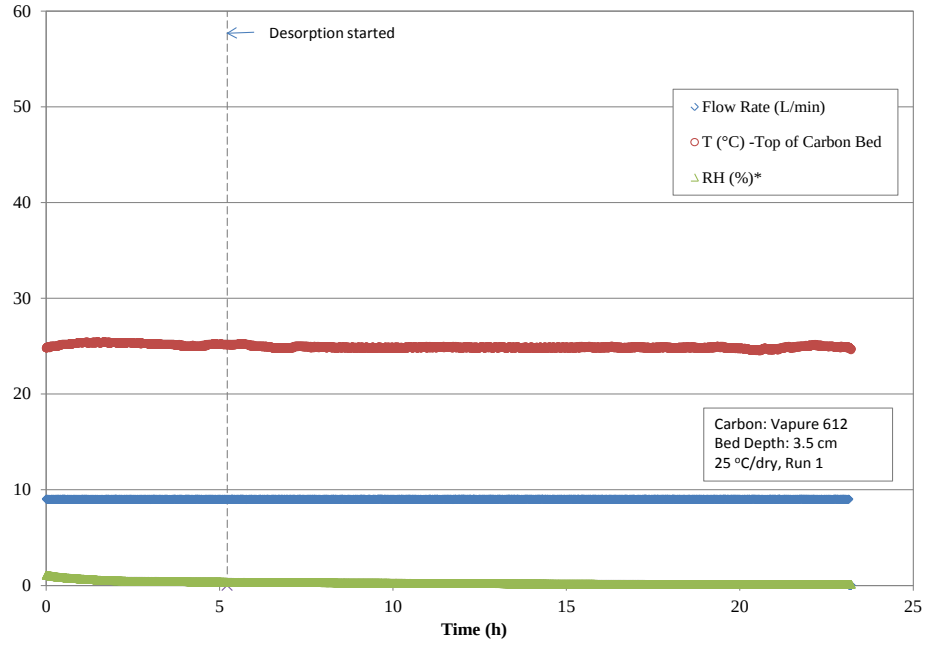

*RH% was monitored at a location before addition of the challenge GB.

Figure C-11. Vapure 612 carbon, 3.5 cm bed depth, 25 °C/dry Run 1.

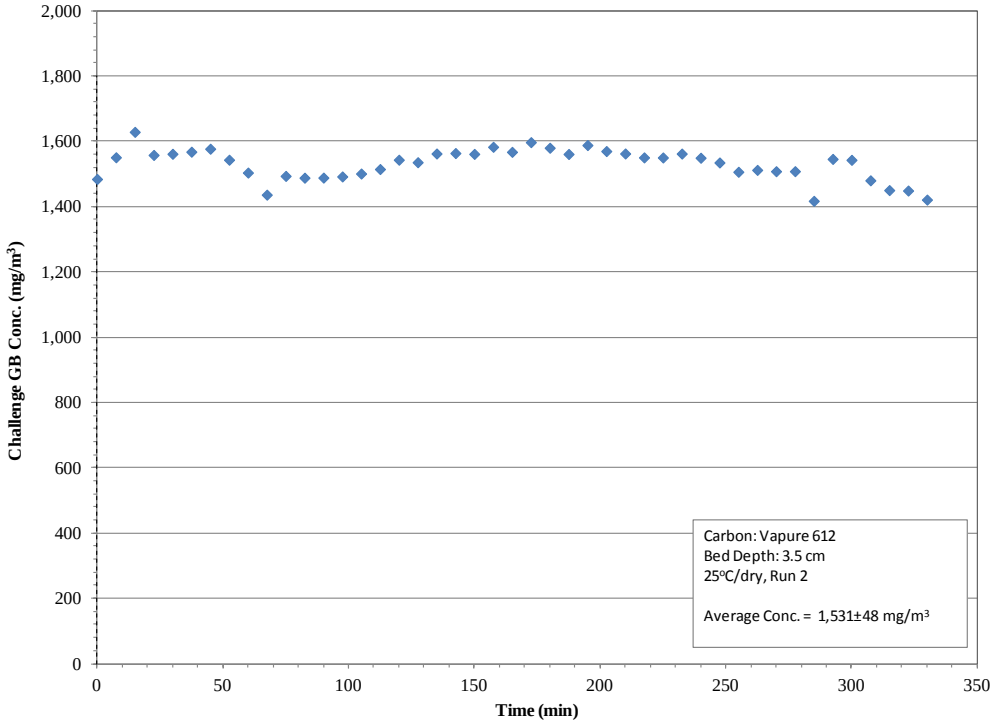

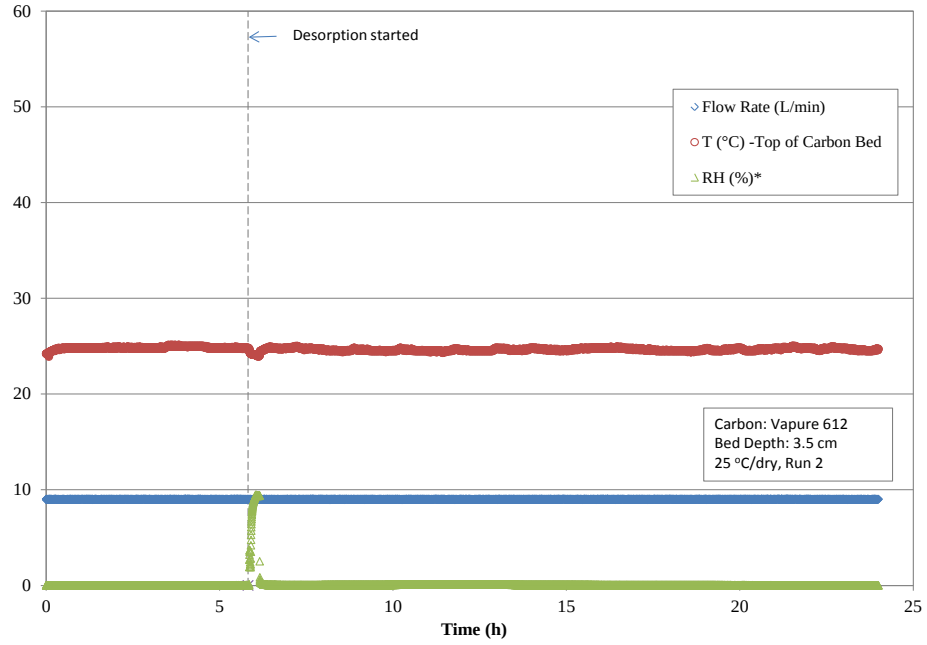

*RH% was monitored at a location before addition of the challenge GB.

Figure C-12. Vapure 612 carbon - 25 °C/dry, 3.5 cm bed depth, Run 2.

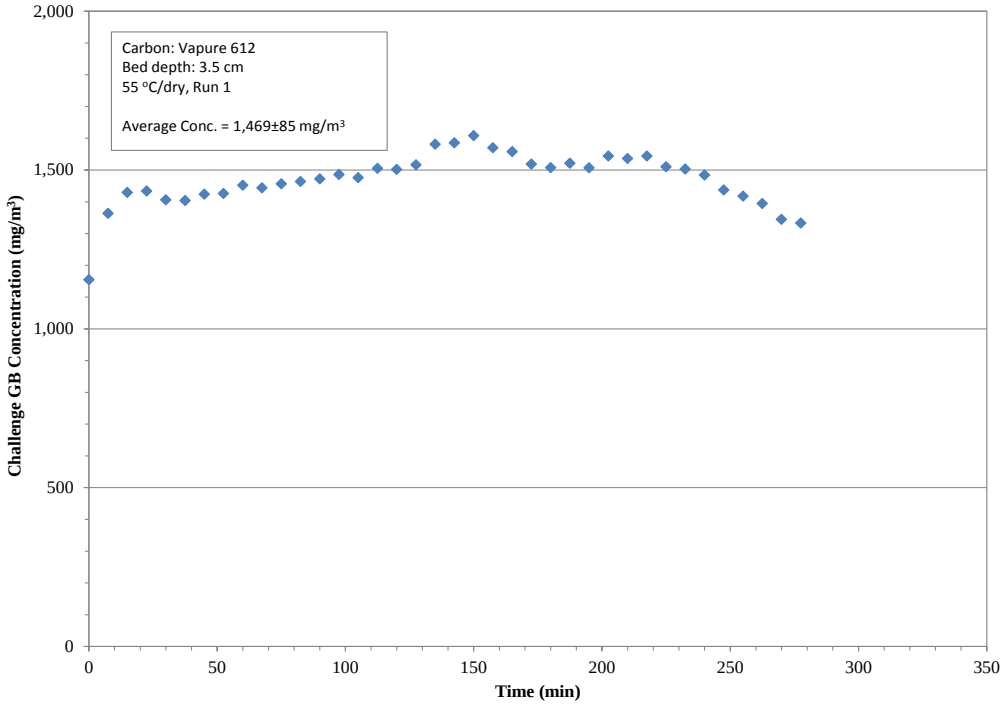

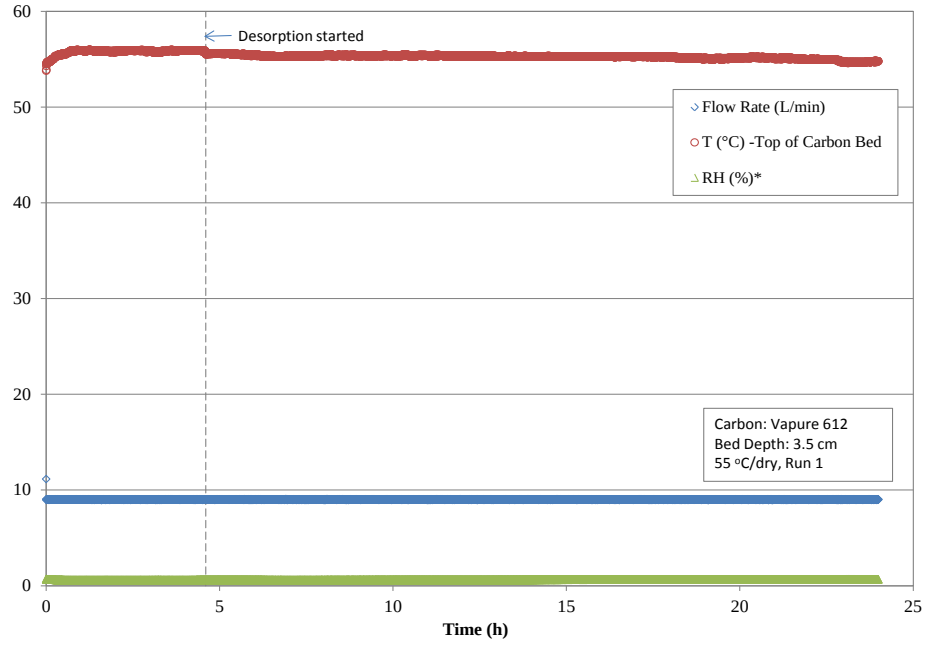

*RH% was monitored at a location before addition of the challenge GB.

Figure C-13. Vapure 612 carbon - 55 °C/dry, 3.5 cm bed depth, Run 1.

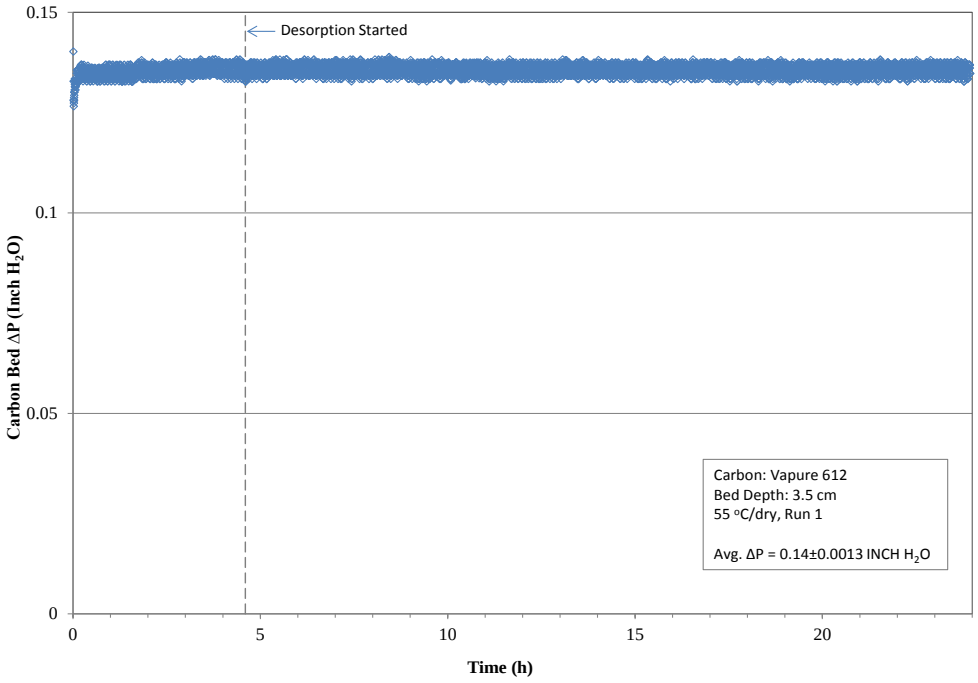

Figure C-14. Vapure 612 carbon - 55 °C/dry, 3.5 cm bed depth, Run 1 (continued).

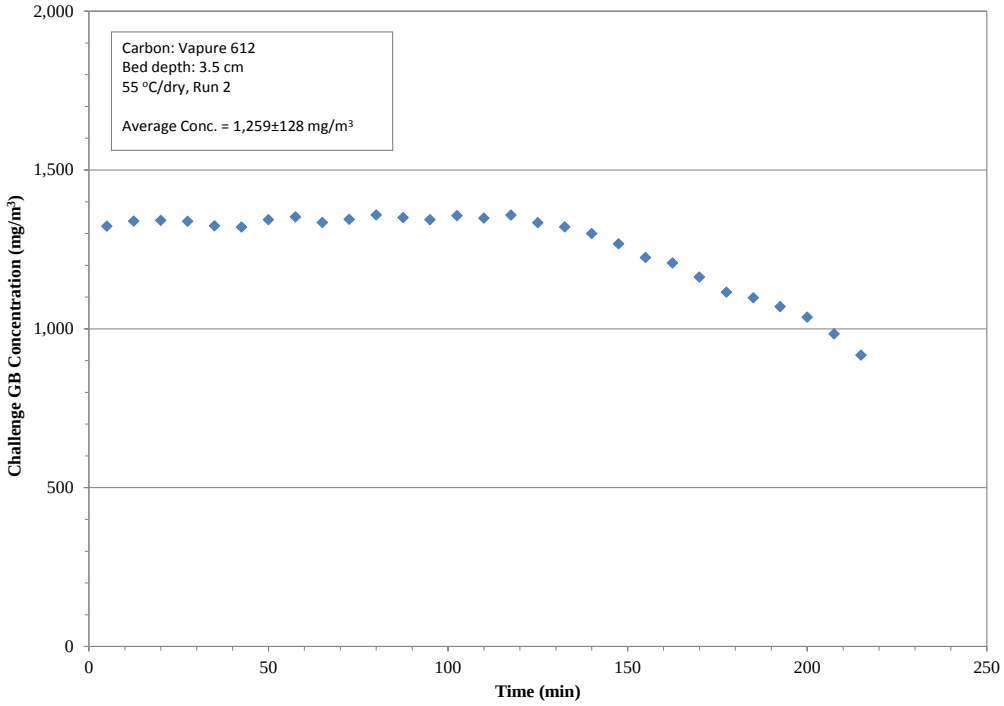

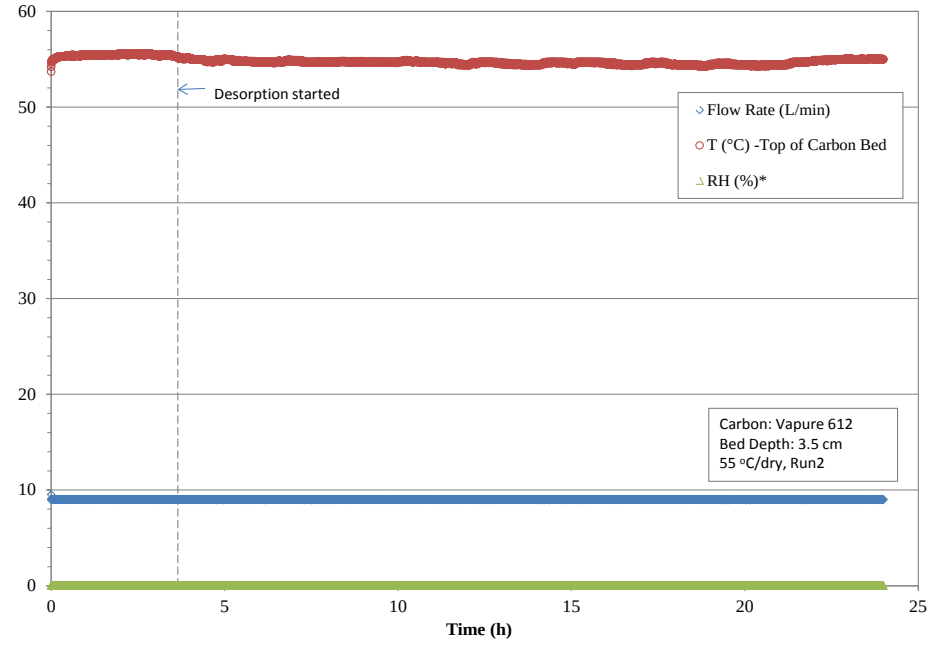

*RH% was monitored at a location before addition of the challenge GB.

Figure C-15. Vapure 612 carbon - 55 °C/dry, 3.5 cm bed depth, Run 2.

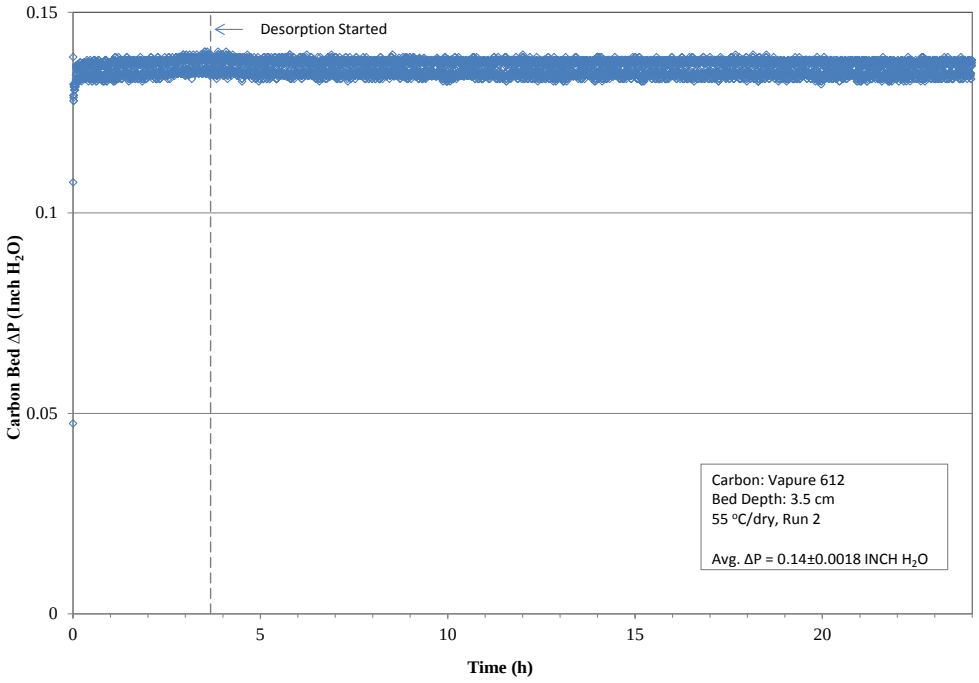

Figure C-16. Vapure 612 carbon – 55 °C/dry, 3.5 cm bed depth, Run 2 (continued).

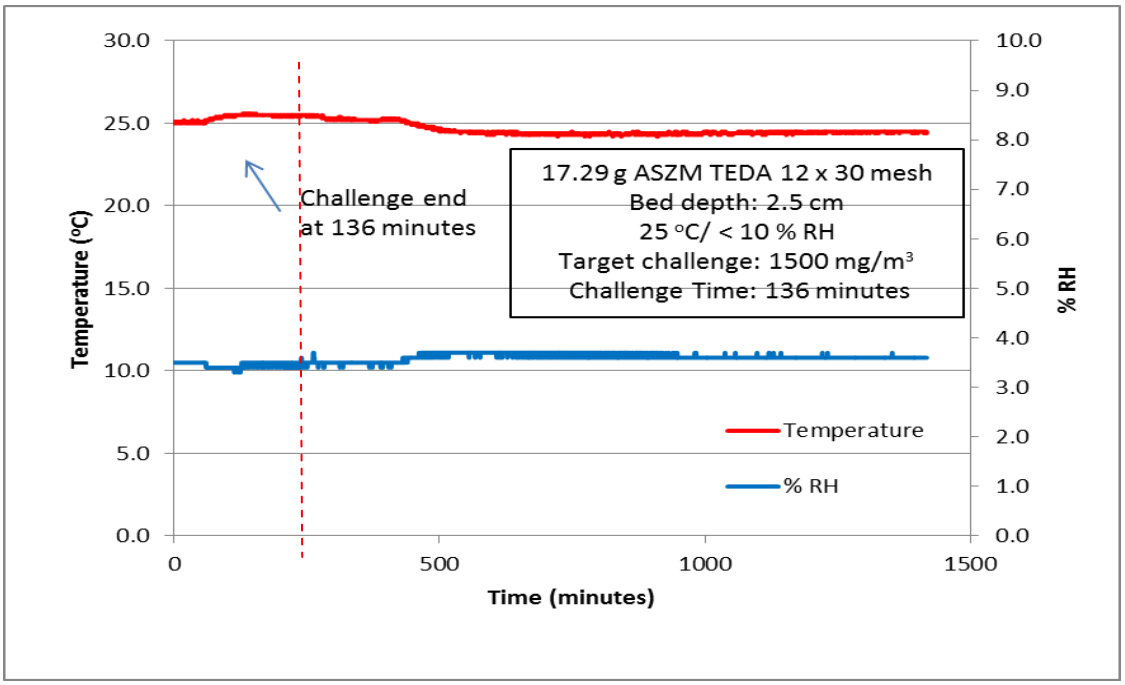

Figure C-17. Temperature and RH measurement for GB adsorption/desorption on ASZM-TEDA (12 × 30 mesh) carbon at 25 °C/dry conditions.

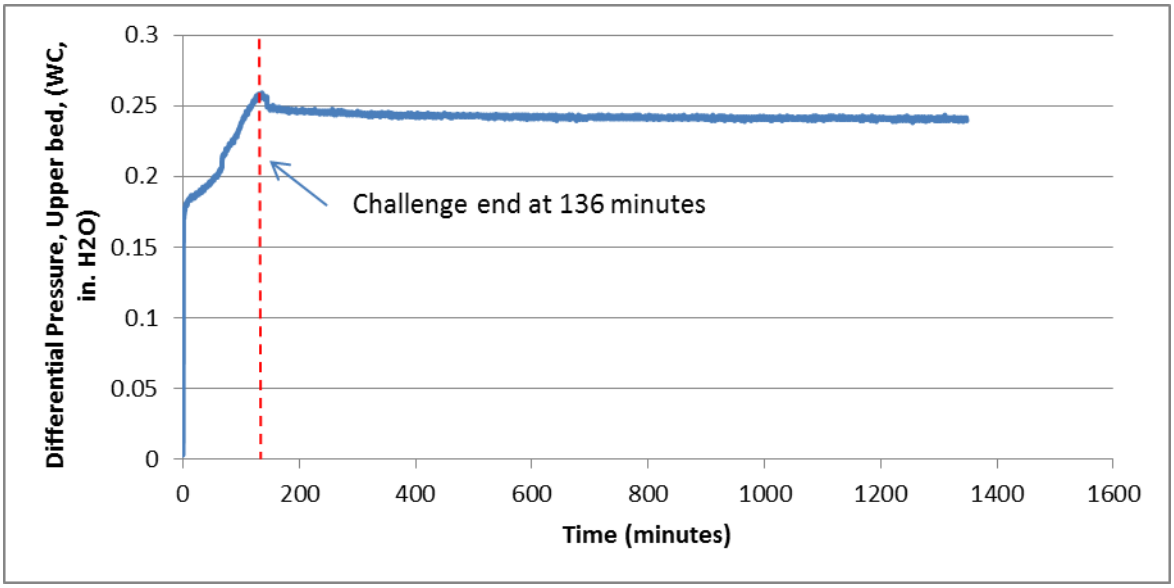

Figure C-18. Pressure differential measurement (upper bed) for GB adsorption / desorption on ASZM-TEDA (12 × 30 mesh) carbon at 25 °/dry conditions.

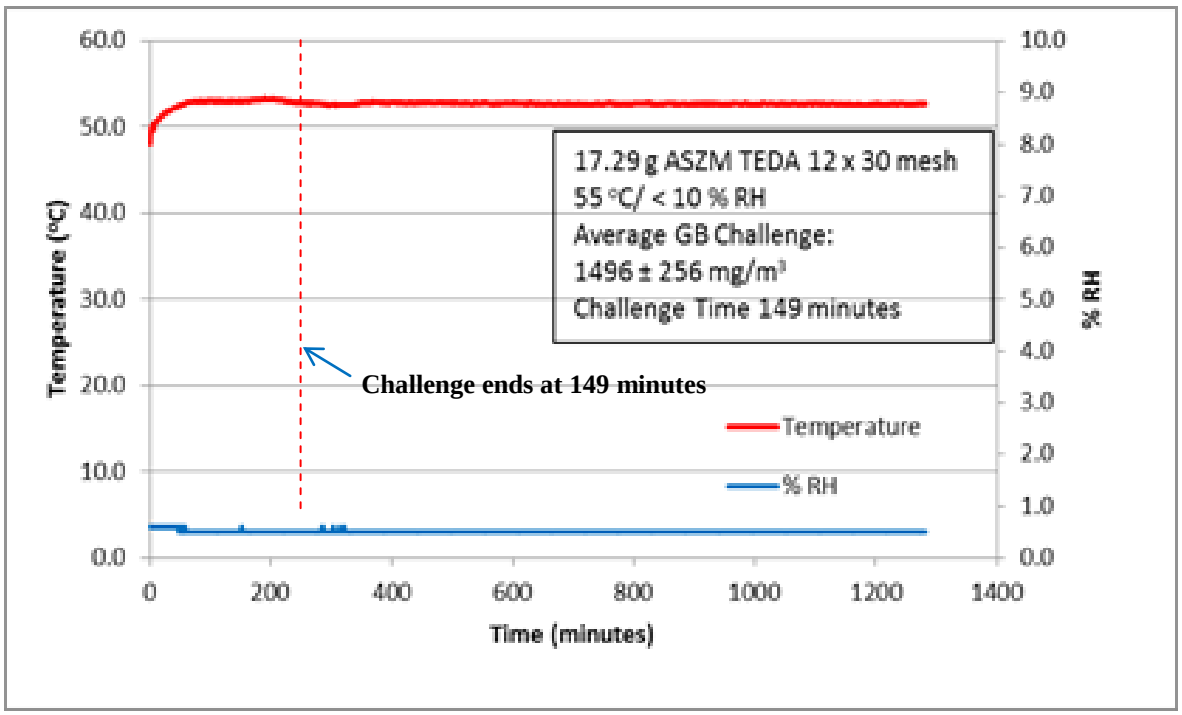

Figure C-19. Temperature and RH measurement for GB adsorption/desorption on ASZM-TEDA (12 × 30 mesh) carbon at 55 ºC/dry conditions.

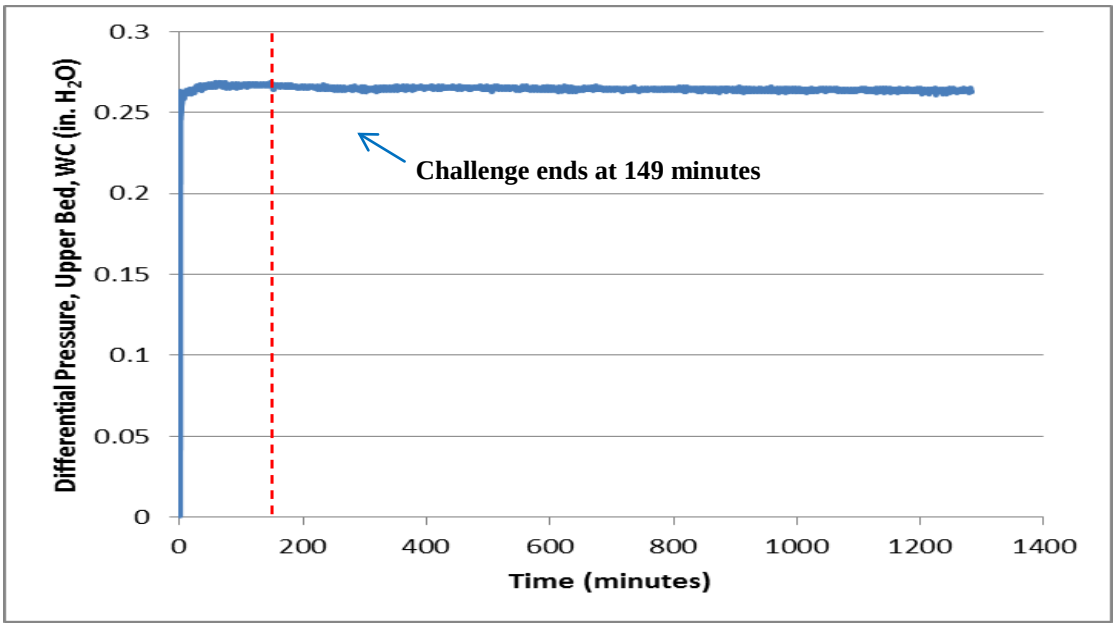

Figure C-20. Pressure differential measurement (upper bed) for GB adsorption/desorption on ASZM-TEDA (12 × 30 mesh) carbon at 55 ºC/dry conditions.

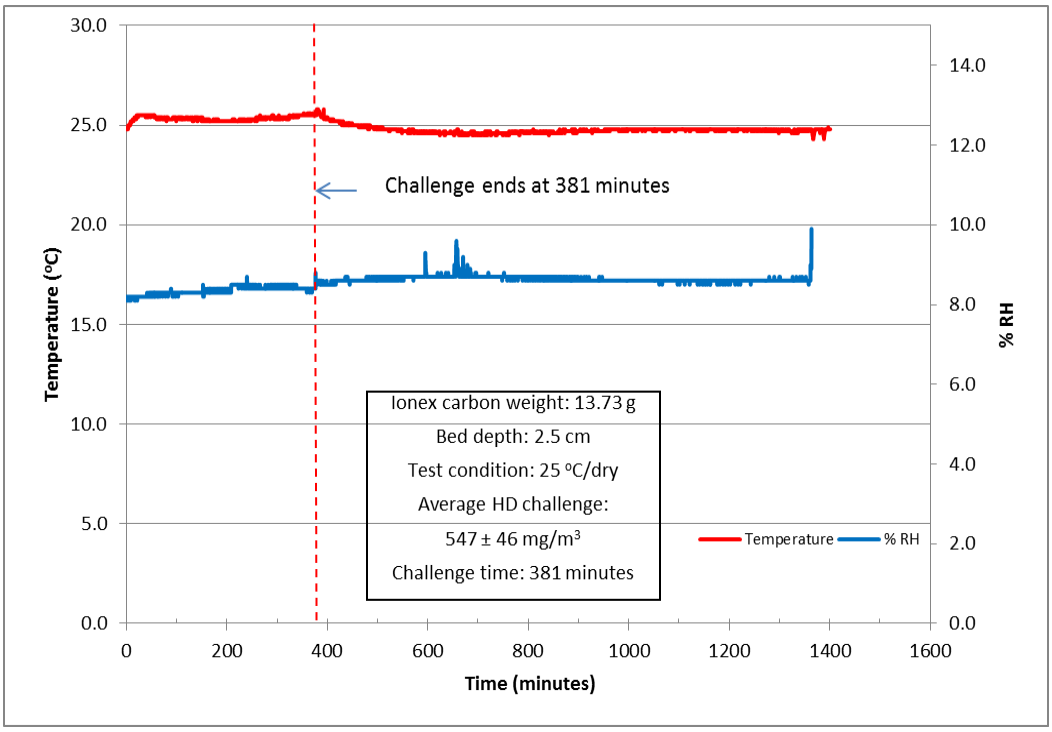

Figure C-21. Temperature and RH measurement for HD adsorption/desorption on IONEX 03-001 carbon at 25 °C/dry conditions.

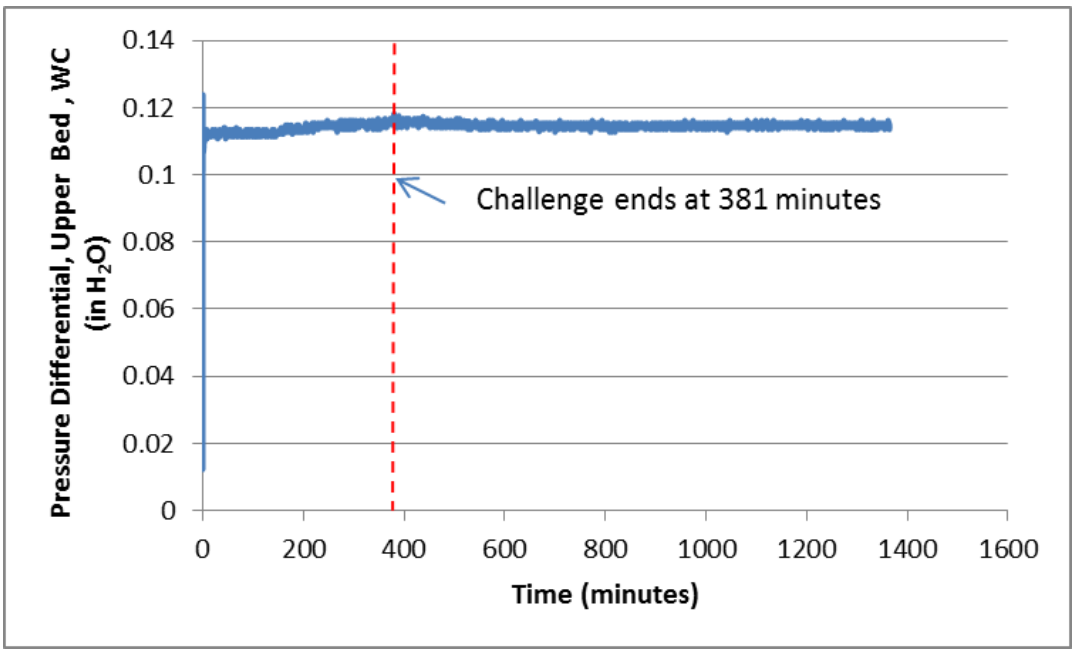

Figure C-22. Pressure differential measurement (upper bed) for HD adsorption/desorption on IONEX 03-001 carbon at 25 °C/dry conditions.

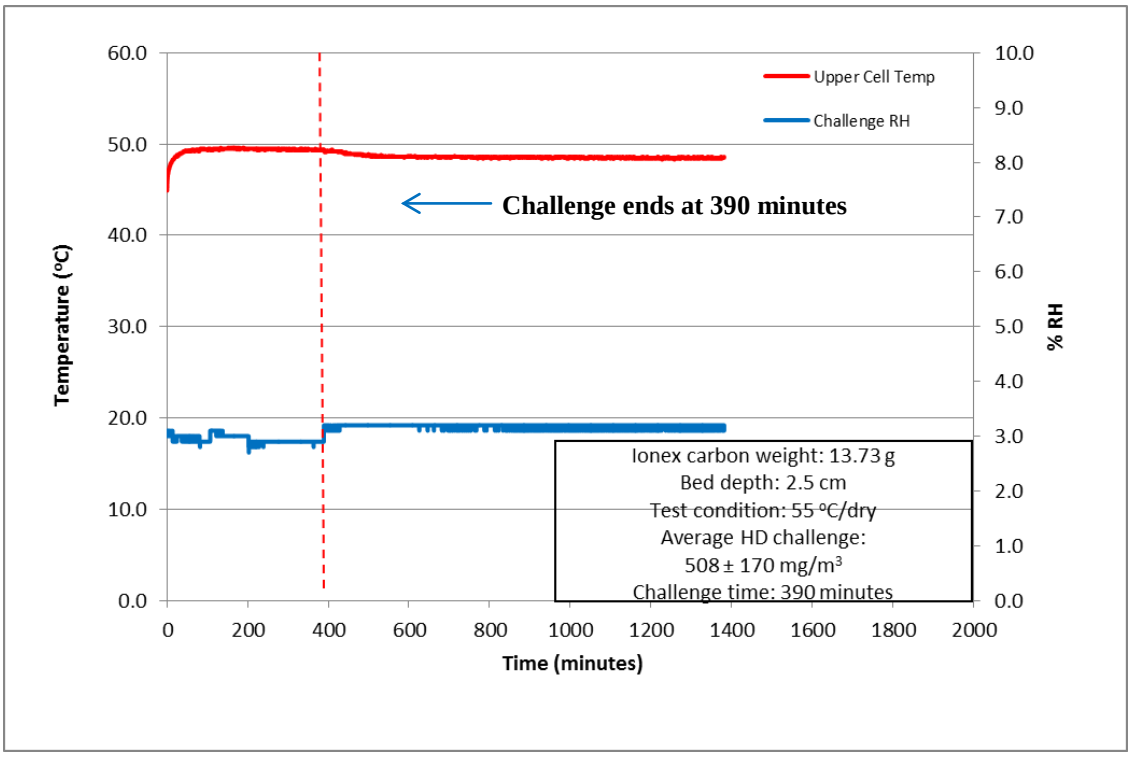

Figure C-23. Temperature and RH measurement for HD adsorption/desorption on IONEX 03-001 carbon at 55 ºC/dry conditions.

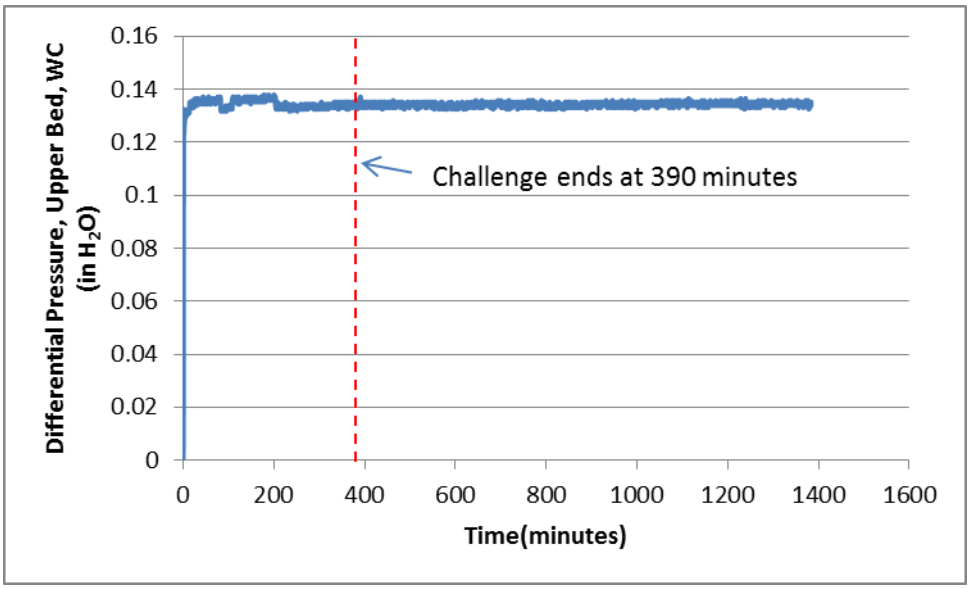

Figure C-24. Pressure differential measurement (upper bed) for HD adsorption/desorption on IONEX 03-001 carbon at 55 ºC/dry conditions.

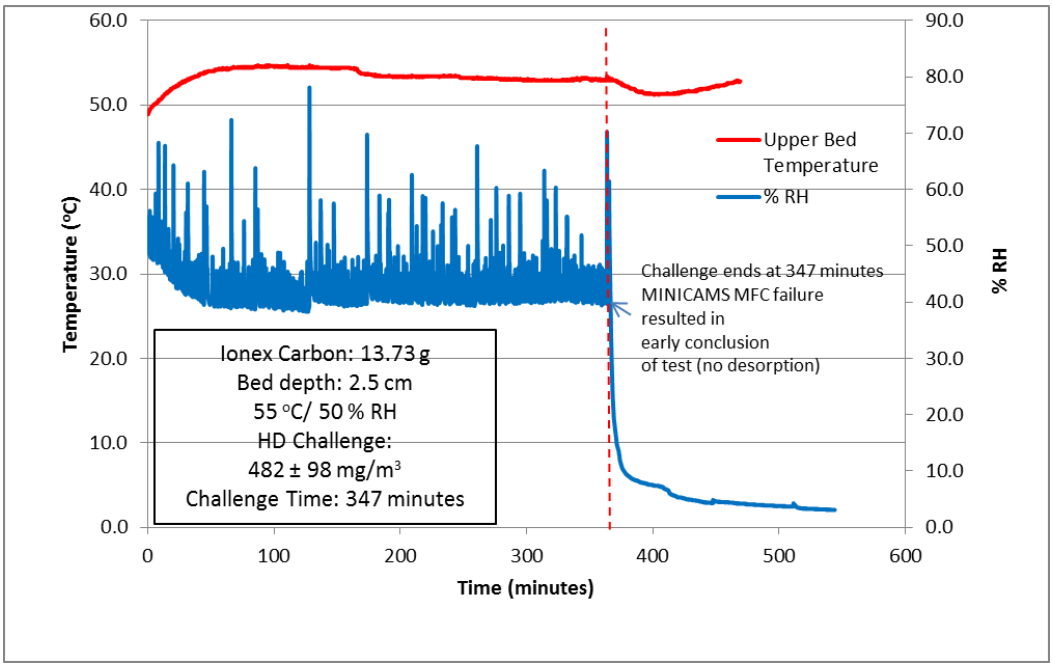

Figure C-25. Temperature and RH measurement for HD adsorption/desorption on IONEX 03-001 carbon at 55 °C/humid conditions.

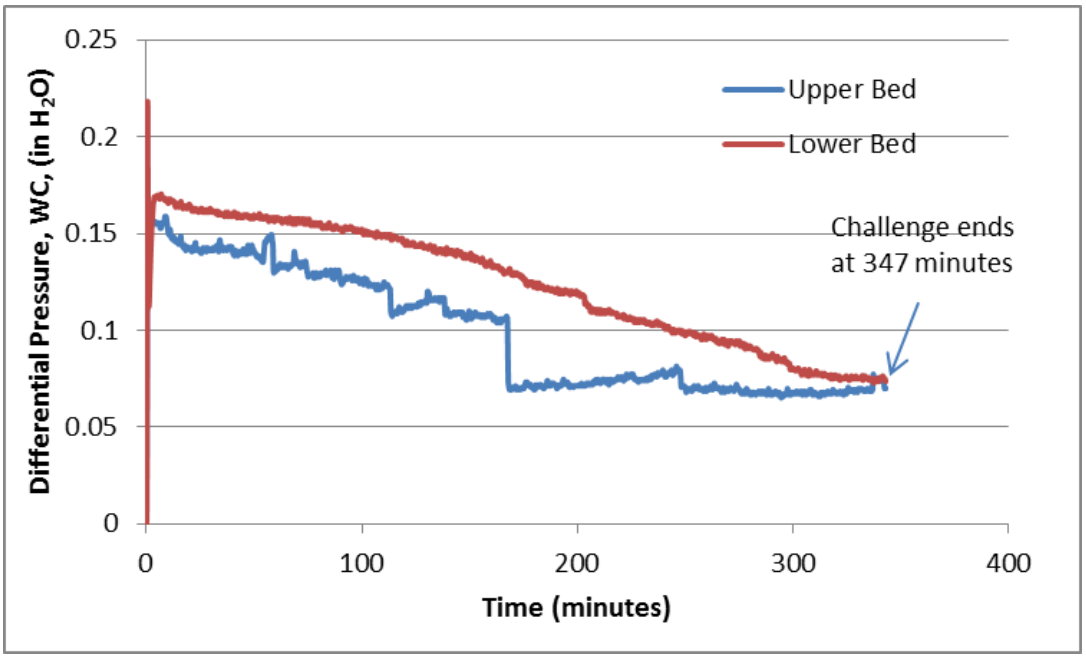

Figure C-26. Pressure differential measurement (upper and lower bed) for HD adsorption/desorption on IONEX 03-001 carbon at 55 °C/humid conditions.[1]

[1] Pressure drop measurements were made above and below the test bed relative to ambient pressure in all tests. Pressure drop results for tests were typically identical at both locations and maintained consistent values. For this test, there was a difference noted between the upper and lower pressure drop measurements. Further, a decreasing trend in pressure drop was noted during the challenge test period (347 minutes). It is unclear whether the changes in pressure drop could be associated with the formation of TDG (and subsequent condensation) on the carbon bed.

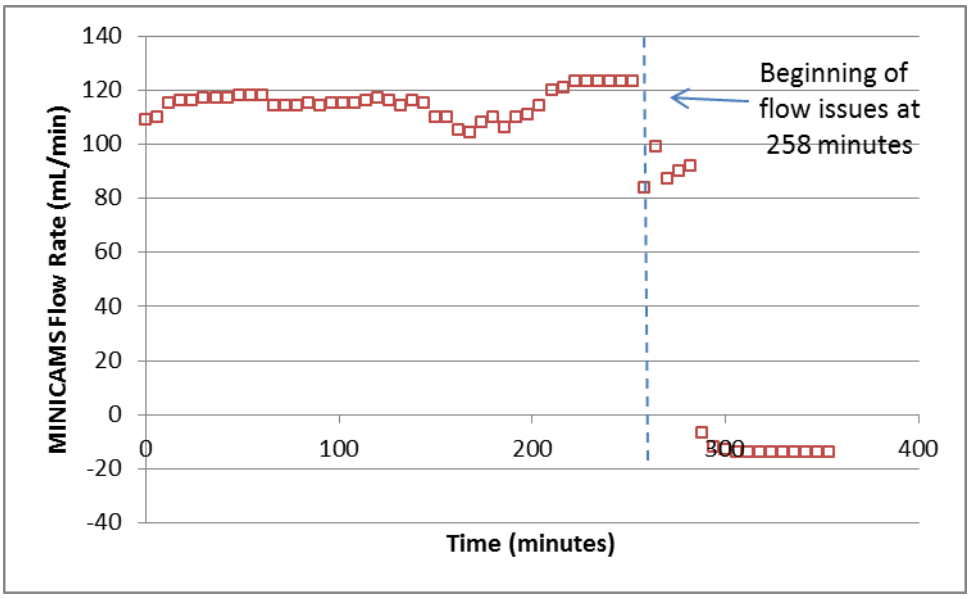

Figure C-27. MINICAMS® sampling flow rate capture data for IONEX 03-001 carbon at 55 ºC/humid conditions.

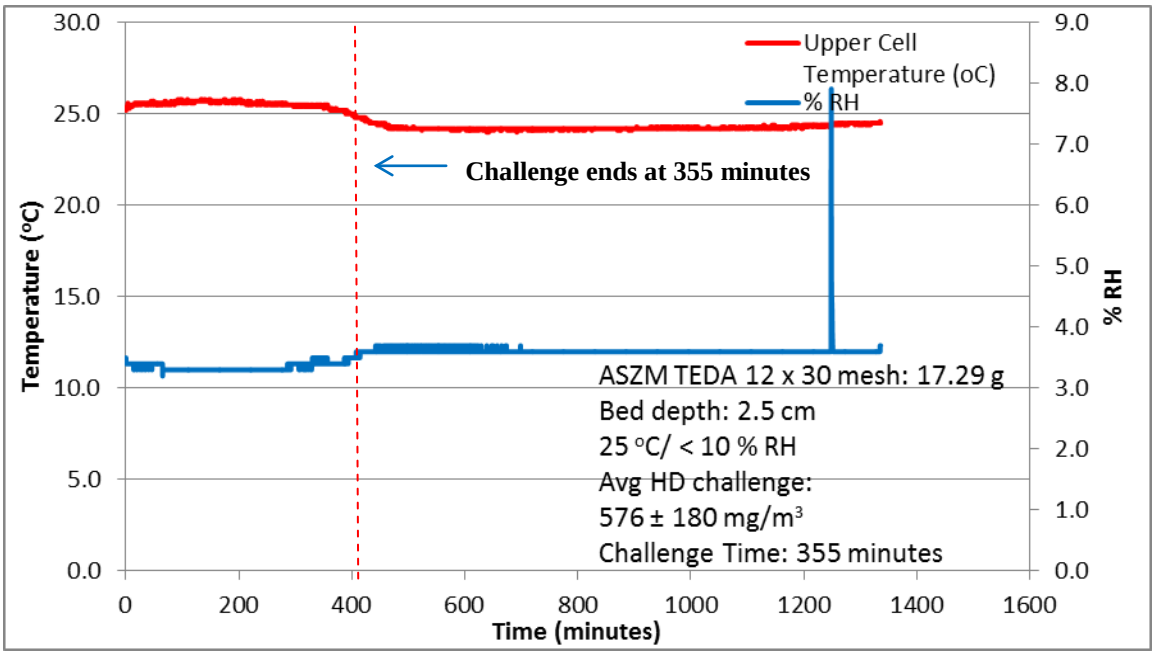

Figure C-28. Temperature and RH measurement for HD adsorption/desorption on ASZM-TEDA (12 × 30 mesh) carbon at 25 °C/dry conditions.

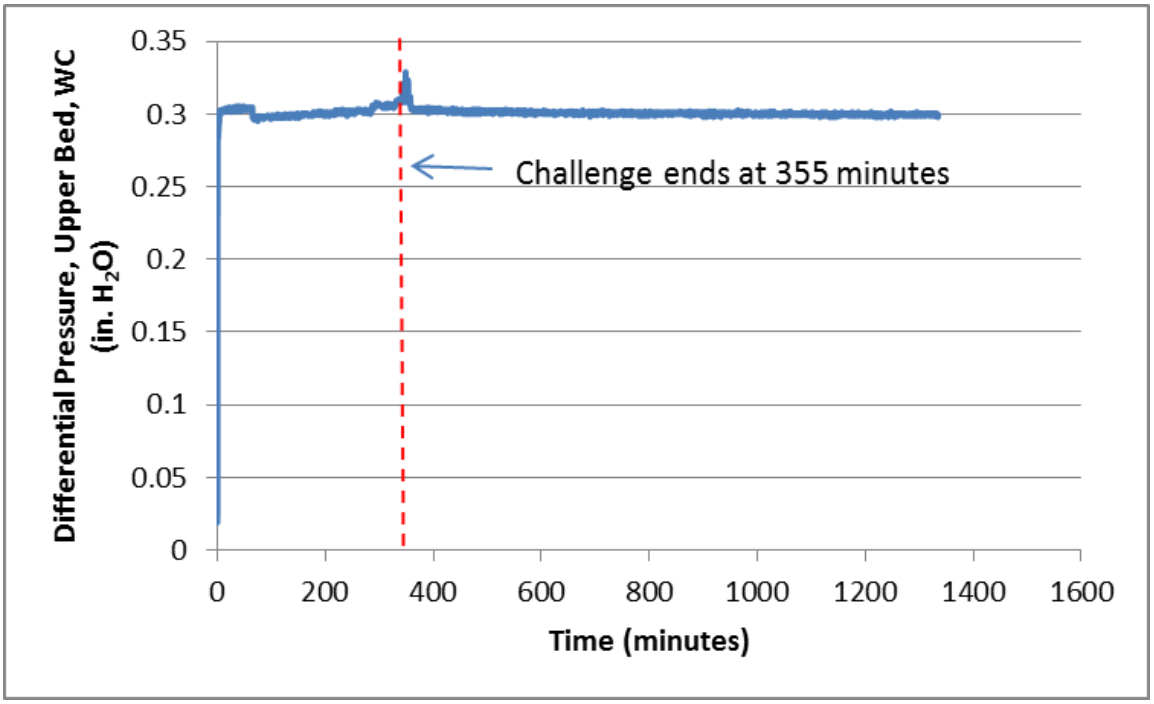

Figure C-29. Pressure differential measurement (upper bed) for HD adsorption/desorption on ASZM-TEDA (12 × 30 mesh) carbon at 25 °C/dry conditions.

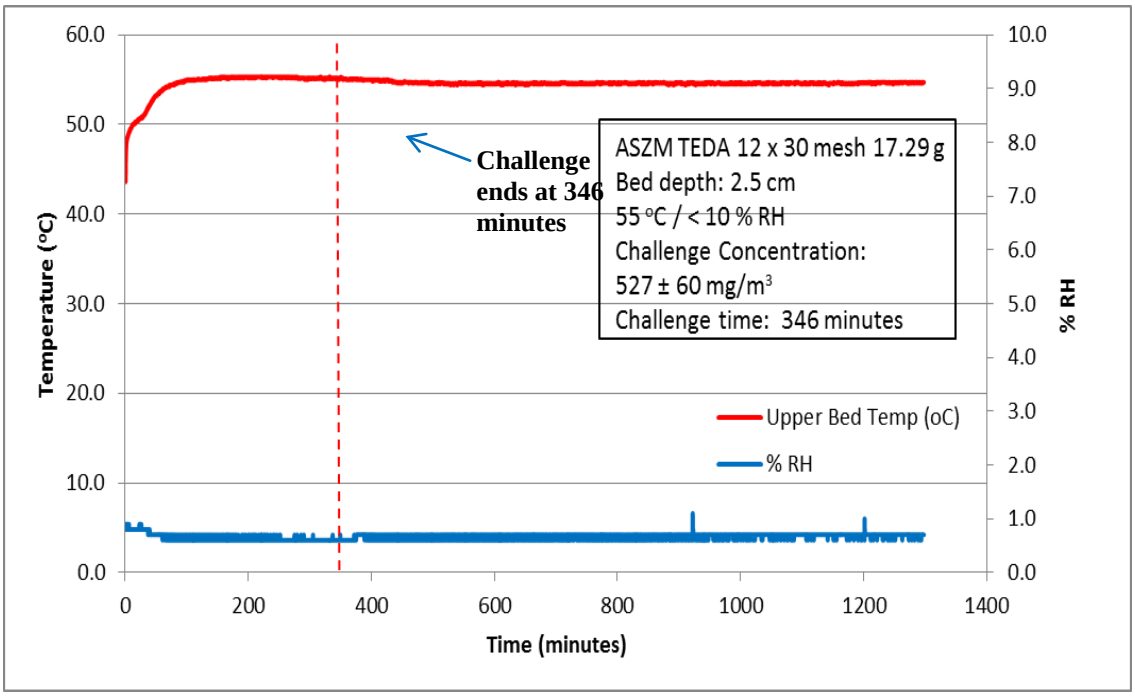

Figure C-30. Temperature and RH measurement for HD adsorption/desorption on ASZM-TEDA (12 × 30 mesh) carbon at 55 ºC/dry conditions.

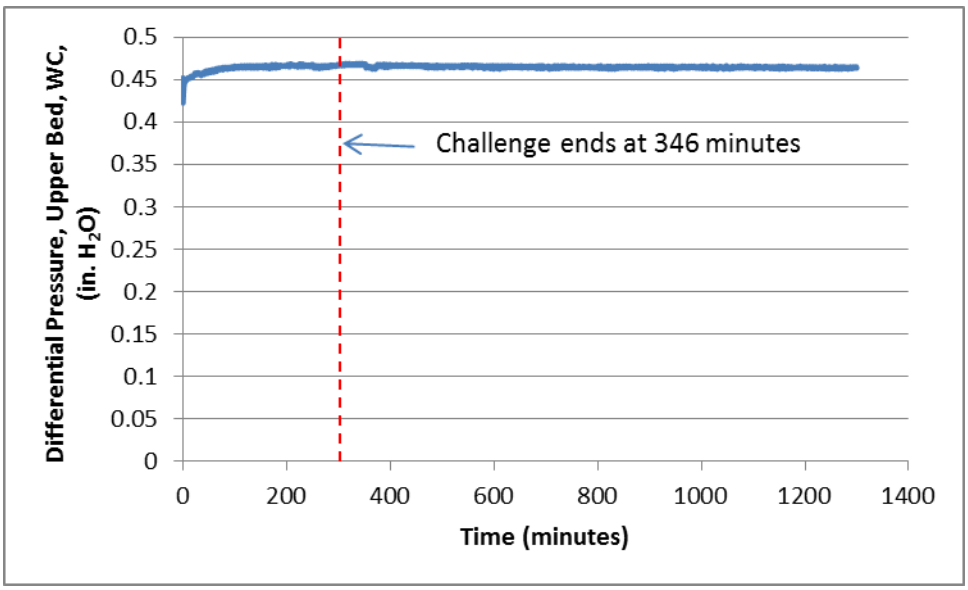

Figure C-31. Pressure differential measurement (upper bed) for HD adsorption/desorption on ASZM-TEDA (12 × 30 mesh) carbon at 55 ºC/dry conditions.

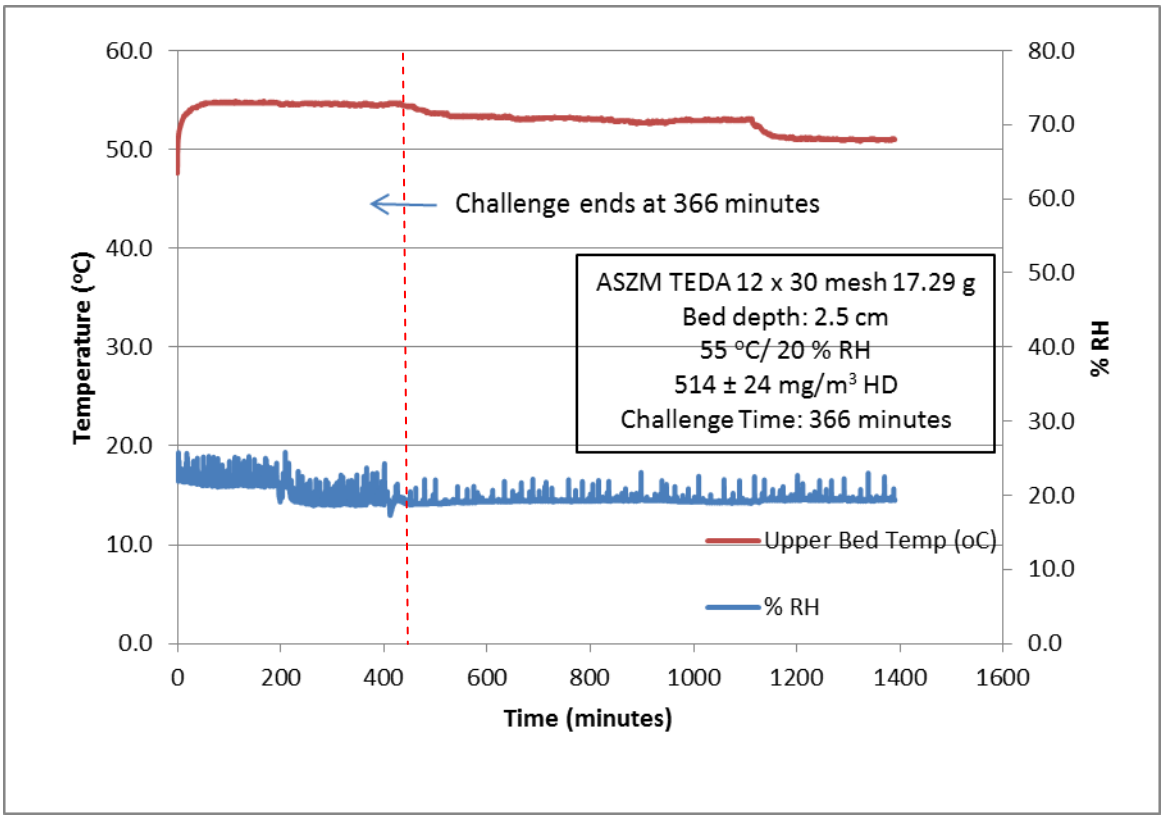

Figure C-32. Temperature and RH measurement for HD adsorption/desorption on ASZM-TEDA (12 × 30 mesh) carbon at 55 °C/humid conditions.

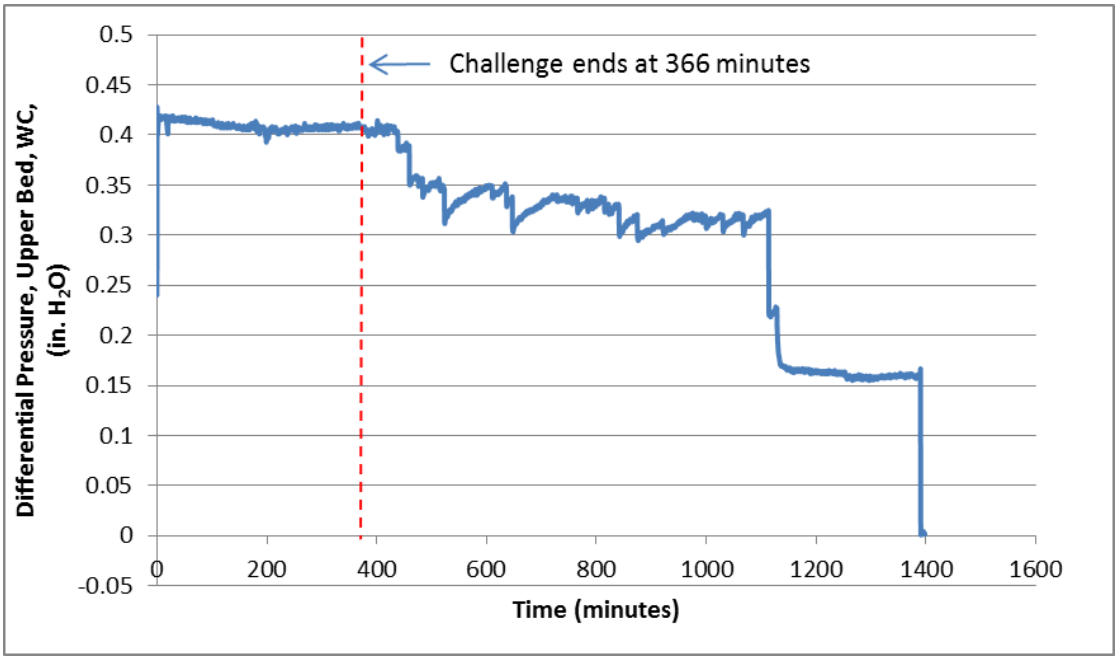

Figure C-33. Pressure differential measurement (upper bed) for HD adsorption/desorption on ASZM-TEDA (12 × 30 mesh) carbon at 55 °C/humid conditions.

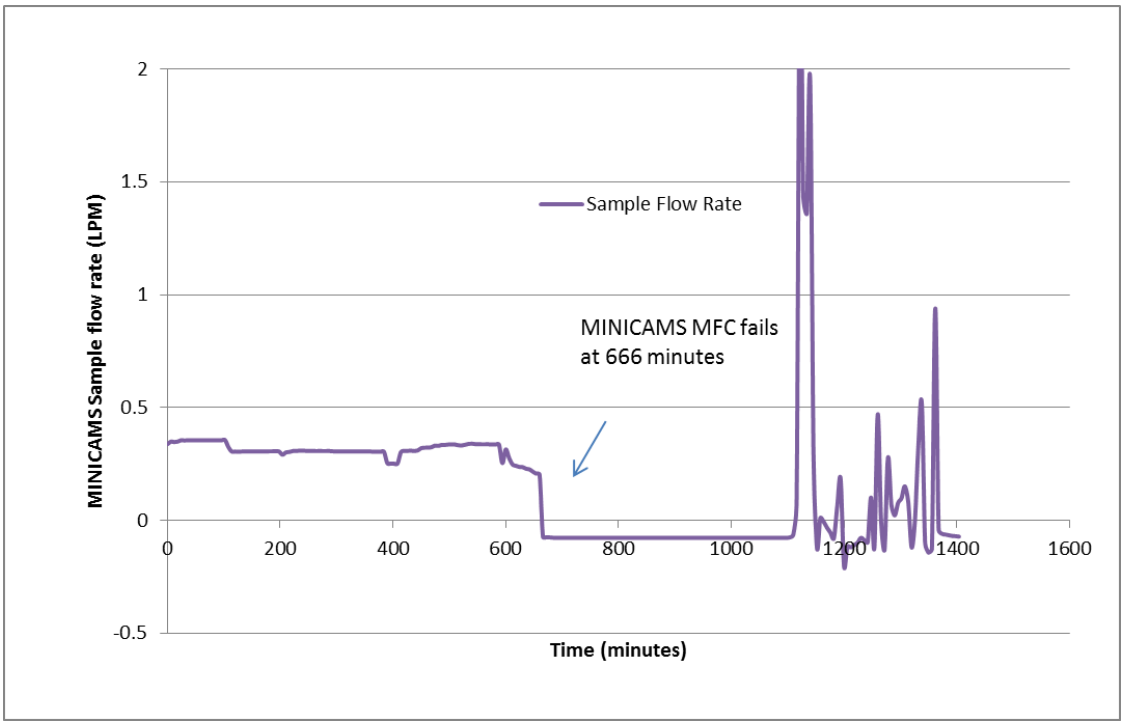

Figure C-34. MINICAMS® sampling flow rate capture data for ASZM-TEDA (12 × 30 mesh) carbon at 55 ºC/humid conditions.

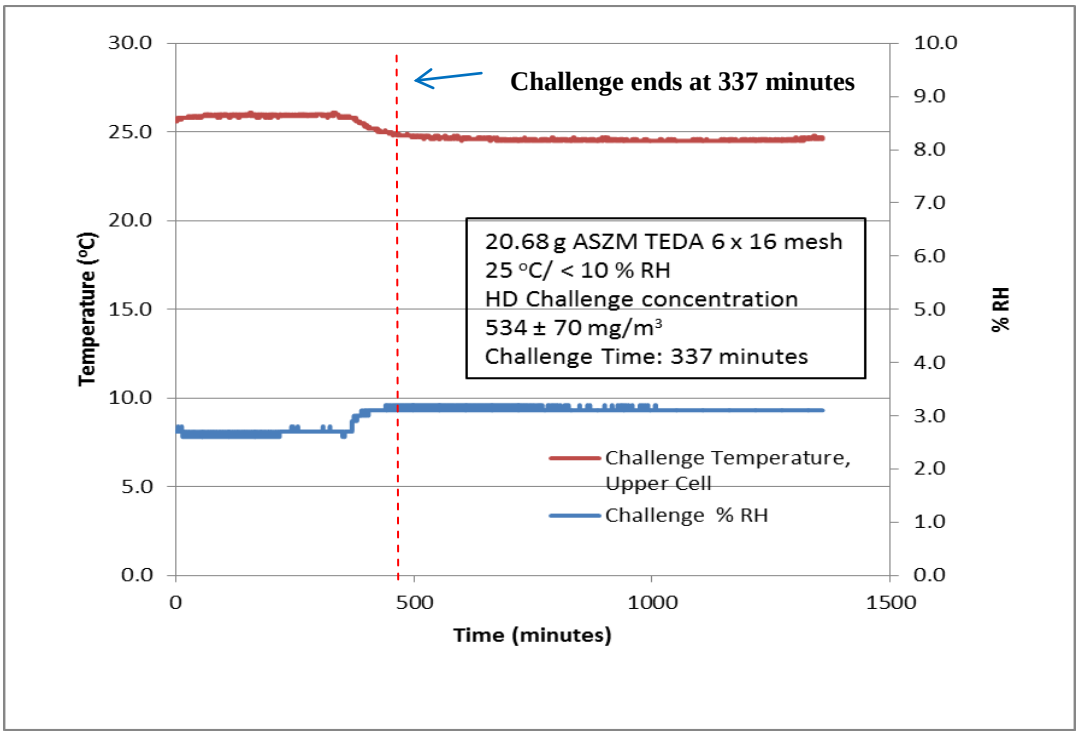

Figure C-35. Temperature and RH measurement for HD adsorption/adsorption on ASZM-TEDA (6 × 16 mesh) carbon at 25 ºC/dry conditions.

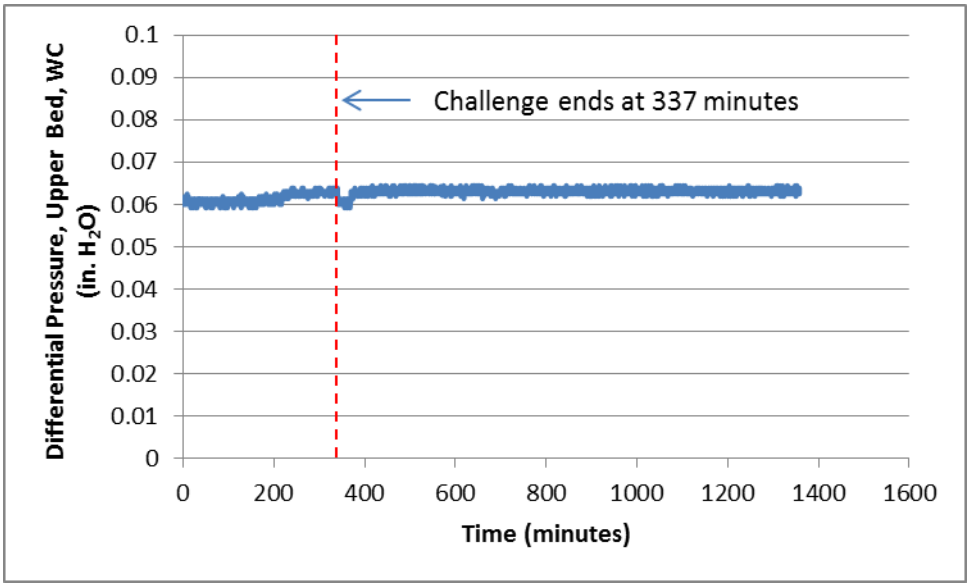

Figure C-36. Pressure differential measurement (upper bed) for HD adsorption/desorption on ASZM-TEDA (6 × 16 mesh) carbon at 25 ºC/dry conditions.

EPA
United States
Environmental Protection
Agency

PRESORTED STANDARD
POSTAGE & FEES PAID
EPA
PERMIT NO. G-35

Office of Research and Development (8101R)
Washington, DC 20460

Official Business
Penalty for Private Use
$300